Title

Novel Injectable Interpenetrating Polymer Network as a Semi-Permanent Injectable Implant for Soft Tissue Augmentation

Author

Leung, Joanne C.

Publication Date

2015

Peer reviewed|Thesis/dissertation

UNIVERSITY OF CALIFORNIA

Los Angeles

Novel Injectable Interpenetrating Polymer Network as a Semi-Permanent Injectable Implant for Soft Tissue Augmentation

A dissertation submitted in partial satisfaction of the
requirements for the degree Doctor of Philosophy
in Biomedical Engineering

By

Joanne Chung On Leung

2014

ABSTRACT OF THE DISSERTATION

Novel Injectable Interpenetrating Polymer Network

as a Semi-Permanent Injectable Implant for Soft Tissue Augmentation

by Joanne Chung On Leung

Doctor of Philosophy in Biomedical Engineering

University of California, Los Angeles, 2015

Professor Benjamin M. Wu, Chair

Injectable fillers have been widely used for soft tissue augmentation in cosmetic procedures, as well as minimally invasive treatment for medical conditions such as urinary and fecal incontinence, vesicoureteral reflux and vocal cord repair. The market for injectable fillers is a multibillion dollar industry worldwide, and each FDA-approved injectable filler has its own drawbacks, namely, lack of durability for temporary fillers, and difficulty in injection for semi-permanent to permanent fillers. A new material that offers solutions to the problems with the existing products will have a big market potential.

The intended application of the novel filler in this study is for treating urinary incontinence. In this thesis, we present a novel injectable filler that lasts > 6 months, is easy to inject, has an elastic modulus that matches the soft tissue to fit the contour, has customizable mechanical characteristics for different application, off-the-shelf, has good biocompatibility, and the feasibility to be co-injected with cells. The novel injectable semi-permanent filler designed in this study is a hydrogel composed of an interpenetrating polymer network (IPN) of random co-pHEMA-PEGMA-TEGDMA intertwined with CMC chains with various degrees of

entanglement, polymer chain lengths, crosslinking and different flow properties. We name this injectable HPTC.

HPTC was found to have the desirable injectability as a soft tissue filler only under a narrow range of optimal conditions. We studied the parameters that govern the injectability of HPTC using Intron injectability assay and rheological testing. We characterized the factors that were important for determining its force of injection, elastic and viscous moduli, oscillatory stress in response to increasing strain, viscosity change under constant shearing, and the percentage loss in elastic modulus after disruptive shearing. The effect of water content, steric hindrance introduced by the CMC pre-polymerization, CMC chain length, and the percentage of TEGDMA all have important contribution to the injectability of HPTC. We showed that optimal HPTC has superior injectability over the major permanent fillers that are FDA approved, which solved the needle-clogging problem.

HPTC also showed good biocompatibility with no signs of fibrotic capsules, durability in vivo for 6 months, good tissue integration, undetectable migration to other organs, and feasibility to be co-injected with cells. It has also been evaluated for its efficacy in the treatment of urinary incontinence in an animal model for 24 weeks, and has shown significant dose-dependent improvement in urethral function by having an increased abdominal leak point pressure (ALPP) compared to the incontinence model alone. Combining its superior injectability, customizable mechanical viscoelastic properties, biocompatibility and effectiveness of restoring the urethral function in a rat incontinence model for 6 months, HPTC is a good candidate as a semi-permanent/ permanent injectable material for soft tissue augmentation.

This dissertation of Joanne Chung On Leung is approved by:

Larissa Rodriguez

James Dunn

Shlomo Raz

Dean Ho

Benjamin M. Wu, Committee Chair

UNIVERSITY OF CALIFORNIA, LOS ANGELES

2015

To my parents, Raymond Leung and Tina Chan,
who always put myself and my siblings before themselves

TABLE OF CONTENTS

LIST OF FIGURES

CHAPTER 2

CHAPTER 3

CHAPTER 4

LIST OF TABLES

ACKNOWLEDGEMENTS

I would like to thank my mentors, Professor Larissa Rodriguez, Professor Ben Wu, and Professor Rong Zhang for your guidance and support. I am truly grateful for the opportunity that you have given me in pursuing a project that I was excited about, and for allowing me the creative freedom in the approach in solving the problems, while guiding me back to the right direction whenever things go awry. You have been monumental in helping me recalibrate the course after each wrong turn, to find the right way out.

I would like to give special thanks to my committee members, Prof. James Dunn, Prof. Shlomo Raz and Prof. Dean Ho for their expertise in their fields, generosity of time and inspirations.

I am grateful that my lab mates and undergraduate researchers have been a great support network for me. Other than giving me invaluable insights into my project because of their expertise, technical support, and asking the right questions to help me focus on the important aspects of my study, they have also been keeping me sane through my graduate career by cheering me up with direly needed snack breaks, inspirational personal stories and keeping things light with necessary goofiness. Prof. Rong Zhang, Suny Kun Harper, Dr. Anne "Lenny" Ackerman, Dr. Forrest Jellison, Dr. Greg Jack, Dr. Ariana Smith, Dr. Andrea Staack, Dr. Nikki Le, Dr. Una Lee, Dr. Leah Nakamura, Dr. Dhiren Dave, Dr. Ja-Hong Kim, Ziva Shulaker, Shannon Wongvibulsin, and Alvin Li, thank you so much for being amazing friends and colleagues.

To those at UCLA who have helped tremendously in my studies: Prof. Thomas Mason, Prof. Pirouz Kavehpour, Dr. Kenny Mayoral, and Kelly Connelly for the remarkable help in the rheology experimental design and countless hours of support, Professor You-Sheng Wilson Lin, Max Ho and Noah Bodzin from the UCLA Nanolab for the help with material characterization including AFM and SEM, Professor Min Lee for the expert advise and support in biomaterials, Dr. April Rodriguez for helping me synthesize chemicals and NMR, Dr. Ichiro Nishimura for

allowing me to carry out multiple experiments in his lab, Prof. Michael Titell for his expertise in identifying cell types that were responsible for the inflammatory response, Joe Severino and Dr. Larry Carlson for helping with viscosity measurements, Matthew Schibler for the guidance in confocal microscopy, Dr. Greg Khitrov for his help with ESI Mass Spectrometry, the TPCL Core for the help with histology, and the Bioengineering staff for all the advice and administrative support--this dissertation would not have been possible without all their major contributions.

I want to express my heartfelt gratitude to everyone who made it possible for me to have a secondary career in photography, which not only was my obsession, but also played a significant role in funding my graduate study. I thank my clients who believed in my craft and trusted my vision.

I cannot imagine being here today without the love and support from my mom Tina Chan, dad Raymond Leung, sister Joie Leung, brother Marcus Leung, nephew little Isaac and grandma Sam Mui Mak. It is because all of you, who let me do whatever I wanted to do with my life, I have finally reached a new milestone in our family's history. Mom and dad, despite the circumstances of your childhoods living in extreme poverty on fishing boats and being discriminated against by most who judged, and having no luxury of financial security to continue beyond high school or primary school education, you did so well to provide all your kids an amazing environment to grow up in and gave us the means to have the best education abroad. I hope that we all make you proud.

Thank you for believing in me and not doubting too many of my impulsive decisions, listening to my whining about school, making sure I am well-fed, making me laugh, insisting on checking out the songs that you wrote that were so fun and catchy, and being a great partner, Julian Chan. Your love and support mean so much to me and I am very grateful for having you in my life.

VITA

B.S. Biochemistry
Northeastern University, Boston, MA

Research Specialist
Neurogenetics Unit
Massachusetts General Hospital and Harvard Medical School, Boston, MA

Research Assistant
Cambridge Institute for Medical Research (CIMR)
Cambridge University, Cambridge, United Kingdom

M.S. Biomedical Engineering
University of California, Los Angeles, CA

CHAPTER 1

INTRODUCTION AND SIGNIFICANCE

1.1. Background

1.1.1. The scope of the soft tissue filler market

Injectable soft tissue filler plays a major role in minimally invasive treatment for cosmetic [1] and non-cosmetic procedures worldwide. The U.S. Food and Drug Administration (FDA) categorize them as permanent (lasts over 6 months) or temporary (lasts less than 6 months) implantable medical devices. Within the realm of injectable soft tissue fillers, just the market share for cosmetic wrinkle fillers alone, was a $1.6 Billion dollar market globally in 2012, with a projected annual growth of 7.6% per year [2] and that was with Botulin Toxin A (Botox) excluded.

Aside from cosmetic applications, injectable soft tissue fillers also have seminal importance for the treatment of various medical conditions, including minimally invasive treatment for urinary incontinence [3] [4], fecal incontinence[5][6], vesicoureteral reflux[7] [8], vocal cord repair [9] [10], and heart infarct size stabilization procedures[11]. The main goal of using these injectable implants is to restore the volume lost in the soft tissues. For example, it can be used in cosmetic procedures to fill the wrinkles by increasing the volume of the dermal [12] and fat layer [13] by biocompatible materials; it can be used in achieving coaptation of loose urethra [3] [14] that have trouble maintaining a higher pressure in the abdomen and the bladder.

Urinary incontinence, which can be debilitating conditions, affect more than 200 million people globally[15], and in the U.S. alone, 25-50% of women suffer from urinary incontinence, according to the National Association for Continence. An estimated 9-13 million patients in the U.S. suffer from severe urinary incontinence symptoms, which make them candidates for

treatments with medications, sling procedure or injection of minimally invasive urethral bulking agents. The market of the U.S. urethral bulking agent for treating urinary incontinence in 2012 totaled approximately $1.2 billion, with an annual growth rate of over 4% in the aging American population [16]. It is a growing market with limited available products, and none of them is ideal.

1.1.2. Commercially available injectable materials used in minimally invasive procedures for soft tissue augmentation

Although the classes of the soft tissue fillers designed for cosmetic procedures, urethral bulking, fecal incontinence treatment and urinary reflux may be marketed under different names and have slight variations adapted for their specific applications, almost all of them in each class are fundamentally the same materials, regardless of the target treatment site, as summarized in Table 1.

Each of the previously or currently FDA-approved soft tissue filler has its own drawbacks, and none of them was ideal. The temporary injectable devices are generally easy to inject, but the problem is that they do not last 6 months, prompting the patients to visit the physician fairly frequently. On the other hand, the semi-permanent to permanent devices last longer, but the ones that are still active in the market are either difficult to inject (Calcium hydroxyapatite beads, Coaptite® and silicone based elastomer beads Macroplastique®) with needle-clogging issues leading to inability to adjust the needle to another injection angle once injection is initiated, requirement of using piston-powered syringe to inject them into the treatment site due to high resistance in the needle, or some have shown concern as low grade chronic infection has been seen in patients, due to the extended time that the implant is in contact

with the body. A soft tissue implant material that is semi-permanent to permanent, easy to inject, and has long term efficacy and safety in vivo does not yet exist in the market, and this prompted us to invent a new product that could fulfill all of these goals. None of the products on the market has been able to fulfill all of these requirements. Finding a material that could solve the problems with needle clogging, fibrotic tissue formation, lack of durability and migration, while having great biocompatibility would have great market potential in the multibillion-dollar industry of soft tissue fillers.

1.1.3. Disadvantages of Injectable Materials formed by physical interactions

The vast majority of injectable biomaterials described in recent biomedical research literature are physical polymer networks linked together by physical associations between nanoparticles or polymer chains. The major drawback with these injectable materials is that they are not durable in nature, and would dissociate or disintegrate in vivo within a period of 1 to 6 months. Presented here are some of the major types of injectable materials that have been under investigation in the recent years.

(1) Alginates are hydrogels that are formed upon the addition of multivalent cations, and the gelation occurs due to Coulombic interactions. To manipulate the injectability, slow release of $CaSO_4$ powder was used to avoid needle-clogging problem [17];

(2) in-situ polymerization of Chitosan is based on pH- and temperature- dependent cationic interactions, of which when a solution of chitosan with hydrated amine groups is admixed with glycerol-phosphate disodium salt, it remains a liquid below room temperature close to physiological pH, and the molecular interactions rearrange upon heating to 37°C [18];

(3) in-situ thermoreversible gelation of poloxamer or Pluronic®, which are non-ionic, amphiphilic tri-block copolymers with hydrophilic blocks (polyethylene) flanking the central hydrophobic block (poly(propylene oxide)), exhibit liquid to solid paste transition due to micelle assembly, that translates into gelation when the temperature is increased over the threshold temperature at critical micellization concentration [19];

(4) fibrin glue is formed by the of interactions between amphipathic fibrous, non-globular protein upon activation, and has been used as biodegradable scaffolds [20];

(5) hyaluronic acid derivatives, but they are subjected to multiple types hyaluronidases in the human body for rapid break down[21];

(6) Bovine Collagen products have been widely used in cosmetic procedures for decades but 3% of the population show signs of rejection, and the longevity of the augmentation is limited to a 2-6 months[22];

One of the main goals of the design of a new material for soft tissue augmentation is to have increased durability while maintaining ease of injection. The injectable gels above that are formed due to physical associations play significant roles in controlled release drug delivery systems and tissue engineering, but they are very limited in retaining the mass or volume in vivo for long-term use for over 6 months, as they are assembled solely by inter-molecular interactions. Injectable biomaterials that are durable and soft as the soft tissue are currently extremely limited and demanded. Efforts have been made to modify some of these injectable materials formed by physical interactions, namely by chemical crosslinking, such as glutaraldehyde on collagen[23], but the extend it which it prolongs the durability of these materials is limited, and sometimes the side effects of toxicity of such treatment outweighs the benefits of the extended durability.

1.1.4. The rationale for the choices of the components in the hydrogel for this study, HPTC

Extensive considerations had been given when it came to choosing the components that have the desired properties that could fulfill the long list of desired characteristics of the final product, that also have good safety records as biomaterials. A novel injectable material, HPTC hydrogel, was designed using very specific combinations and concentrations of 4 major starting materials to give rise to a range of final products that fit the design specifications. HPTC was named after the first letter of its 4 main components listed below:

- 2-Hydroxyethylmethacrylate (HEMA)—when polymerized to poly-HEMA, or pHEMA, has a long history as a non-degradable biomaterial [24], well known for its inertness, high water content and safety record, with both hydrophobic and hydrophillic characteristics. pHEMA has been widely used as a contact lens material, intraocular lenses, and in dentistry
- poly(ethylene glycol) methyl ether methacrylate (PEGMA) is chemically similar to HEMA, except with a slightly longer side-chain with higher hydrophilicity. It is added to improve the general hydrophilicity and biocompatibility of pHEMA as implant materials, drug release device, and coating for blood-contacting surfaces[25]
- Tetraethylene glycol dimethacrylate (TEGDMA)– a covalent crosslinker to improve the injectability of the hydrogel by providing a flexible linker in its backbone. It has been used extensively in dental applications [26] [27].
- Carboxymethyl cellulose (CMC)—it is an inert derivative from cellulose obtained from plants and has a long safety record for both for FDA approved devices such as carrier for

the hydroxyapatite beads in injectable filler Coaptite®, lubricant for medical implants such as hip prosthesis [28], artificial tears [29], and human consumption in the food industry such as food thickeners found in sauces and ice cream.

Poly((HEMA)-based materials and its conventional use in medicine HEMA polymerization was first reported in the 1934 patent filed by Woodhouse (Woodhouse et al 1934). At the time, he did not realize that the polymerized HEMA in a white powder format was extremely hydrophilic and could swell many times its weight in water. HEMA's hydrophilic properties and thus the potential as an important biomaterial was discovered by Wichterle and Lim in 1951, as they developed the world's soft contact lenses with it. Since then, clinical trials with HEMA as an implant have been used for intraocular lens implant [30] [31], artificial cornea [32] , breast implants [33] [34] [35], surface coating by polymer grafting of cochlear implant electrodes [36], drug delivery device for the eye [37] , bioactive synthetic bone graft for dentistry [38] and various dental adhesive and composite resins [39] [40].

In this study, we transformed the typically uninjectable pHEMA-based hydrogel into its injectable counterpart by polymerizing the monomers (HEMA, PEGMA and TEGDMA) around a solubilized entanglement of carboxymethyl cellulose, using photo-initiated free radical polymerization under a set of well-defined parameters to yield a material with the optimal mechanical properties as an injectable soft tissue filler.

1.1.5. The desirable characteristics of an improved permanent to semi-permanent implantable medical device for soft tissue augmentation

The following list of desirable properties that were taken into consideration:

- Ease of injection—a material that does not clog the needle during the application, or is too thin to control the flow;
- lasts at least 6 months to avoid frequent visit to the physician for reinjection
- components of the materials are FDA-approved in other devices with a track record for safety;
- off the shelf, no refrigeration;
- suitable physical attributes for soft tissue augmentation—soft and compliant, smooth rather than lumpy or rugged,
- shear-thinning property suitable for delivering the material into the injection site so that it can adequately accommodate the narrowness of the needle, but viscoelastic enough to remain in the injection site immediately following the needle withdrawal up to months after the injection;
- easy to inject regardless of the number of times or the extended time it takes the physician needs to readjust the position of the needle during injection, and improvement of symptom for over 6 months.
- processing method does not require harsh conditions;
- Ability to customize the mechanical characteristics for specific applications—balancing injectability, ease of control of volume, and modulus of the material;
- low cost to manufacture.
- Inert and biocompatible--Non-immunogenic, minimal scar tissue/ fibrotic capsule
- Maximal tissue integration--blends well with the host tissue and matching the modulus
- minimal migration to the blood stream and other organs;

- feasibility of co-injecting cells with therapeutic potential along with the material into the soft tissue.

HPTC is designed, fabricated, and tested with these criteria in mind in the following chapters.

1.2. Research objectives

The primary goal of this study is to develop a new injectable material within the semi-permanent to permanent implantable medical device category that provides better injectability than the currently FDA approved products in the same category.

The aims of this thesis are:

Aim 1: To develop HPTC, a non-degradable HEMA-based hydrogel that is injectable

(a) to fabricate the typically solid and uninjectable pHEMA hydrogel into an injectable form by manipulating the conditions of an interpenetrating network, while maintaining its non-biodegradable status targeted for long-term treatment;

(b) to define and characterize the parameters that govern the physical properties of the injectable pHEMA hydrogel that make it a desirable material for soft tissue augmentation implanted by injection;

(c) to have the ability to customize the viscoelastic to suit individual needs for different applications;

(d) to achieve greater injectability compared to the leading FDA-approved soft tissue fillers in the semi-permanent to permanent injectable category;

Aim 2: To evaluate HPTC's biocompatibility and efficacy as a treatment for urinary incontinence

(a) to evaluate HPTC's biocompatibility;

(b) to evaluate HPTC as a treatment effectiveness as a soft tissue filler, using a rat incontinence model;

(c) to evaluate the feasibility of co-injecting HPTC with cells.

Type of injectable biomaterial	FDA implantable device category	Pros	Cons	Applications
Hyaluronic acid	Temporary	-easy to inject	-lasts <6 months	Restylane®, Juvederm® and Prevelle® for facial filler, Deflux® and Solesta® for fecal incontinence, Zuidex® and Deflux® for urinary incontinence and urinary reflux
Crosslinked collagen	Temporary	-easy to inject	-lasts ~3-4 months	Evolence® and Zyplast® for the facial filler, Contigen® for urinary incontinence, and Cymetra® for fecal incontinence
Poly-Lactic Acid (PLLA) microspheres	Temporary	-easy to inject	-lasts <4 months	Sculptra® and New Fill® for facial filler
Autologous tissues (fat, stem cells, myoblasts, fibroblasts) *	Temporary	-fairly easy to inject -no rejection	-lasts <6 months	facial filler , body sculpting, incontinence
Calcium Hydroxyapatite microbeads	Permanent/ semi-permanent	-lasts 18 months for the face and 12+ months in the urethra -well tolerated	-very difficult to inject -clogs needle	Radiesse® for facial filler, Coaptite® for urinary incontinence and vocal cord, Radiesse® for fecal incontinence
Crosslinked Silicone elastomer beads	Permanent/ semi-permanent	-lasts over a year	-very difficult to inject (power piston syringe required) -fibrotic capsule	Macroplastique® for urinary incontinence, PTQ® for fecal incontinence
Polymethyl methacrylate (PMMA) microspheres in collagen	Permanent/ semi-permanent	-possible to use 26G needle -lasts over a year	-hard pieces of Plexiglas -low grade infection reported	Both Artefill® and Artcoll® are used as facial filler and trials for urinary and fecal incontinence
Carbon-coated beads	Permanent/ semi-permanent		-withdrawn due to migration	Duraspheres® for urinary and fecal incontinence
Teflon (PTFE) particles	Permanent/ semi-permanent		-withdrawn due to migration	Urinary and fecal incontinence

Table 1. Summary of the types of injectable biomaterials either currently on the market or have been on the market in the past, along with their respective FDA implantable medical device category, pros and cons, as well as their applications. The major temporary devices are Hyaluronic acid, crosslinked collagen, and poly-lactic-acid (PLLA) microspheres, while the major permanent/semi-permanent devices are Calcium hydroxyapatite microbeads, crosslinked silicone elastomer beads, polymethyl methacrylate (PMMA) microspheres in collagen, carbon-coated beads and Teflon particles.

Reference

[1] D. W. Buck, M. Alam, and J. Y. S. Kim, "Injectable fillers for facial rejuvenation: a review," *J. Plast. Reconstr. Aesthetic Surg.*, vol. 62, no. 1, pp. 11–18, 2009.

[2] iData Research, "U.S. Cosmetic Surgery, Facial Aesthetics and Medical Laser Devices Market," 2013.

[3] M. S. Kirchin V, Page T, Keegan PE, Atiemo K, Cody JD, "Urethral injection therapy for urinary incontinence in women (Review)," *Cochrane Collab.*, vol. 2, pp. 1–59, 2012.

[4] M. Imamura, P. Abrams, C. Bain, B. Buckley, L. Cardozo, J. Cody, J. Cook, S. Eustice, C. Glazener, a Grant, J. Hislop, D. Jenkinson, M. Kilonzo, G. Nabi, J. N. Dow, R. Pickard, L. Ternent, S. Wallace, J. Wardle, S. Zhu, and L. Vale, "of the Effectiveness and Cost-Effectiveness Stress Urinary Incontinence," vol. 14, no. 40, 2010.

[5] Y. Maeda, S. Laurberg, and C. S. Norton, "Perianal injectable bulking agents as treatment for faecal incontinence," *Cochrane Database Syst. Rev.*, no. 3, 2009.

[6] J. J. Tjandra, J. F. Lim, R. Hiscock, and P. Rajendra, "Injectable silicone biomaterial for fecal incontinence caused by internal anal sphincter dysfunction is effective," *Dis. Colon Rectum*, vol. 47, no. 12, pp. 2138–2146, 2004.

[7] P. Puri, B. Kutasy, E. Colhoun, and M. Hunziker, "Single center experience with endoscopic subureteral dextranomer/hyaluronic acid injection as first line treatment in 1,551 children with intermediate and high grade vesicoureteral reflux," *J. Urol.*, vol. 188, no. 4 SUPPL., pp. 1485–1489, 2012.

[8] S. Kocherov, I. Ulman, S. Nikolaev, J. P. Corbetta, Y. Rudin, A. Slavkovic, Z. Dokumcu, A. Avanoglu, L. Menovshchikova, S. Kovarskiy, T. Skliarova, S. Weller, J. I. Bortagaray, J. C. Lopez, V. Durán, C. Burek, C. Sager, M. Dmitriy, T. Garmanova, A. Djamal, Z. Jovanovic, N. Vacic, W. Abu Arafeh, and B. Chertin, "Multicenter Survey of Endoscopic Treatment of Vesicoureteral Reflux Using Polyacrylate-Polyalcohol Bulking Copolymer (Vantris)," *Urology*, vol. 84, no. 3, pp. 689–693, 2014.

[9] R. Lakhani, F. Jm, N. Bleach, D. Costello, M. Birchall, R. Lakhani, J. M. Fishman, N. Bleach, D. Costello, and M. Birchall, "Alternative injectable materials for vocal fold medialisation in unilateral vocal fold paralysis (Review) Alternative injectable materials for vocal fold medialisation in unilateral vocal fold paralysis," no. 10, 2012.

[10] R. Mikaelian, DO, Lowry, LD, Sataloff, "Lipoinjection for Unilateral Vocal Cord Paralysis," *Laryngoscope*, vol. 101, no. 5, p. 465, 1991.

[11] J. Wu, F. Zeng, X. P. Huang, J. C. Y. Chung, F. Konecny, R. D. Weisel, and R. K. Li, "Infarct stabilization and cardiac repair with a VEGF-conjugated, injectable hydrogel," *Biomaterials*, vol. 32, no. 2, pp. 579–586, 2011.

[12] R. J. Rohrich, A. Ghavami, and M. a Crosby, "The role of hyaluronic acid fillers (Restylane) in facial cosmetic surgery: review and technical considerations.," *Plast. Reconstr. Surg.*, vol. 120, no. 6 Suppl, p. 41S–54S, 2007.

[13] R. J. Rohrich and J. E. Pessa, "The fat compartments of the face: anatomy and clinical implications for cosmetic surgery.," *Plast. Reconstr. Surg.*, vol. 119, no. 7, pp. 2219–2227; discussion 2228–2231, 2007.

[14] N. F. Davis, F. Kheradmand, and T. Creagh, "Injectable biomaterials for the treatment of stress urinary incontinence: Their potential and pitfalls as urethral bulking agents," *Int. Urogynecol. J. Pelvic Floor Dysfunct.*, vol. 24, no. 6, pp. 913–919, 2013.

[15] M. Rozensky, RH, Tovian, SM, Gartley, CB, Nichols, TR, Layton, "A Quality of Life Survey of Individuals with Urinary Incontinence Who Visit a Self-Help Website: Implications for those Seeking Healthcare Information," *J. Clin. Psychol. Med. Settings*, vol. 20, pp. 263–302, 2013.

[16] Frost_Sullivan_Research_Services, "U.S. Direct-energy Based Medical Devices Market - Aesthetics; Cardiovascular; Gynecology; Orthopedics; Urology," 2011.

[17] C. Cao, Y, Rodriguez A, Vacanti, M, Ibarra, C, Arevalo, C, Vacanti, "Comparative study of the use of poly(glycolic acid), Calcium alginate and pluronics in the engineering of autologous porcine cartilage.," *J. Biomater. Sci. Polym. Ed.*, vol. 9, no. 5, pp. 475–487, 1998.

[18] a Chenite, C. Chaput, D. Wang, C. Combes, M. D. Buschmann, C. D. Hoemann, J. C. Leroux, B. L. Atkinson, F. Binette, and a Selmani, "Novel injectable neutral solutions of chitosan form biodegradable gels in situ.," *Biomaterials*, vol. 21, no. 21, pp. 2155–2161, 2000.

[19] L. Yu and J. Ding, "Injectable hydrogels as unique biomedical materials.," *Chem. Soc. Rev.*, vol. 37, no. 8, pp. 1473–1481, 2008.

[20] K. L. Christman, H. H. Fok, R. E. Sievers, Q. Fang, and R. J. Lee, "Fibrin glue alone and skeletal myoblasts in a fibrin scaffold preserve cardiac function after myocardial infarction.," *Tissue Eng.*, vol. 10, no. 3–4, pp. 403–409, 2004.

[21] D. D. Allison and K. J. Grande-Allen, "Review. Hyaluronan: a powerful tissue engineering tool.," *Tissue Eng.*, vol. 12, no. 8, pp. 2131–2140, 2006.

[22] A. W. Klein and M. L. Elson, "The history of substances for soft tissue augmentation," *Dermatologic Surg.*, vol. 26, no. 12, pp. 1096–1105, 2000.

[23] A. S. Hoffman, “Hydrogels for biomedical applications,” *Adv. Drug Deliv. Rev.*, vol. 64, no. SUPPL., pp. 18–23, 2012.

[24] O. Wichterle and D. Lím, “Hydrophilic Gels for Biological Use,” *Nature*, vol. 185, no. 4706, pp. 117–118, 1960.

[25] J. Jin, W. Jiang, Q. Shi, J. Zhao, J. Yin, and P. Stagnaro, “Fabrication of PP-g-PEGMA-g-heparin and its hemocompatibility: From protein adsorption to anticoagulant tendency,” *Appl. Surf. Sci.*, vol. 258, no. 15, pp. 5841–5849, 2012.

[26] M.-L. Henriks-Eckerman, K. Suuronen, R. Jolanki, and K. Alanko, “Methacrylates in dental restorative materials.,” *Contact Dermatitis*, vol. 50, no. 4, pp. 233–237, 2004.

[27] V. B. Michelsen, G. Moe, M. B. Strøm, E. Jensen, and H. Lygre, “Quantitative analysis of TEGDMA and HEMA eluted into saliva from two dental composites by use of GC/MS and tailor-made internal standards,” *Dent. Mater.*, vol. 24, no. 6, pp. 724–731, 2008.

[28] S. Flanagan, E. Jones, and C. Birkinshaw, “In vitro friction and lubrication of large bearing hip prostheses.,” *Proc. Inst. Mech. Eng. H.*, vol. 224, no. 7, pp. 853–864, 2010.

[29] H. Roth, T. Conway, and D. a Hollander, “Artificial Tears in Patients With Mild To Moderate Dry Eye,” pp. 73–78, 2011.

[30] a J. Khan and S. P. Percival, “12 Year Results of a Prospective Trial Comparing Poly(Methyl Methacrylate) and Poly(Hydroxyethyl Methacrylate) Intraocular Lenses.,” *J. Cataract Refract. Surg.*, vol. 25, no. 10, pp. 1404–1407, 1999.

[31] G. Barrett, “Multicenter Trial of an intraocular hydrogel lens implant,” *J. Cataract Refract. Surg.*, vol. 13, no. 6, pp. 621–626, 1987.

[32] G. J. Crawford, C. R. Hicks, X. Lou, S. Vijayasekaran, D. Tan, B. Mulholland, T. V. Chirila, and I. J. Constable, “The Chirila Keratoprosthesis: Phase I human clinical trial,” *Ophthalmology*, vol. 109, no. 5, pp. 883–889, 2002.

[33] K. Kliment, M. Stol, K. Fahoun, and B. Stockar, “Use of spongy hydron in plastic surgery.,” *J. Biomed. Mater. Res.*, vol. 2, no. 2, pp. 237–243, 1968.

[34] J. S. Calnan, “Assessment of Biological Properties of Implants Before their Clinical Use,” *Proc. R. Soc. Med.*, vol. 63, no. 11 Pt 1, pp. 1115–1118, 1970.

[35] Z. Voldrich, Z. Tománek, J. Vacík, and J. Kopecek, “Long-term experience with poly(glycol monomethacrylate) gel in plastic operations of the nose.,” *J. Biomed. Mater. Res.*, vol. 9, no. 6, pp. 675–685, 1975.

[36] H. Mirzadeh and F. Abbasi, “Segmented detachable structure of cochlear-implant electrodes for close-hugging engagement with the modiolus.,” *J. Biomed. Mater. Res. B. Appl. Biomater.*, vol. 68, no. 2, pp. 191–198, 2004.

[37] D. Gulsen and A. Chauhan, “Dispersion of microemulsion drops in HEMA hydrogel: A potential ophthalmic drug delivery vehicle,” *Int. J. Pharm.*, vol. 292, no. 1–2, pp. 95–117, 2005.

[38] S. J. Froum, M. a Weinberg, and D. Tarnow, “Comparison of bioactive glass synthetic bone graft particles and open debridement in the treatment of human periodontal defects. A clinical study.,” *J. Periodontol.*, vol. 69, no. 6, pp. 698–709, 1998.

[39] D. M. Yourtee, R. E. Smith, K. a. Russo, S. Burmaster, J. M. Cannon, J. D. Eick, and E. L. Kostoryz, “The stability of methacrylate biomaterials when enzyme challenged: Kinetic and systematic evaluations,” *J. Biomed. Mater. Res.*, vol. 57, no. 4, pp. 522–531, 2001.

[40] J. Szczepanska, T. Poplawski, E. Synowiec, E. Pawlowska, C. J. Chojnacki, J. Chojnacki, and J. Blasiak, “2-Hydroxylethyl methacrylate (HEMA), a tooth restoration component, exerts its genotoxic effects in human gingival fibroblasts trough methacrylic acid, an immediate product of its degradation,” *Mol. Biol. Rep.*, vol. 39, no. 2, pp. 1561–1574, 2012.

IMPROVED EASE OF INJECTION AND VISCOELASTIC PROPERTIES OF A NOVEL NON-ABSORBABLE INJECTABLE MEDICAL IMPLANT FOR SOFT TISSUE AUGMENTATION

2.1 Introduction

2.1.1 Advantages of Interpenetrating Network compared to injectable materials made with polymers held together by physical interactions

Interpenetrating network is a polymer composed of two or more networks that are interlaced but not covalently bonded to each other. Due to the interpenetrating properties, the network cannot be physically separated unless chemical bonds are broken to release the networks from one another. Unlike physical polymer networks that have "junction points or zones formed by physically interacting chains which need not be permanent"[1] HPTC formed by sequential interpenetrating polymer network is resistant to dissolution due to changes in physical parameters such as temperature, pH, ionic strength, crosslinker concentration, surface area, which on the other hand, are crucial factors that affect the structural integrity of materials held by physical associations [2].

In order to break down the interpenetrating network of HPTC, covalent bonds must be broken. In order to achieve the goal of making it a permanent or semi-permanent implant, the types of covalent bonds involved have been engineered to be resistant to major biological degradation mechanisms. In this study, we designed HPTC to consist mostly of -C-C- backbones for the HEMA/PEGMA chains, and -C-C-O- bonds within the TEGDMA molecule itself at the branch points. With the low abundance of ester bonds such as those found in poly-galactic acid (PGA) or poly-lactic acid (PLA) that are prone to hydrolysis, acidic degradation and enzymatic digestion, these backbones and branch points of HPTC are extremely resilient to the common enzymatic degradation or water erosion. The interpenetrating network is also

resilient enough to withstand drastic changes in pH, temperature, surface area, and ionic strength, in which case materials held together by physical interactions will crumble, and therefore short in-vivo and in-vitro presence has been widely reported[3-6]. The body of research for interpenetrating networks is limited to non-injectable applications currently, such as those for bone regeneration and drug delivery.

2.1.2 HPTC is designed to be a durable injectable implant

A novel interpenetrating network of HPTC hydrogel has been developed to transform a classically solid uninjectable pHEMA polymeric hydrogel into an injectable material with customizable physical flow properties and moduli to be used for different applications. The initial limitation of design was the chemical components, which need to have a proven safety record in pre-existing medical devices and are FDA-approved for use in medical devices. Next, the goal of the design is to best mimic the natural physical properties of the soft tissues, which are elastic, supple, inert, while ensuring that the material is still in an injectable form for minimally invasive procedures. Since none of the semi-permanent to permanent medical devices for injection on the market are easy to inject in the clinical setting, often facing challenges with clogged needles one of the main goals of designing this p(HEMA) injectable material is to have significant improvement in ease of injection compared to other nonabsorbable/ semi-permanent injectable materials on the market.

We put the emphases on the flow characteristics of these pHEMA-based gels and other physical attributes that make them desirable for use in soft tissues.

pHEMA based polymers and copolymers have been widely used in the medical field as a biocompatible material since its development as a solid biomaterial that was brittle when dry, and soft and compliant when wet, initially developed for use as soft contact lenses by Wichterle and Lim in 1960 [7]. pHEMA based hydrogels have been widely researched for application in the Biomedical field in the past 5 decades, ranging from intraocular lenses [8], keratoprosthesis or artificial cornea [9-13], experimental breast implants in the 60s [14], membrane for artificial liver [15-18], interface for biosensors [19-21] to scaffolding material for tissue engineering, such as biomaterial to repair spinal cord injury [22].

Despite the wide use of HEMA in the biomedical field, having HEMA as a building block as an injectable material has been very limited. The only applications of pHEMA as an injectable material has been limited to (1) fabricating them into nanoparticles so they could pass through syringes, such as those for drug delivery purposes [23], (2) conjugating pHEMA with Poly (N-isoproylacrylamide) or PNIPA, which is a temperature-responsive polymer that when heated in water above 32 °C , it goes through phase-transition from a swollen hydrated state to a shrunken dehydrated state, making it a great candidate for controlled release drug delivery applications [24-25] or 3D-cell-culture [4], (3) conjugating chitosan with HEMA as a controlled drug release vehicle, in which the assembly of the hydrogel network is driven by ionic interactions between cations and chitosan [3]. All of these methods involve making either very small particle sizes of the polymer, or small molecular structure with HEMA as a component with another class of chemical that induces the capability of gelling in situ once the smaller components leave the syringe and needle. In this study, we describe the a novel method of introducing HEMA as a pre-polymerized polymer network before it is being injected rather than fabricating them into microspheres, or leaving them as pre-polymerized monomers before

injection and polymerizing the monomers post-injection, which could have many of its own problems in controlling the polymerization environment to achieve consistent results, leakage, and side effects of unreacted monomers exposed to the patients.

The aim for this chapter is to fabricate a range of injectable HPTC hydrogels that fall within the desirable range of mechanical characteristics as a soft implant material for different medical applications, and is can last more than 6 months. The characterization of the parameters that affect the injectable force and viscoelasticity are presented.

2.2 MATERIALS AND METHODS

2.2.1 Materials

2-Hydroxyethyl methacrylate (HEMA) containing ≤250 ppm monomethyl ether hydroquinone as inhibitor (product number 128635), Triethylene glycol dimethacrylate (TEGDMA) containing 80-120ppm MEHQ inhibitor (product no. 261548), Carboxymethyl cellulose (CMC) at M.W. 90000, 250000, and 700000 (product numbers 419273, 419311, 419338), 1-vinyl-2-pyrrolidinone (product no. V3409) were purchased from Sigma (St. Louis, MO). Polyethylene glycol-200-monomethylether monomethacrylate (PEGMA) containing 100ppm MEHQ and 300ppm BHT (product no. 16664) De-Hibit 200 (product no. 24013) were purchased from Polysciences (Warrington, PA). 2,2-dimethoxy-2-phenyl-acetophenone or Irgacure® 651 (Ciba® , I651) photoinitiator was purchased from BASF (Florham Park, NJ). All syringes were purchased from Becton Dickinson (Franklin Lakes, NJ). 3-Way stopcock with swivel male luer lock (product no. MX5311L) were purchased from Smiths Medical (Brisbane,

Australia). Human foreskin fibroblast cell line HFF-1 (product no. SCRC-1041) and macrophage cell line J774A macrophages (ATCC-TIB-67) was purchased from ATCC® (Manassas, VA).

2.2.2 Preparation of the materials

Inihibitors, namely hydroquinone in HEMA and MEHQ in TEGDMA were removed by passing the HEMA, PEGMA, and TEGDMA in separate columns containing activated De-hibit-200 beads (according to the technical data sheet) at flow rate lower than 4 bed volumes per hour twice, and saved for immediate use. De-hibit-200 columns were used no more than 20 bed volumes before a regeneration wash with a backflow of 2.5 bed volumes of methanol takes place for 1 hour, well under the recommended 170 bed volumes capacity for 100ppm inhibitor, or the equivalent of 56 times for 300ppm inhibitor concentration.

Carboxymethycellulose at either MW 90,000 g/mol, 250,000 g/mol or 700,000g/mol were dissolved in ultrapure water with mechanical mixing, and left to fully dissolve for at least 24 hours.

2.2.3 Fabrication of interpenetrating network of CMC and HEMA

2.2.3.2 Photoinitiated radical polymerization method

Inhibitor-removed HEMA, PEGMA, TEGDMA and 0.1% volume of 1% wt Irgacure 651 dissolved in 2-pyrrolidinone were mixed, and then added to the carboxymethylcellulose slurry, followed by vigorous mechanical mixing. The slurries are then loaded into a Luer lock syringe, connected to a 3 way stop cock with an empty syringe connected to one of the remaining valves. The trapped air layer is purged 3 times with Argon gas, before being carefully pushed out of the release valve on the stopcock. The slurries are mixed well by pushing the mixtures back and

forth between the empty syringe and the loaded syringe through the narrow passageway of the stopcock, and the mixing continued for an extra few minutes after the mixtures appear visibly homogenously mixed. The homogeneous slurry is then immediately loaded into polypropylene or polycarbonate syringes with Luer lock. Slurries of monomers are subjected to photoinitiation of free radical polymerization directly on a UV Transilluminator (UVP High-Performance UV Transilluminator) at 302nm with 25-Watt tubes for 20 minutes, alternating the surface of which the UV is exposed to every 5 minutes. Polymerized polymers are stored for characterization or in other experiments.

2.2.3.2 Heat-activated radical polymerization method

Inhibitor-removed HEMA, PEGMA, TEGDMA and 0.01% of Azobisisobutyronitrile (AIBN) were mixed with the CMC slurry as described above. The handling method is identical as above except for the polymerization process. Instead of using photo activation with UV, heat was applied to initiate the radical formation of AIBN with temperature regulated water baths at 50°C, 60° or 70° degrees, for 4 hours, 1 hour, and 20 minutes respectively.

2.2.4 Preparation of HPTC with different compositions

To make it feasible to fine tune the mechanical properties of the range of injectable materials for specific applications that have slightly different requirements, such as flow property and needle size compatibility, here we investigate the various composition of pre-polymerization mixtures to gain insight on the contribution of mechanical characteristics by each component. For example, if a product for filling fine lines is required, a material with a lower elastic modulus and higher tan delta that shear thins to flow through a finer gauge needle might have more desirable

mechanical properties for that particular application. On the contrary, if a product is meant for coapting the anal canal and injected through a wider gauge needle, a product with higher elastic modulus that coapts the lumen better that can remain intact in the injection site without excessive leaking from the high pressure of defecation would be more desirable.

The variables of the composition can be found in Table 1. They are namely:

(1) percentage of water;

(2) molecular weight of CMC (90k, 250k or 700k);

(3) concentration of CMC;

(4) for the precursors, which include the monomers and crosslinkers, is prepared in the stated percentages in Table 1. The mole ratio between HEMA and PEGMA is kept constant throughout the study. For the sake of simplicity, we will refer to these monomer composition solely by the TEGDMA percentages for the rest of this thesis, which are rounded up to **0%, 4.6%, 12.6%, 19.3% and 32.4% TEGDMA**, while in reality the HEMA and PEGMA concentrations vary as listed accordingly.

In a subset of experiments, Tetraethylene glycol (TEG) was used as a control for the effect TEGDMA as it has an identical backbone as TEGDMA, and the only difference is that it does not have the methacrylate group to participate in polymerization. The mole percentages of TEG used in these experiments are the same as the TEGDMA mole percentages above. 150 different samples were made, and only a fraction of them fall within the desirable range of mechanical properties as a material for soft tissue augmentation.

2.2.5 Qualitative injectability test on small intestines in rats

To assess the injectability and ease of control of injection, a target of 0.1 ml of HPTC is being injected to the submucosal layer of a freshly harvested rat small intestine with a 25G and 21G needle from 1mL syringes to evaluate the ease of priming of the needle, ease of injection, control of material placement, control of volume, ease of control of flow, and integrity of HPTC at the injection site once the needle is retracted, based on how well the sample stays at the injection site without leaking out, and whether the borders are distinct. These qualitative evaluation was rated on a scale of 1 to 5, with 1 being difficult inject or bad at staying intact in the tissue, and 5 being very easy to inject and stays well in the tissue. Each of these test started at the syringe fill volume of 0.5mL, primed with 0.1mL of HPTC, and a targeted 0.1mL is injected. Injection was performed in duplicate syringes fitted with 21G and 25G needles.

2.2.6 Quantitative Injectability assay with Instron mechanical testing

The Instron 5564 model with Bluehill Software was used for all the Instron mechanical testing experiments. We recorded the force required to compress the plunger of the syringe down at real time, at a constant rate of 5.00mm/min. All samples are loaded into 1 ml syringes and filled at the 0.30 ml mark. Half inch blunt end luer lock 21G needles were fitted on the syringes and all needles are primed with HPTC, until the plunger aligns with the 0.20ml mark prior to making contact with the Instron compressor to ensure uniformity for comparison. Syringes with primed needles were positioned on a rigid fitted stand to hold the syringe in a vertical position with the needle pointing downwards, with a 3 cm gap between the needle tip and the bottom surface, ensuring that the accumulated sample leaving the needle do not contribute to the reading for the compression test. The compression surface was a flat rigid surface larger than the plunger's surface area on the syringe, and the compressor pushes the

plunger downward motion with a constant velocity of 5.00mm/min. The end of test was assigned to be 5mm compression.

To compare the ease of injection with HPTC compared to the commercially available products on the market, the HPTC sample that has the most desirable properties was also compared to two existing FDA-approved semi-permanent/ permanent injectable medical devices for soft tissues, Coaptite® and Macroplastique®. In this set of Instron mechanical testing, a long 21G Sidekick® needle, same as the ones used with Coaptite in the clinical settings, is used. The Sidekick® rigid needle (product no. M0068903040, Boston Scientific, Marlborough, MA) has a needle length of 14.6 inches (370mm), 18.5G (1.2 inner diameter) cannula for 14.1 inches of the length, and has tapered to a smaller diameter 21G(0.8mm inner diameter) at the tip of the needle (0.5 inch/ 13mm), with a 15° point. A custom made stand that holds the syringe and Sidekick® needle in a vertical position with a 3-inch gap from needle tip to the bottom of the test surface was used. Testing conditions was designed to simulate the problem encountered often in the clinic for Coaptite®, which was when the physician pauses injection and readjust the needle position, the needle would often be reported as clogged up. For this experiment, the plunger of the syringe is compressed down at 2mm increments, with a 1-minute break between each push, for a total of 8 pushes for a total compression of 16mm. Any differences in the responses registered on the Instron were recorded.

2.2.7 **Oscillatory rheologic characterization with Frequency Sweep**

All rheological characterization injectable HPTC were performed on the AR2000 rheometer by TA Instruments (New Castle, DE) outfitted with a solvent trap to prevent drying of the samples, and a temperature controller set at 25°C unless otherwise stated. HPTC samples were

characterized using 20mm diameter parallel plates at 1000μm gap. All samples were loaded between the parallel plates with care to ensure that the entire gap is filled with the sample, and excess material is being scooped off from the sides. DI water is used to fill the solvent trap. Frequency sweep experiments were performed at 1% strain and angular frequency between 0.1 and 100 radians/s (equivalent to 0.01-15.92 Hz) with dynamic oscillations over a period of 750 seconds. A new sample is used for each test and duplicates were tested for all rheological experiments.

2.2.8 Oscillatory shear rheologic studies

Strain sweep experiments were performed with the same equipment and sample loading conditions described in 2.2.7. Samples undergo oscillatory shear from 0% to 500% strain at constant angular frequency of 1Hz over a time period of 480s. Oscillatory stress, G', G", tan delta are recorded for the duration. A fresh sample is used for each test and duplicates were tested.

2.2.9 Dynamic shear rheometry followed by time sweep

To test the effect of uni-directional shearing with constant shear rate on the viscosity of the samples for 10 minutes, and its loss in elastic modulus 10 minutes post-test to allow enough time for the hydrogel to relax, we performed dynamic shear rheometry followed by time sweep experiment immediately. Shear rate is held constant at 1/s with an angular velocity of 0.01rad/s, and the test was performed for 10 minutes while the viscosity is recorded over time. At the end of the dynamic shear rheometry, time sweep experiment is started immediately at 1% strain at 1 rad/s angular frequency. The G', G", and tan delta are measured over the 10 minute duration.

2.2.10 Parameters tested for injection force as rheological testing

We one variable at a time for HPTC, which are:

1. **The effect of water content**, varying from 80% to 90%, with these fixed parameters: 0.125 g/ml 90k CMC, and 12.6% TEGDMA
2. **The effect of the concentration of CMC**, varying from 0 to 0.25g/ml CMC for 90k CMC (or alternatively, varying from 0 to 0.05g/ml 700k CMC) with these fixed parameters: 12.6% TEGDMA and 87.5% water
3. **The effect of the molecular weight of CMC**, varying from 90k, 250k, and 700k CMC for 90k CMC with these fixed parameters: 12.6% TEGDMA and 87.5% water, and 0.05 g/ml CMC concentration. Note that the 0.05g/ml is chosen because the solubility of 700k CMC is saturated at this concentration.
4. **The effect of the TEGDMA percentage**, varying from 0% to 32.4 mol % TEGDMA with these fixed parameters: 87.5% water, and 0.125 g/ml 90k CMC.
5. **The effect of the substituting a "non-participating" negative control for the TEGDMA crosslinker, TEG for TEGDMA**, with these fixed parameters: 87.5% water, and 0.125 g/ml 90k CMC.

2.2.11 Digestion of TEGDMA's PEO backbone by Fenton oxidation

To test the hypothesis that the polymer's HEMA/ PEGMA chain length is shortened with increasing ratio of TEGDMA, we specifically target the –C-C-O- PEO backbone in TEGDMA without affecting existing –C-C- covalent bonds within the pHEMA/PEGMA or CMC chains.

The hypothesis is tested by comparing the injectability of HPTC before and after digesting the polyether bonds by Fenton oxidation, found exclusively in TEGDMA in the components in HPTC. 20mg $FeCl_2 \bullet 4H_2O$ was dissolved in 25ml of H_2O. H_2O_2[26], to create hydroperoxyl radicals.

(1) $Fe^{2+} + H_2O_2 \rightarrow Fe^{3+} + HO\bullet + OH^-$
(2) $Fe^{3+} + H_2O_2 \rightarrow Fe^{2+} + HOO\bullet + H^+$

The solution is added slowly to HPTC samples prepared in 1mL syringes, with the plunger removed temporarily, and the digestion was allowed to take place for 2 hours. A 2mm diameter hole is then drilled on the wall of the syringe at the level at which the HPTC gels remains, and the plunger is returned back into the syringe, and trapped air is allowed to escape through the drilled hole. Post-Fenton oxidation digest Instron analysis of the injectability of the HPTC is then tested.

2.3 RESULTS

2.3.1 A novel injectable HEMA-based hydrogel, HPTC, was developed

An interpenetrating network of HEMA, PEGMA, TEGDMA and CMC has been developed to be injectable through 21 and 25G needles, with components that are already approved by other FDA devices, with the chemical structure of each of the component shown in figure 1. Stepwise interpenetrating network was formed by dissolving large molecular weight CMC with different percentages of HEMA, PEGMA, and TEGDMA together with 0.01% of photoinitator Irgacure 651 in water, followed by photoinitiation by free radical polymerization with UV for 20 minutes. As the monomers and crosslinkers find their way to polymerize with

one another randomly around the long CMC chains, a homogeneous interpenetrating network with chain entanglement is formed.

The results of two polymerization methods, UV-initiated free radical polymerization using Irgacure 651®, and heat-activated free radical polymerization with AIBN are compared. UV-initiation results in more consistent results with a 100% success rate, while heat-activated polymerization resulted in inconsistent success, at an average of about 75% for the 70°C polymerization condition, and below 50% success rate for the lower temperature with longer polymerization periods. Even when the gels are formed, marbling appearance of the gel with bands of translucent material swirling between layers of white, opaque layers of gel is observed occasionally, suggesting inhomogeneous polymerization. In contrary, UV-initiated polymerization yields hydrogels that are homogeneous in appearance. After attempts at troubleshooting, we have abandoned using the heat polymerization method and only used UV-initiation as the only method of sample fabrication for this study. It is quick, results in homogeneous hydrogels, and provided very consistent success rate.

2.3.2 Characteristics of different HPTC compositions and qualitative injectability test on rat intestine

All 150 variations of HPTC have been tested for injectability using rat intestines as a sample soft tissue. Injectability was assessed based on ease of initiation of the injection, control of volume, whether the injected material stays in the injected site or partially leaks out from the puncture point, and presence of a distinct outline (Figure 3). Only a fraction of the HPTC made was injectable. Among them, only a minority of the gels has the desirable characteristics as an injectable material. Based on the observations, we roughly narrowed down the boundaries by

which the HPTC components must have in order to be injectable. We then tested the range of parameters that seemed to affect the injectability of HPTC in the following sections by changing one variable at a time.

2.3.3 The effects of water content in HPTC on the injectability and viscoelastic properties

Despite the fact that HPTC is a highly porous hydrogel that consists of mostly water, the percentage of water the gel contains greatly affects its injectability, and only a narrow range of water percentage under other optimal conditions can produce an injectable hydrogel with desirable characteristics. We tested the force of injection and viscoelastic properties of HPTC between 80-90% water in this experiment.

Force of injection

Increasing water content of HPTC from 80% to 85% (while the other components of HPTC are kept under optimal composition) significantly lowers the force of injection (Figure 5a). At 80% water, HPTC is uninjectable, requiring a force of 90.0±16.4 N to inject through a ½" 21G needle, as determined by Instron mechanical testing. For easily injectable materials, the force of injection is ≤ 20N. When the water content is raised to the 85-90% range, the force required for injection drop to 14.5±2.4, 13.0±0.4, and 13.6± 2.8 N for 85%, 87.5% and 90% water respectively, which are all easy for hand-held injection without mechanical assistance. Within the 85% -90% range, the increase in water content does not further decrease the injection force, with p-values all above 0.05, which suggests that once the threshold water % between 80 and 85% is met, the injectability of HPTC remains similar between 85-90%.

Rheology

Further investigation of the water content on the viscoelastic properties of HPTC was performed on 82.5% and 87.5% water content with rheological testing (Figure 5b), which is around the region that has the drop in injection force. The oscillatory stress during strain sweep (at 1% strain) seems decreased slightly with increased water content from 12.6±1.5 Pa to 8.6±0.8 Pa but the difference is not statistically significant, with a p-value of 0.077.

During frequency sweep at 1Hz frequency, both the elastic modulus G' and loss (or viscous) modulus G" seem to decrease slightly when the water content is increased, from G' of 877±59 N to 652±24 N, and G" of 797±59 N to 642±21 N, at 82.5% water and 87.5% water respectively, but the difference is not statistically significant, with p-values of 0.052 and 0.11 respectively. The tan delta, an equivalent of G"/ G', is used as a measure of readiness to flow. As the viscous modulus to elastic modulus ratio increases, tan delta increases, and it indicates that the flow modulus approaches or exceeds the elastic modulus in response to shear-thinning. The tan delta of 87.5% water, 0.98±0.00, is significantly higher than that of the 82.5% water, 0.91± 0.01, with p-value of 0.022. A schematic summarizing the effect of water content is shown in Figure 8.

2.3.4 **The effects of the concentration of CMC in HPTC on injectability and viscoelastic properties**

Carboxymethyl Cellulose is a crucial component in making HPTC an injectable hydrogel. When the concentration of CMC is below a certain minimum threshold value, HPTC is uninjectable, on the other hand, when the CMC concentration keep increasing above the optimal range, CMC injectability decreases again.

Force of injection

In the absence of CMC, or if the concentration is too low, In figure 9a, Instron injectability assay of 90k CMC shows that the force of injection decreases dramatically from 46.1±6.5 N, 42.3±2.3 N, 41.4±2.8 N and 37.6±0.9 N for 0.000, 0.0001, 0.001 and 0.01 g/ml respectively, to 2.2±0.1 N, 3.2±1.3 N, 7.3±0.2 N, 13.3±0.5 N, and 19.3±1.1 N for CMC concentrations 0.01, 0.05, 0.075, 0.100, 0.125 and 0.150 respectively. A note about the injection force below the threshold CMC concentration is that the forces are likely underestimated in those samples in the Instron injectability test. In those particular cases, the gels would at first seem injectable, but if the injected material is examined closely, the extruded volume being pushed out of the hydrogel was only water, leaving a more dense polymer network in the syringe. Since the gels were made at 87.5% water, even though all the needles were primed prior to the injectability test, a high percentage of water is left in these samples to be further compressed out. If the polymer network does not flow together with the water being pushed out, the injectability would be underestimated during the test.

Rheology

During strain sweep, the oscillatory stress at 1% strain (figure 9c) is by far the highest when there is no CMC, at 1114±189 Pa. As little as 0.01g/ml 90k CMC brings the oscillatory stress about 11 times lower to 97±39 Pa. The oscillatory stress appears the lowest at 0.125 g/ml CMC, at 8.6±0.8 Pa, and increases again at 0.25g/ml CMC, at 81±22 Pa, which is a similar trend observed in the Instron injectability assay. When the percentage strain increases from 1% to

10% (figure 9d), the oscillatory stress increases 6 to 10 times the value, at 8601±1629, 546±1143, 83.8±9.6, and 791±218 Pa for 0, 0.01, 0.125 and0.25 g/mL 90k CMC respectively.

During frequency sweep at 1Hz, both the G' and G" are at least 12 times higher in the absence of CMC than any other sample with CMC tested, showing a similar trend as the oscillatory stress graph in Figure 9c. The moduli are the lowest at 0.125 g/ml CMC at G' 652±24 Pa and G" 642±21 Pa, which are at least 10 times lower than those of the other samples tested, with G' in the range of 7340 to 105240 Pa, and G" between 3114 and 23598 Pa. Tan delta peaks at 1.0 with CMC concentration of 0.125g/ml. It is significantly higher than the tan delta for 0, 0.01, and 0.25g/ml CMC, with p-values of 0.00035, 0.045, and 0.0025 respectively, suggesting that this concentration has the highest readiness to flow under shear stress.

2.3.5 **The effects of the molecular weight of CMC in HPTC on injectability and viscoelastic properties**

Force of injection

Increasing the molecular weight of CMC increases the force of injection of HPTC through a 21G needle, as measured by the Instron injectability assay (Figure 13a). The injection forces of HPTC made with 0.125g/ml 90k, 250k and 700k CMC are 3.4±0.5 N, 4.8±0.4 N, and 7.1±0.3 N respectively, all of which are within the injectable range.

Rheology

Increasing molecular weight of HPTC increases the oscillatory stress during strain sweep at 1% strain, at 0.5Pa, 2.7Pa to 12.7Pa for 90k, 250k, and 700k CMC respectively (Figure 13b). Increasing the molecular weight of CMC also increases both the elastic modulus G' and viscous

modulus G", but dramatically decreases the tan delta during the frequency sweep, from 2.87±0.27, 0.8±0.01, 0.37±0.01 for 90k, 250k, and 700k CMC respectively, indicating lower degree of shear-thinning and more resistance to flow (Figures 14a and b). During the steady rate sweep experiment where the sample is constantly sheared for 10 minutes, we observed that the viscosity increases dramatically as the MW of CMC increases. At 30 seconds of shearing, the viscosities with the three MW are significantly different from each other, at 5.12±0.81, 199.8±16.3 and 905±7.35 Pa•s for 90k, 250k and 700k CMC respectively and p-values of 0.0035 and 0.0032. Over the 10-minute constant shearing, the viscosity for the 90k CMC did not change significantly, to 5.97±4.75 Pa•s with p-value of 0.79. However, there is a significant drop in viscosity over 10 minutes for 250k and 700k CMC. At 10 minutes of constant shearing, the viscosity for the 250k CMC dropped to 148.5±5.2 with p-value 0.051, and the viscosity for the 700k CMC dropped significantly to 492.8±18.4 Pa•s with the p-value of 0.0011. Lastly, there is no significant difference in the G' loss in all three MW tested ($p>0.05$), which is between 69% and 82%.

2.3.6 The effects of the TEGDMA percentage in HPTC on injectability and viscoelastic properties

Force of injection

The force of injection first drops dramatically from 21.3±0.4 N to 8.0±1.8 N when TEGDMA mol % is increased from 0% to 4.6% ($p = 0.005$). It then increases significantly to 13.2±0.5 N at 14.6% TEGDMA ($p = 0.02$), drops down slightly to 10.4±1.14 N ($p = 0.06$), before it rises back to 14.6±0.0N at 32.4% TEGDMA ($p = 0.008$). The only sample that is not easy to inject within the range of TEGDMA % tested (0% - 32.4%) is 0% TEGDMA, as its

required force of injection is above 20N, the level below which is easy to perform hand-held injection.

Rheology

During the strain sweep test, the oscillatory stress were similar across all samples at 1% strain, but as the strain increases to 10%, there is a significant difference in the oscillatory stress between 0% TEGDMA and all the other samples with 4.6-32.4% TEGDMA. This suggests that 0% TEGDMA is not optimal for injection, while 4.6-32.4% TEGDMA have lower stress and therefore likely to be easier to inject.

During the frequency sweep at 1Hz, the G' and G" are not significantly different across all the samples except for the G' with 0% TEGDMA, which is significantly higher than the rest of the samples (all $p < 0.05$). The tan delta from the same test shows the lowest flow property when there is no TEGDMA at 0.67±0.00, and highest at 0.97±0.01 and 0.98±0.00 when TEGDMA is 4.6% and 12.6% respectively (both $p<0.05$ compared to tan delta at 0% TEGDMA). The tan delta then drops to 0.89±0.03 and 0.91±0.04 at 19.3% and 32.4% TEGDMA.

During the 10-minute steady rate sweep with dynamic shearing, the initial viscosity (at 30 seconds) is the highest with no TEGDMA at 872±56 Pa.s, which is significantly higher than those viscosities for 4.6%, 12.6% ad 19.3% TEGDMA at 490±21, 573±62, 616±16 Pa.s respectively, with all p-values < 0.05. The viscosity increases gradually from 490±21 Pa.s at 4.6% to 712±54 Pa.s at 32.4% TEGDMA.

There is no difference in the percentage loss in G' before and after the steady rate shear, with between 63% and 69% loss.

2.3.7 The effects of digesting the PEG backbone found specifically in TEGDMA crosslinkers in HPTC by Fenton Oxidation

To test the hypothesis that the polymer chains are shorter with higher degree of branching in the higher TEGDMA mol % sample (32.4%) compared to the lower TEGDMA % sample, we used Fenton reaction to specifically digest the –C-C-O- backbone found only in TEGDMA within HPTC after polymerization. We used Instron injectability assay to assess the relative ease of injection, which is affected by the polymeric chain length and entanglement.

Force of injection

The force of injection first drops dramatically from 21.3±0.4 N to 8.0±1.8 N when TEGDMA mol % is increased from 0% to 4.6% ($p = 0.005$). It then increases significantly to 13.2±0.5 N at 14.6% TEGDMA ($p = 0.02$), drops down slightly to 10.4±1.14 N ($p = 0.06$), before it rises back to 14.6±0.0N at 32.4% TEGDMA ($p = 0.008$). The only sample that is not easy to inject within the range of TEGDMA % tested (0% - 32.4%) is 0% TEGDMA, as its required force of injection is above 20N, the level below which is easy to perform hand-held injection.

2.3.8 The effects of the replacing 12.6% TEGDMA with a non-polymerizing control, Tetraethylene Glycol, TEG

To test the hypothesis that the improvement in injectability in the presence of TEGDMA is not due to an eluent effect or lubricating effect of TEGDMA, we substituted TEGDMA with TEG, which has the identical tetraethylene glycol backbone, but instead of having methacrylate end

groups available for polymerization, they are alcohol groups instead. TEGDMA participates in the polymerization with the HEMA/ PEGMA network, while TEG does not.

Force of injection

The force of injection between the TEGDMA (13.2±0.4 N) and TEG (12.2±0.5N) are not different from each other, with p-value of 0.68 (Figure 21a).

Rheology

During the strain sweep test, the oscillatory stress seems to increase slightly when TEGDMA is substituted with TEG, at 8.6±0.8 Pa and 12.1±_0.9 Pa with a p-value of 0.057, which is not statistically significant (Figure 21b).

During the frequency sweep at 1Hz, the G' and G" both increase significantly when TEGDMA is replaced by TEG. G' increased from 652.4±8.6 Pa to 900.8±19.5 Pa ($p = 0.0002$*), and G" increased from 642.0±20.7 Pa to 796.7±12.5 Pa ($p = 0.045$*). The tan delta from the same test shows a significant decrease in Tan delta when TEGDMA is replaced by TEG, from 0.98±0.00 to 0.91± 0.00($p = 0.003$*).

During the 10-minute steady rate sweep with dynamic shearing (Figure 21c), the viscosity did not change significantly when TEGDMA is replaced by TEG, at 574± 62 Pa.s and 711±103 Pa.s ($p = 0.25$), and viscosity at 600 seconds at 411±38 and 508±13 respectively ($p = 0.07$).

There is no difference in the percentage loss in G' with the replacement of TEGDMA by TEG (Figure 21d), with between 63% and 85% G' loss ($p = 0.37$). The schematic of the TEGDMA replacement by TEG is shown in Figure 23.

2.3.9 The effects of the replacing TEGDMA with a non-polymerizing control, Tetraethylene Glycol, TEG over the range of 0 – 32.4%

Rheology

During the frequency sweep at 1Hz (Figure 24a), tan delta increases steadily with increasing TEG concentration, from 0.67±0.00 at 0% TEG, to 0.80±0.04, 0.87±0.00, 0.87±0.01, 0.93±0.01 for 4.6%, 12.6%, 19.3% and 32.4% TEG respectively. For TEGDMA, tan delta initially increases, from 0.67±0.00 at 0% TEGDMA, to 0.97±0.01, 0.98±0.00 for 4.6% and 12.6% respectively, and it decreases to 0.89±0.03 and 0.91±0.04 at 19.3% and 32.4% respectively. There is a significant difference between the tan delta at low percentage (4.6% and 12.6%) TEG vs. TEGDMA

TEGDMA's tan delta is significantly higher than TEG's at low percentage (4.6% and 12.6%), with p-value of 0.033 and 0.0031 respectively. However when the percentage is raised to 19.3% and 32.4%, there is no statistical difference between the tan delta of TEGDMA and TEG, with p-values of 0.49 and 0.57 respectively.

The oscillatory stress at 1% strain (Figure 24b) for TEG shows a general decreasing trend with increasing TEG concentration, from 13.22±1.71 Pa at 0% TEG, to 14.12±1.04 Pa, 12.13±0.93 Pa, 8.99±0.53 Pa, and 7.70±0.12 Pa respectively. However, for TEGDMA, the oscillatory stress initially decreases from 13.22±1.71 Pa at 0% TEGDMA to 8.53±0.95 Pa and 8.62±0.82 Pa at 4.6% and 12.6% TEGDMA, and increased to 13.64±8.54 Pa and 9.43±0.45 Pa at 19.3% and 32.4% TEGDMA respectively. The p-values for the difference between TEG and TEGDMA are 0.085, 0.057, 0.52 and 0.035 at 4.6%, 12.6%, 19.3% and 32.4% respectively.

2.3.10 Passage of HPTC through a 21G needle does not significantly affect its viscoelastic properties

To test whether passing HPTC through a 21G needle has any effects on its viscoelastic properties, which could give us valuable insights as to whether HPTC injected into the soft tissue would have similar properties as before the material leaves the syringe, we put samples of HPTC before and after the 21G needle extrusion through the test on the rheometer.

Rheology

During the strain sweep test, the oscillatory stress did not change, at 8.62± 0.82 Pa and 7.63 ± 0.62 respectively ($p = 0.90$) (Figure 26a).

During the frequency sweep at 1Hz (Figure 26b), the G' and G" have no significant difference after passing through the 21G needle, from G' 652.4± 2.05 Pa to 507.9±2.05 Pa, and G" of 642.0± 20.7 Pa to 549.1± 0.9 Pa ($p = 0.003$*).

During the 10-minute steady rate sweep with dynamic shearing (Figure 26d), the viscosity did not change significantly after passing HPTC through the needle, at 574.0± 62.2 Pa.s and 420.1±47.0 Pa.s ($p = 0.16$), and viscosity at 600 seconds at 411.4± 37.9 Pa.s and 375.6± 41.4 Pa.s respectively ($p = 0.30$).

There is no difference in the percentage loss in G' with the passage of HPTC through a 21G needle (Figure 26e) with % G' loss at 64.6% and 65.2% ($p = 0.22$).

2.3.11 HPTC's injectability surpasses those of Coaptite® and Macroplastique® by Instron mechanical testing

HPTC's injectability is compared against the two FDA-approved semi-permanent to permanent injectable implants on the market, Coaptite® and Macroplastique®.
In the first test, HPTC shows better injectability through short ½ inch 21G needle compared to Macroplastique® during the initiation of the flow post-needle-priming, with the force of injection at 18N for HPTC, compared to 47N for Macroplastique®. When HPTC is compared to Coaptite®, their force of injection during initiation are similar, at 12N and 18N respectively (Figure 4a). However, as time passes, the force required to inject Coaptite® drastically increased to 48N at 20 minutes and then 187N at 30 minutes, while the force of injection remained low for HPTC, at 15N at 20 minutes and 10N at 30 minutes.

In the second experiment, we examined the needle clogging aspect observed in the Coaptite further, with more closely simulated conditions at which the clogging phenomenon was observed in the clinic. We use the 14.6" 21G Sidekick® needle, which is the needle that comes with the Coaptite® product to be used in the procedure rooms, for the Instron injectability assay. We simulated the trigger for needle clogging, by simply pausing injection for 60 second-periods of time between each 2mm compression (over a period of 30 seconds) of the plunger of the syringe. Figure 4b showed that HPTC's force of injection remained relatively unchanged through a cycle of 2 pauses from time 0s to 180s, between 40-50N, while the Coaptite®'s force of injection started at about 60N, and increased to 90N, which is very difficult to be inject by hand, after a single 1-minute pause. It then further elevated to over 180N after an additional 1-minute pauses. This further elucidates the superior injectability of HPTC compared to Coaptite, as it has a longer working time and allow the physicians to have the time it needs to reposition the needle before it gets clogged up.

2.4 DISCUSSION

In this study, we present a novel approach of fabricating an injectable form of pHEMA hydrogel. To the best of our knowledge, the only other way to produce a non-degradable but injectable hydrogel with pHEMA is by fabricating them into microbeads [27]. This study presents an alternative way of making injectable pHEMA-based hydrogel that is not easily biodegradable. The method is to mix precursors of HEMA, PEGDMA, TEGDMA, CMC and water together to create an interpenetrating network of HPTC by free radical polymerization using UV photo-initiation, where the HEMA, PEGMA and TEGDMA polymerize around the preexisting strands of CMC, to form an intertwined, entangled network. The resulting gel is resistant to degradation, injectable through 21G and 25G needles if fabricated under the right conditions.

We have gathered evidence to support that the viscoelastic property and injectability of HPTC is governed by (1) the structural scaffolding at the pre-polymerization stage provided by the pre-existing CMC, (2) the proximity of monomers and crosslinkers to each other demonstrated by variable water content; (3) the percentage of crosslinkers in the precursor volume, (4) the chain length of the CMC. A delicate balance of these factors must be achieved in order to obtain a range of desirable properties of HPTC.

First, the effect of water in HPTC's viscoelastic properties and injectability was studied. As illustrated in Figure 8, when the water percentage is increased, there is a lower likelihood for the precursors (monomers and crosslinkers) to react with each other, and shorter polymer chains are expected. We observed that when water percentage is increased, tan delta increases, and oscillatory stress decreases, which lead to easier injectability.

Second, we studied the effect of the polymerization hindrance by varying the concentration of CMC. CMC is a crucial component that must be added to HPTC pre-polymerization order to make it injectable. As illustrated in Figure 12, when there is 0 g/ml CMC, or if the CMC concentration falls below the minimum threshold, HPTC has huge injection force, oscillatory stress, and viscosity, as well as low tan delta, all of which indicate poor injectability. As the concentration of CMC moves towards the optimum range, the injection force, oscillatory stress decrease, making HPTC more injectable. On the contrary, having too much CMC has a detrimental effect on injectability. Decreasing it from a high concentration down to the optimal range decreases injection force, oscillatory stress and viscosity, while increasing the tan delta, making HPTC more injectable. The hypothesis is that the presence CMC acts as a steric hindrance for polymerization. In the absence of CMC, there is a massive growth of the HEMA/PEGMA/TEGDMA network, and it results in an uninjectable as it is too difficult to have high enough flow property to shear thin the polymer network enough to make it flow through the needle. With the optimal concentration of CMC, there is just the right amount of hindrance in the polymerization to result in a desirable combination of optimal chain length of HEMA/PEGMDA/TEGDMA that is entangled with the desirable amount of CMC, to have the desirable viscoelastic properties as a desirable injectable material. With too much CMC, the effect of entanglement of CMC chains with the newly formed HEMA/PEGMA/TEGDMA chains becomes too high, and therefore injection is difficult.

Third, the molecular weight of CMC contributes to the injectability as well. We tested 3 molecular weights of CMC in this study, 90k (short), 250k (medium), and 700k (long), as illustrated in Figure 12. Injection force, oscillatory stress, viscosity and G' loss from shearing all decrease with the length of CMC The tan delta increases with the lower molecular weight,

making the short CMC the most desirable injectable out of the 3 molecular weights tested. We expect the HEMA/PEGMA/ TEGDMA chains to have similar lengths among the groups, and we postulate that with short CMC, there is low entanglement. That is evident when we looked at the viscosity during steady rate sweep carefully where the sample is being sheared in one direction over a period of 10 minutes. There is no detectable drop of viscosity over this period for the short CMC, suggesting that there could be considerable slipping of HEMA/PEGMA/TEGDMA chains past these short CMC without physically breaking the chains from the one-directional shearing. On the other hand, with long CMC, we observed very high viscosity along with a dramatic decrease over the 10 minutes shearing, which suggests that entanglements between CMC and HEMA/PEGMA/TEGDMA chains is high, and the shearing could play a role in either untangling or physically breaking the strands, rendering the post-shear HPTC less viscous.

Next, the effect of TEGDMA percentage within the precursor composition was investigated. When TEGDMA percentage is zero, HPTC has high oscillatory stress, G', G" and viscosity, and it also has poor flow property with a low tan delta, and therefore HPTC with no TEGDMA is uninjectable. However, when the TEGDMA % is raised to 4.6-32.4%, the whole range collectively have similarly low oscillatory stress, G' and G", and with similarly high Tan delta, which agrees with the observation that as long as there is some % of TEGDMA between 4.6-32.4% under optimal conditions of the rest of the components, HPTC becomes injectable. The viscosity is the only parameter that shows a trend from low to high viscosity as the TEGDMA% is increased. The observed results could be explained by the balance between the density of branches and the flexibility introduced in the polyethylene portion of the TEGDMA. When there is no TEGDMA, all chains are just linear and stiff, and therefore hard to inject. However, when TEGDMA is present, the chains become shorter, and the density of branches is

higher. It translates to better injectability compared to no TEGDMA because of the added flexibility in the crosslinkers.

To test the hypothesis that the HEMA/PEGMA linear chains are shorter in the high TEGDMA%, we specifically digested the TEGDMA and then determined the force of injection using the Instron injectability assay. Digestion of polyether groups present exclusively in TEGDMA supports the hypothesis that when TEGDMA % is high, the HEMA/PEGMA chains become shorter, because the force of injection for the highest TEGDMA % sample went from being the most difficult to inject, to the easies to inject after the digestion.

To further understand the mechanism by which TEGDMA contributes to the increase in the flow properties of HPTC, a non-polymerization-participating TEGDMA substitute, Tetraethylene glycol, TEG, which has the same tetraethylene backbone as TEGDMA but instead of having polymerizable methacrylates on each end, they are substituted by alcohol groups instead.

When we only compared the TEG substituting TEGDMA at its optimal concentration 12.6%, we found that TEG-substituted HPTC has higher oscillatory stress, G' and G", and a lower tan delta, suggesting that it does not flow as well as TEGDMA. Since TEG is not participating in the polymerization, we postulate that the linear chains of HEMA/ PEGMA will grow slightly longer than the TEGDMA counterpart, because there is no option for chain to branch off during the explosive free radical polymerization but to make linear additions when there is no crosslinker around. 12.6% TEG is thought to result in slightly longer, and stiffer HEMA/PEGMA polymer chains with a complete lack of branching, compared to 12.6% TEGDMA, which has plenty of opportunity for HEMA to collide with a TEGDMA to make branches. In the TEG-substituted HPTC, since there is a lack in the flexible tetraethylene

glycol linker integrated into the polymer network, the flow property decreases, resulting in a poorer injectable compared to the TEGDMA counterpart.

When we take one step further to analyze not only the 12.6% TEGDMA vs. 12.6% TEG, but all the concentrations of TEGDMA tested: 0%, 4.6%, 12.6%, 19.3%, and 32.4% we discovered one more factor that affects the effectiveness of the flexible crosslinkers in making HPTC have better flower properties (high tan delta). It was found that when these crosslinkers are in a high density at higher than 15% TEGDMA %, the effect of entanglement due to the increased number of branch points starts to become detrimental to the overall flow property of HPTC. With more of these branch points, although they are still flexible, it makes HPTC's tan delta decrease instead of increase further. It is further confirmed by analyzing the oscillatory stress of TEGDMA versus TEG: the oscillatory stress is much lower for lower % TEGDMA than it is of TEG, further suggesting that low density flexible branch points improves the flow properties of HPTC. On the contrary, the flexibility effect can be overwhelmed by the sheer number of branches that add resistance to the neighboring chains when it attempts to slip past each other during shearing, as it was seen that the oscillatory stress of TEGDMA increases beyond the TEG counterpart , suggesting high number of branches with shorter chains in TEGDMA flow with higher resistance than the slightly longer linear chains that have no branches but are stiff. The schematic in Figure 25 summarizes that at 4-12.6% TEGDMA, there is lower oscillatory stress in TEGMDA and higher Tan delta in TEGDMA.

Lastly, the viscoelasticity of HPTC before and after passing through a 21G needle was compared. Since the number of samples in each group shown in Figure 26 was 2, the reason why there was no statistical significance in any differences in oscillatory stress, G', G", tan delta, viscosity at 30s and 600s during the steady rate one dimensional shear test, and % G' loss could

be attributed to the small sample size. If the averages are analyzed further disregarding the lack of significant difference, the G' and G" decreased to 75% and 85% of its original value, and Tan delta increased slightly by about 10%, which is not surprising as some of the entanglements would have been pre-sheared once through the needle already. There could have been a drop in viscosity as well, which could again be attributed to the untangling of the chains during the shearing in the needle.

Finally, the 4 major parameters that determine HPTC's injectability and viscoelastic properties are summarized in Figure 27. If the optimal condition on each side of the diagram is met, the HPTC would be within the injectable range. The four major parameters are water content, polymerization hindrance with the CMC concentration, percentage of flexible branching by varying the percentage of TEGDMA, and the chain length of the CMC. The shaded yellow area represents the range of HPTC that is within the desirable range for the purpose of injection. The characteristics can be further customized to suit the particular need of the application. For example, if a runnier consistency is desired for face injection with a finer gauge needle, the viscosity and G' can be decreased by increasing the water content and adjusting the TEGDMA concentration. On the other hand, if a stiffer consistency that has a higher G' and higher viscosity is desired for applications such as fecal incontinence, where it is preferable to have the material stay intact in the injection site despite being exposed to higher pressure, one might do so by increasing the TEGDMA concentration and CMC concentration to achieve such consistency to suit the needs.

For the purpose of treating urinary incontinence in rats, we chose the composition of HPTC to be 87.5% water, 0.125 g/ml of CMC at MW 90k, and 12.6% TEGDMA.

2.5 CONCLUSIONS

A novel injectable hydrogel that is an interpenetrating network resistant to biodegradation, HPTC, was developed in this study. Characterization of the force of injection and viscoelastic properties with rheological tests show that the major parameters in injectability are water content, polymerization hindrance by the CMC concentration, TEGDMA percentage with respect to the other monomers, and the molecular weight of the CMC. The results show that when the optimal range of each of the 4 parameters are met, not only is HPTC injectable, it can also have a range of customizable viscoelastic properties such as oscillatory stress, G', G", tan delta during low and high strain, G', G" and tan delta to different frequency responses, viscosity during shear, and the percentage of permanent loss in G' is resulted from constant stress. HPTC also shows lower force of injection compared to an FDA-approved semi-permanent filler Macroplastique®, as well as much longer working time when compared with Coaptite®. The optimal condition for HPTC for the purpose of rat urethral injection for incontinence is determined as 87.5% water, 0.125g 90k MW CMC, and 12.6 mol % TEGDMA (with 87.5 mol % HEMA and 0.19 mol % PEGMA) based on the desirable viscoelastic properties and its ability to be injected through a 25G needle, which is a requirement for urethral injection in the rat model..

2.6 Table

a

Water %	Precursor %	CMC
80-90%	10-20%	Either 90k, 250k, or 700k within their range

b

Precursor composition 1		
HEMA mol %	PEGDMA mol %	**TEGDMA** mol %
99.78%	0.21%	0%
95.22%	0.21%	4.57%
87.24%	0.19%	12.57%
80.50%	0.17%	19.33%
67.46%	0.15%	32.39%

c

Precursor composition 2		
HEMA mol %	PEGDMA mol %	**TEG** mol %
99.78%	0.21%	0%
95.22%	0.21%	4.57%
87.24%	0.19%	12.57%
80.50%	0.17%	19.33%
67.46%	0.15%	32.39%

d

CMC	Concentration tested
90k CMC	0-0.25 g/ml
250k CMC	0-0.15 g/ml
700k CMC	0-0.05 g/ml

Table 1. Composition of HPTC, and a list of ranges of each component tested for this study. (a) All HPTC hydrogels have some combination of water, precursors, and CMC, with variable amount of each component. One of the precursor combinations listed in b or c is used in each unique HPTC combination, and they are listed in (b) for when TEGDMA crosslinkers are used, or (c) when TEG was used instead of TEGDMA. For the CMC composition, the range of concentrations tested with each molecular weight is listed in (d).

2.7 Figures

a

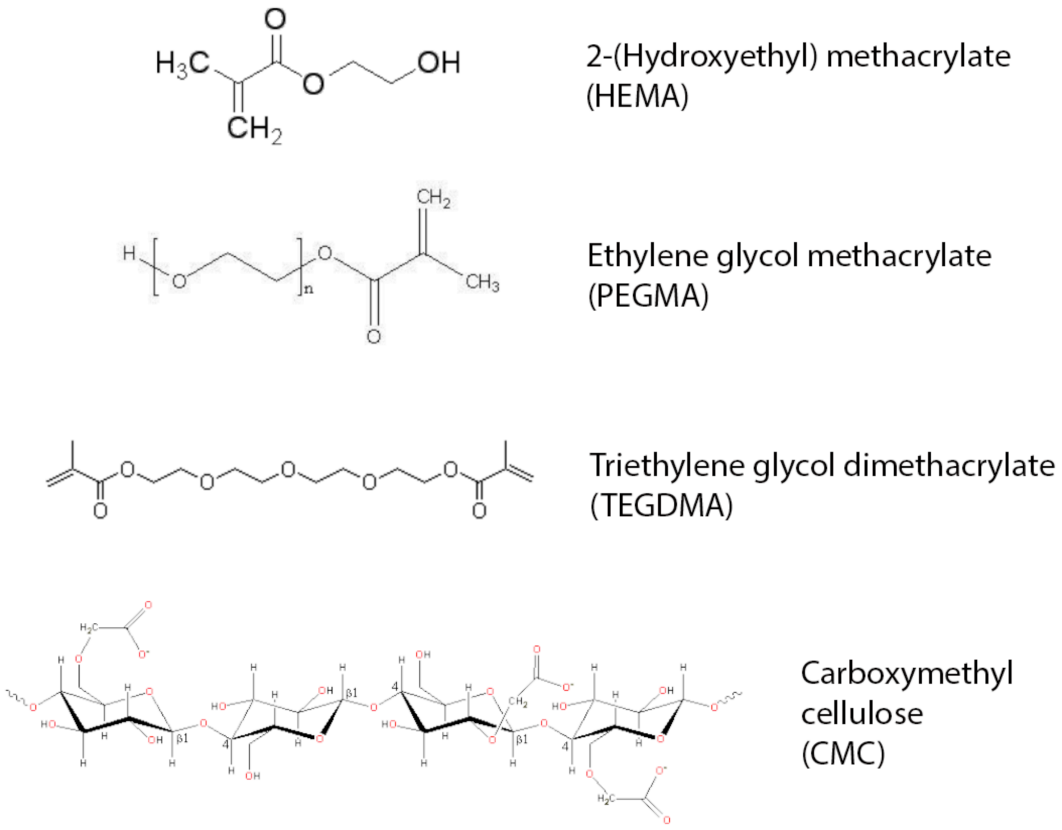

b

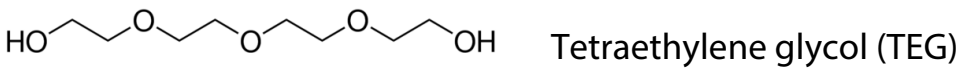

Figure 1. The chemical structures of the major components of the HPTC hydrogel are presented. (a) HEMA, PEGMA, TEGDMA and CMC are the major components of HPTC. These molecules are solubilized in water before photoinitiated free radical polymerization with photoinitiator Irgacure® 651 to form HPTC. (b) TEG is used in place of TEGDMA as a non-participating crosslinker negative control in a set of experiment.

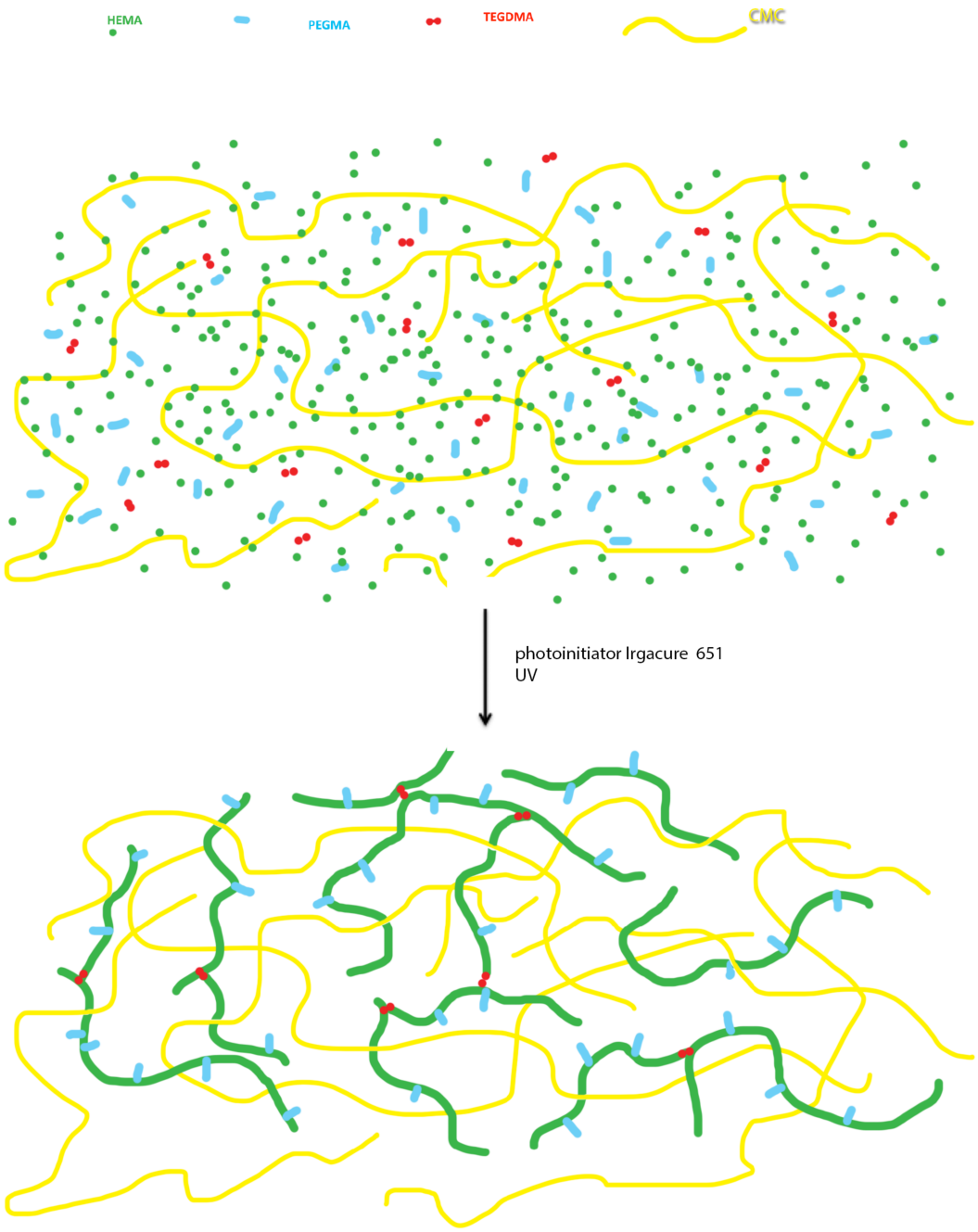

Figure 2. The schematic of photo-polymerization of HEMA, PEGMA, TEGDMA within pre-solubilized CMC. Monomers HEMA and PEGMA are suspended with crosslinker TEGDMA in a homogenous CMC solution along with photoinitiator Irgacure 651. The slurry is well-mixed by passing the mixture through a stop-cock between two interconnecting syringes, and photopolymerization is initiated under airtight conditions.

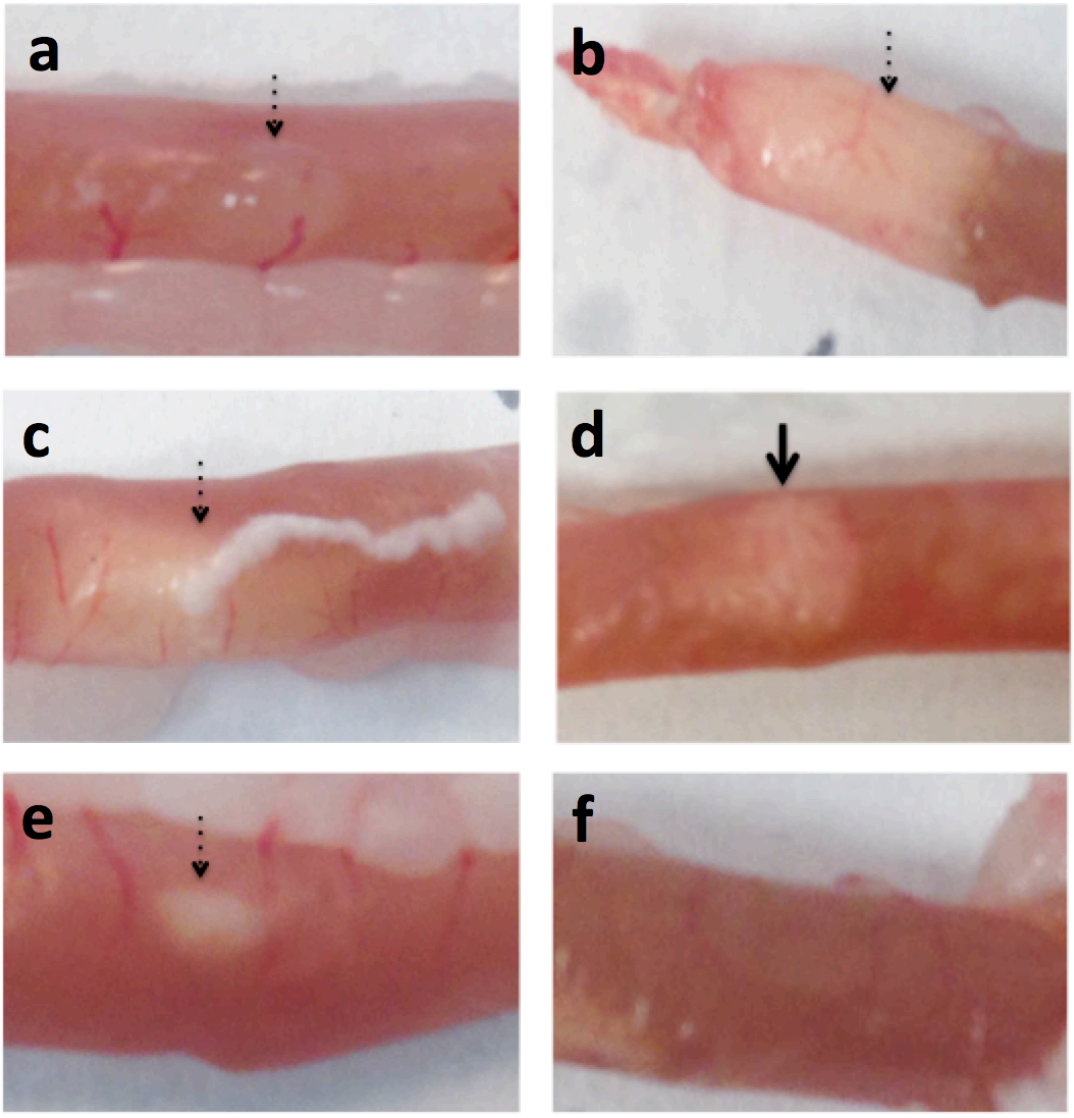

Figure 3. Injection of HPTC onto the walls of rat intestine was performed to screen the ease of injection through 25G needle for each of the 150 samples made. The dashed arrows indicate the undesirable consistency of the HPTC for injection. Injection was difficult when the consistency of the injectable material was too thin or runny under different circumstances: (A) when the polymer stays behind in the syringe while the water in the hydrogel is being pushed out, the injected volume would consist of mostly water, as indicated as a translucent bubble; (B) when the polymer is extremely runny and little resistance was offered during the injection, the volume of injection and the dispersion of the injected volume was difficult to control; (C) when the polymer has high flow modulus to elastic modulus ratio, the HPTC gel leaks out from the needle entry point upon withdrawal of the needle. The solid arrow in D indicates a well-controlled injection with satisfactory resistance and good consistency with a distinct outline of the material once the HPTC is injected into the tissue. When the polymers are too thick, much higher force would be needed to inject HPTC. (E) required at least double the force used in D in order to inject a small volume, though it was injectable. F indicates an uninjectable formulation of HPTC.

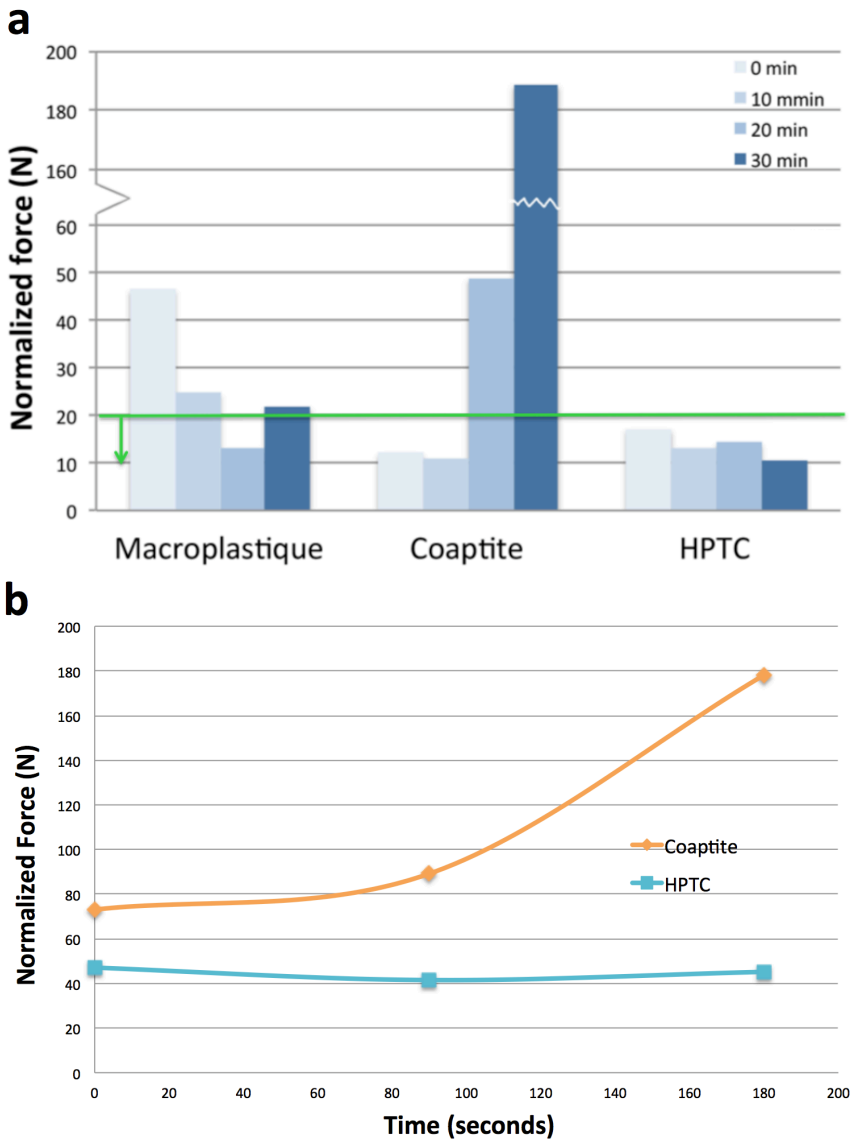

Figure 4. HPTC remains easy to inject over time, while Macroplastique ® and Coaptite ® require significantly higher force to inject. (a) Macroplastique ®, Coaptite ® and HPTC's injectability are compared over a period of 30 minutes with the Instron injectability test, using half inch long 21G blunt needle. Macroplastique had the highest resistance upon initiation at above 40N, but with decreased force of injection after 10 minutes. Coaptite started at a relatively low resistance, but after being exposed for 20 minutes it drastically became more difficult to inject through the short needle, with force required increased to above 45N at 20 min, and above 180N at 30 min. HPTC remains the easiest to inject among all three samples, below 20N force required (hand injectable) to inject throughout the 30-minute test period. (b) Instron injectability assay repeated with the longer, 14.6" 21G Sidekick® needle commonly used in the clinic with Coaptite®, with 1 minute pauses between injection at each trial. HPTC and Coaptite were injected every 90 seconds between data points to simulate the clinical challenge with the injectable materials more closely. HPTC remained relatively easy to inject, while Coaptite became very difficult to inject at around 180N in just 3 minutes, demonstrating the short working time.

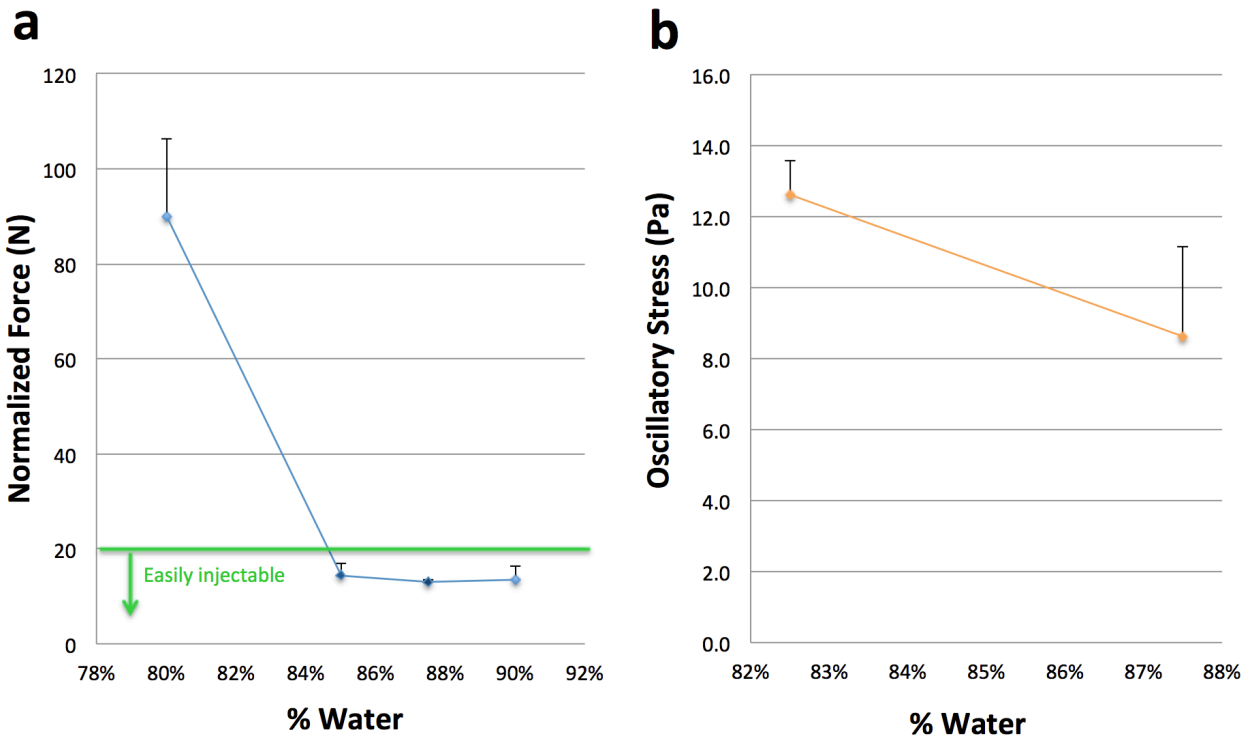

Figure 5. Increasing water content of HPTC increases the ease of injection, as shown by Instron injectability assay (a) and rheological testing under strain sweep (b). (a) The ease of injection dramatically increases when the water content increases from 80% to 85%. HPTC with 3X TEGDMA, 0.15g/ml 90k CMC at different % of water content were subjected to an injectability assay with Instron mechanical testing, through a 21G half inch needle from a 1mL syringe, at the compression rate of 5mm/min. The force recorded was an indicator of the resistance of injection, and it shows that the injectability dramatically improves once the water content goes above 85%, consistent with the qualitative testing of injectability by hand. (b) Rheological study shows a similar trend in the ease of injection increasing with increasing water content in HPTC during strain sweep testing. Shown here is 82.5% water content has higher oscillatory stress compared to 87.5% water content at 1% strain.

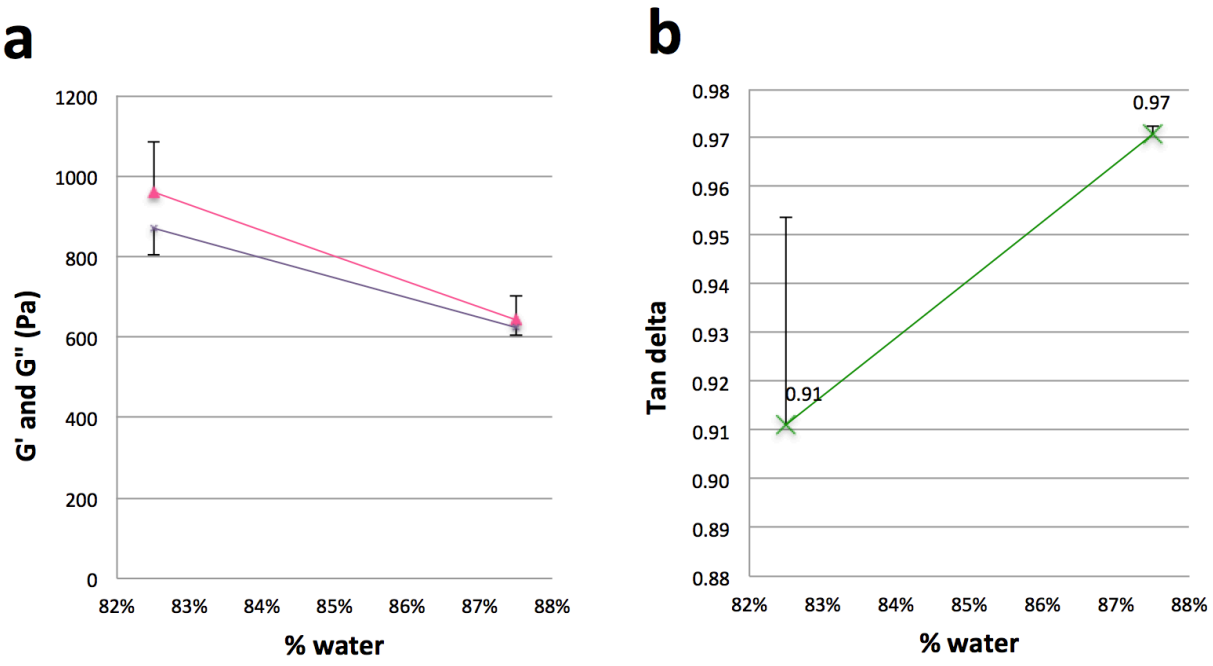

Figure 6. Increasing water content of HPTC does not change the G' and G" significantly, but increases the Tan delta significantly to improve its flow property, as shown by rheological testing under frequency sweep. Both the elastic modulus, G', and the viscous modulus, G" showed a slight decrease with increasing water content from 82.5% to 87.5% (a), but the decreases are statistically insignificant with p-value of 0.052 and 0.11 respectively. (b) tan delta increases significantly from 0.91 to 0.97 with a p-value of 0.022, suggesting a material that has better shear thinning properties at the higher water content.

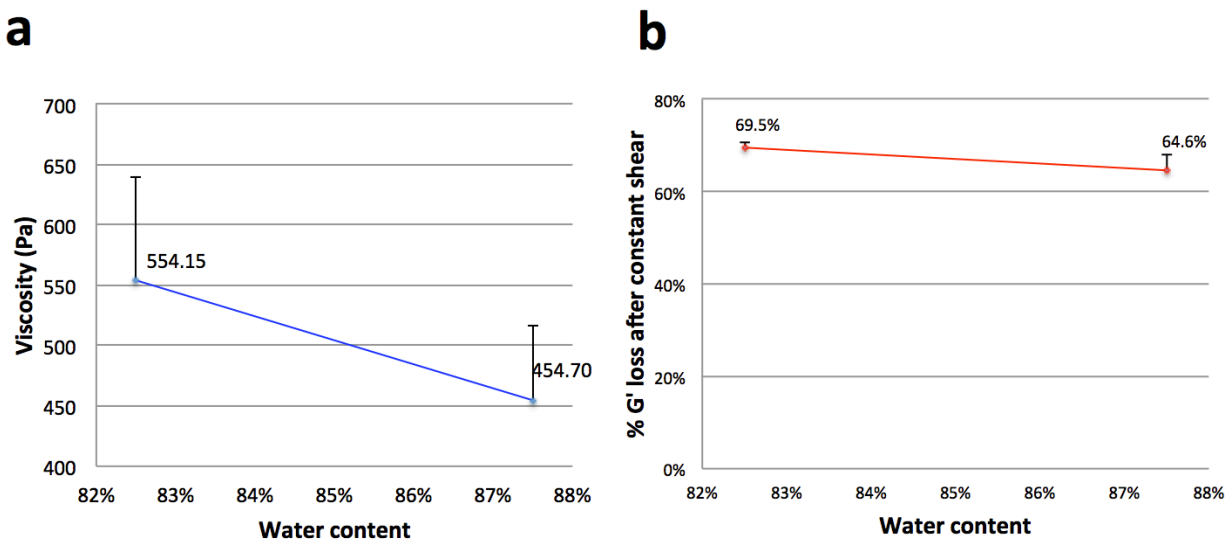

Figure 7. Water content does not affect the viscosity or the percentage G' loss significantly, measured at 10 minutes after the continuous dynamic shear. (a) There was no statistically significant change in the viscosity during dynamic steady rate shear, with the p-value of 0.16. (b) There is no significant difference in the percentage of G' loss 10 minutes after the continuous dynamic shearing, with p-value of 0.95.

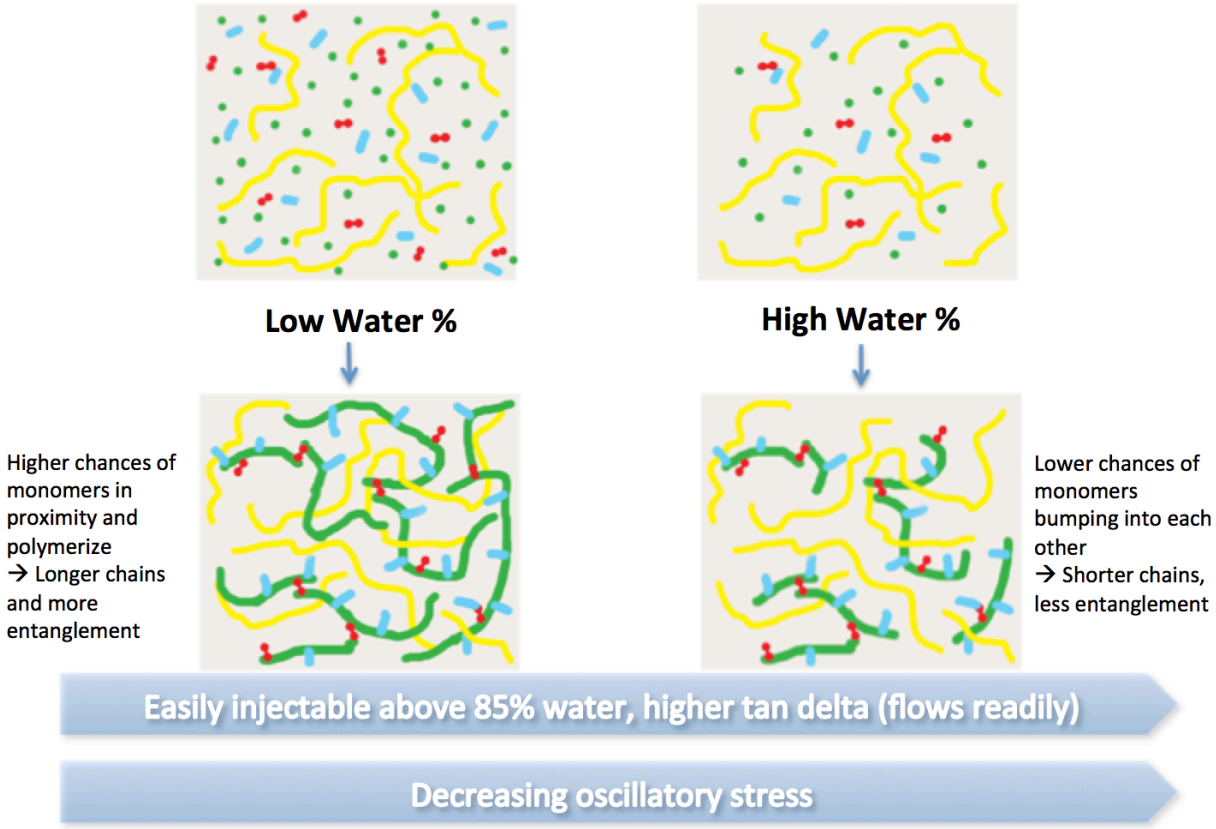

Figure 8. The increasing ease of injection with increasing water content can be explained by the likelihood of monomers in colliding with other monomers, and forming new bonds during polymerization in this schematic. As water content increases, it is less likely for the monomers to bump into each other, resulting in shorter polymer chains with less entanglement with the surrounding chains of polymers and CMC.

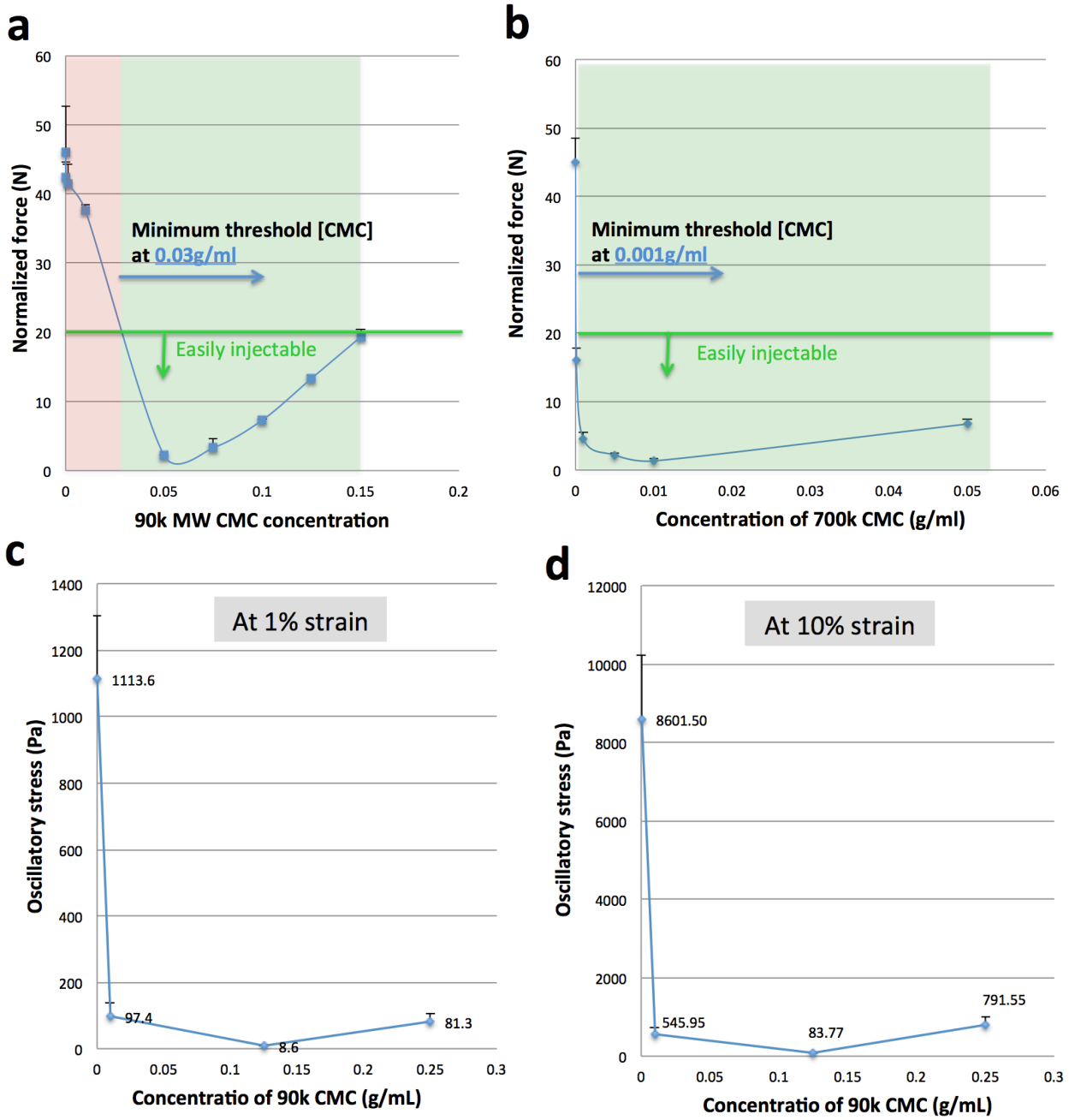

Figure 9. A minimum threshold of CMC concentration must be met in order to make HPTC injectable. (a) The injection force through a 21G needle for 90k CMC is too high for easy hand held injection when the CMC concentration is below 0.03g/ml 90k CMC. Once the concentration is above the minimum threshold, the injection force tested with Instron increases again with increasing CMC concentration. (b) A similar trend is observed for another MW CMC, 700k, except that the minimum threshold is lower at 0.001g/ml 700k CMC. (c, d) The oscillatory stress during strain sweep is the highest without any CMC, and drops as soon as 0.01g/ml of CMC is added, and the trend is similar to the trend observed for the injectability assay with Instron. The oscillatory stress for all samples tested increase as the strain percentage increases from 1% to 10%(d). 87.5% water content and 12.6% TEGDMA were present in all the samples.

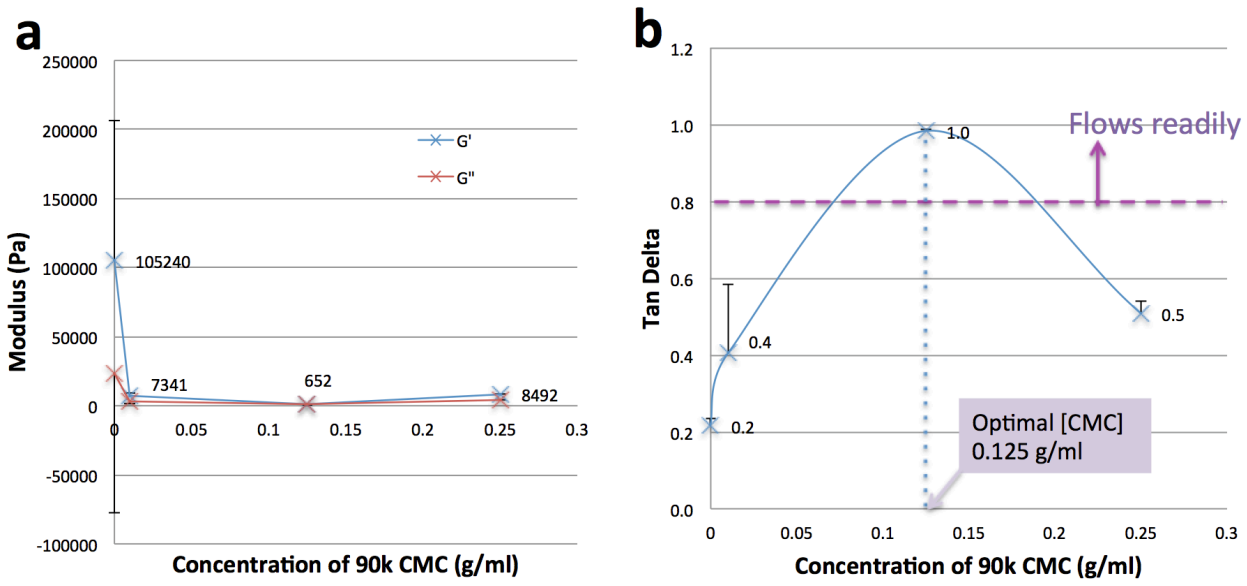

Figure 10. Frequency sweep of rheological study shows that G' and G" both decrease as small amount of CMC is added, and the tan delta peaks at the optimal CMC concentration and falls back down at a higher concentration. (a) The G' and G" are higher in the uninjectable samples, 0, 0.01, and 0.25 g/ml CMC concentrations than the injectable one at optimal CMC concentration, 0.125 g/ml. (b) Tan delta for the 0.125g/ml CMC sample is close to 1, and is significantly higher than the rest of the samples that are uninjectable. 87.5% water content and 12.6% TEGDMA and 90k CMC were present in all the samples.

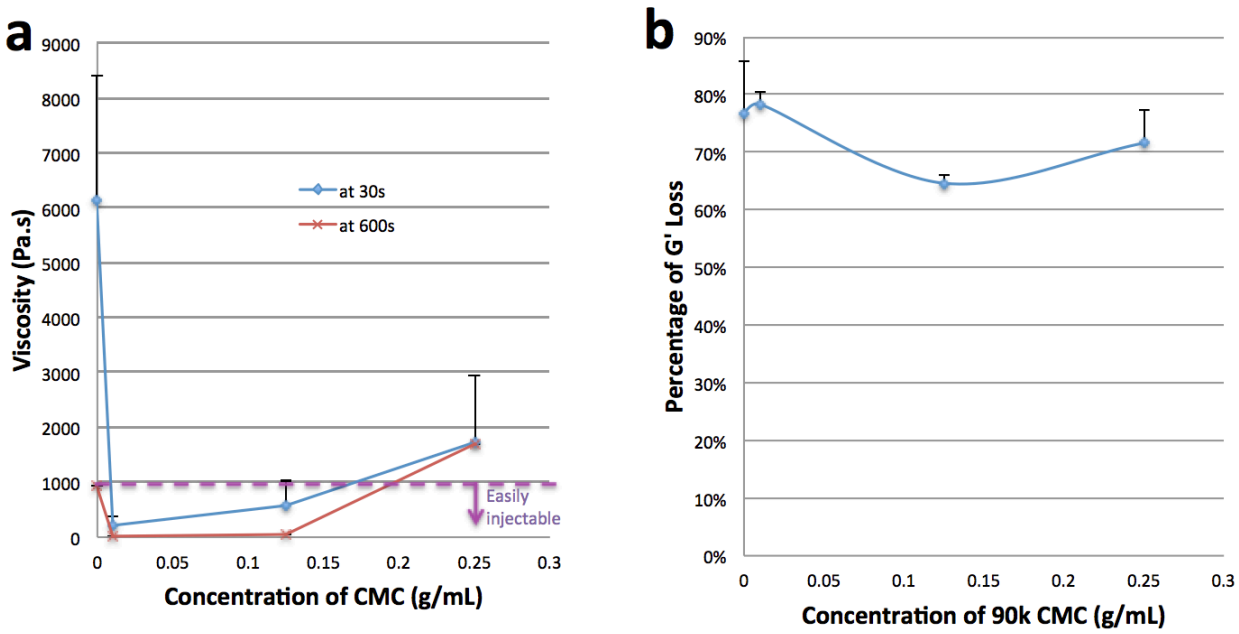

Figure 11. The viscosity of CMC drops dramatically with the addition of CMC, and it increases gradually with the increases in the concentration of CMC, and the G' loss percentage is the lowest at 0.125g/ml CMC. (a) The viscosity during steady rate sweep in rheology shows a very high viscosity in the absence of CMC, and increasing viscosity once the threshold CMC concentration is achieved. (b) At the end of the 10-minute time sweep experiment after the dynamic shear, the percentage of G' loss for the optimal CMC concentration at 0.125g/ml is not significantly lower than the other samples except for 0.01g/ml.

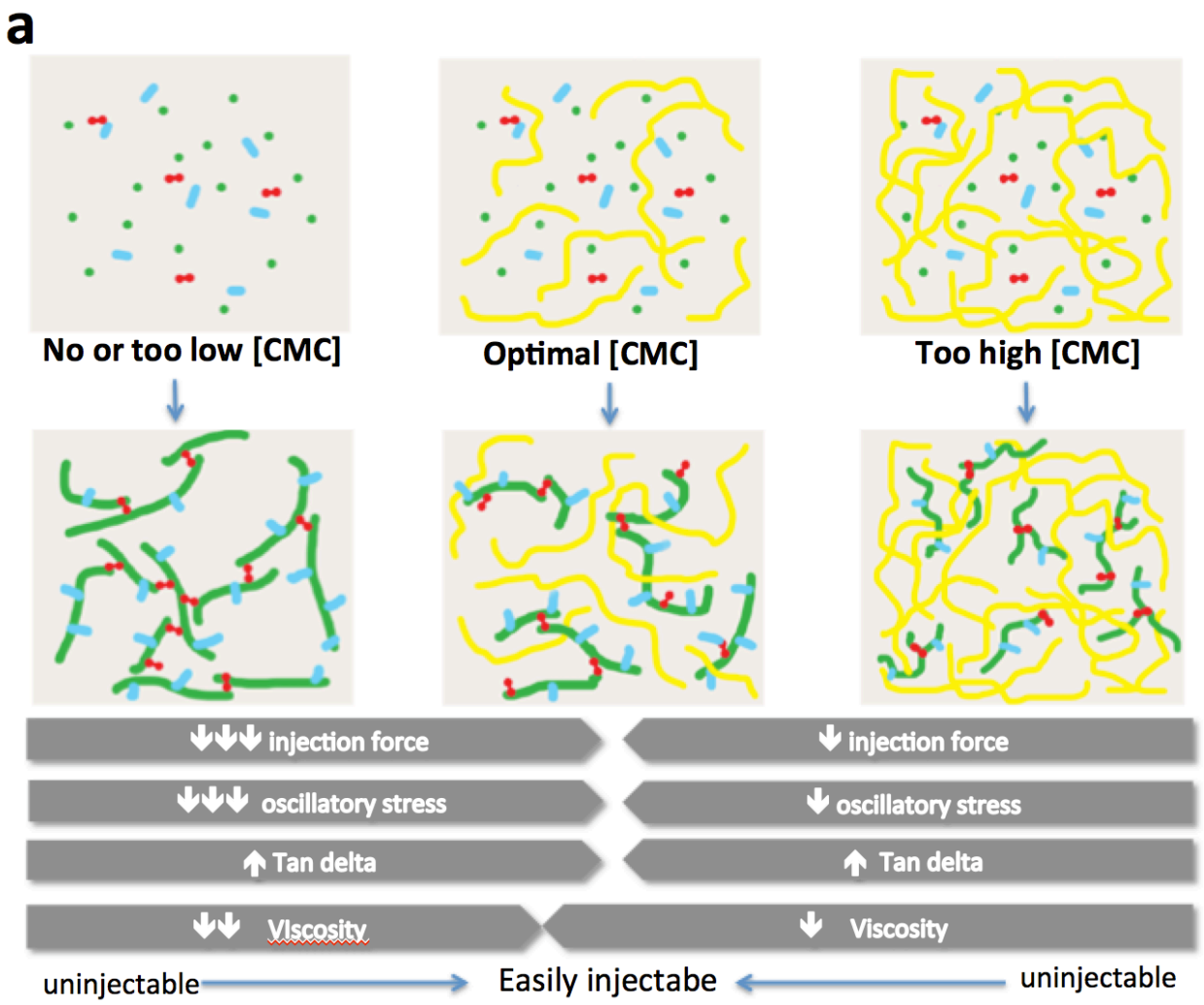

Figure 12. The effects of CMC concentration on HPTC's viscoelasticity and injectability are summarized in this schematic. In the absence of CMC (or very low concentration of CMC), there is no scaffolding or steric hindrance to interrupt with the polymerization, and the polymer chains are allowed to grow very long and interconnected. On the other end of the spectrum, when the CMC concentration is too high, the effect of CMC entanglement compounding with the newly formed polymer chains makes the viscosity high, tan delta low and difficult to inject. The polymer chains are expected to be short. When the CMC concentration is at the optimal range, CNC provides appropriate steric hindrance to limit the polymer size, interferes growing chains with the scaffolding of CMC, leading to an interpenetrating network with an appropriate amount of entanglement. The optimal polymer chain size that allows easy flow through the needle is promoted.

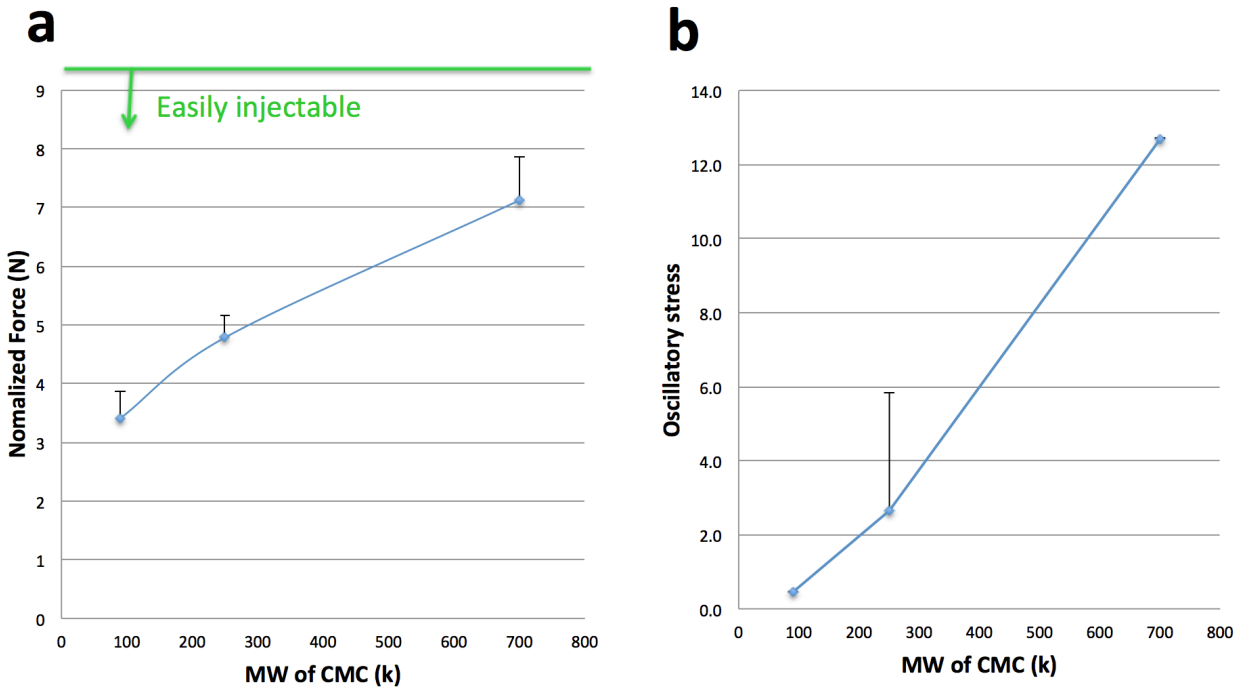

Figure 13. Increasing the molecular weight of CMC increases the force required to inject HPTC through a 21 G needle and the oscillatory stress during strain sweep rheological test. (a) Instron mechanical testing of HPTC made with increasing molecular weights, 90k, 250k and 700k showed increasing force required to inject through a 21G needle. (b) rheological testing shows that increasing molecular weight of HPTC increases the oscillatory stress during strain sweep, at 1% strain. In both graphs, the HPTC samples are at 12.6% TEGDMA, 87.5% water, and CMC concentration of 0.05g/ml as it is the limitation of the maximum solubility of 700k CMC.

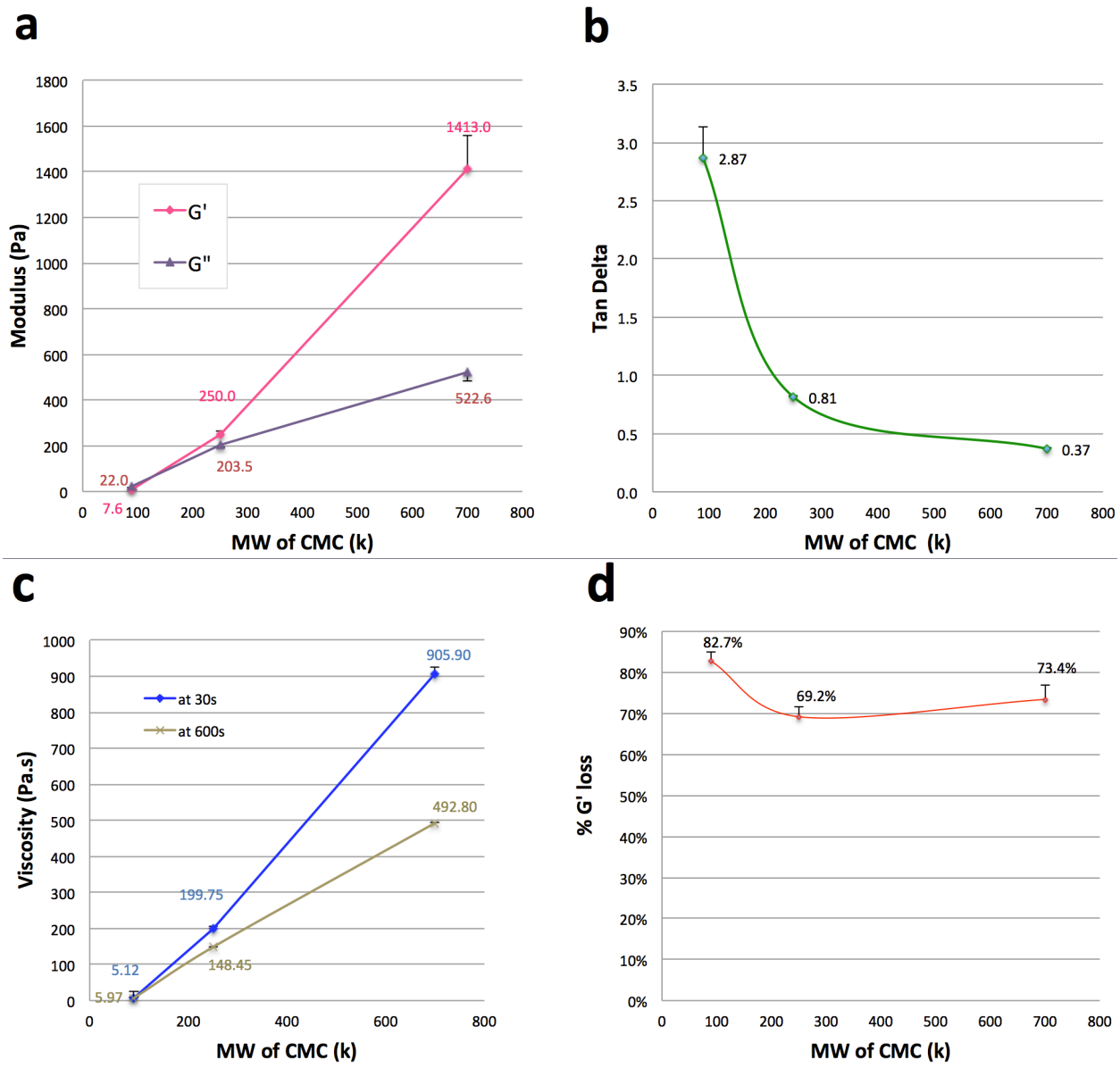

Figure 14. Increasing the molecular weight of CMC increases both the elastic modulus G' and viscous modulus G", but decreases the tan delta during the frequency sweep rheological experiment. It also increases the viscosity of HPTC, while not significantly affect the loss in G' after 10 minutes of dynamic shearing. HPTC made with increasing molecular weights, 90k, 250k and 700k showed (a) increasing G' and G" during frequency sweep at 1Hz; (b) but the G" to G' ratio, tan delta, decreases dramatically from 2.87 for the 90k CMC to 0.37 for the 700k CMC, suggesting that flow characteristic of HPTC is the highest when the low molecular weight CMC, 90k, is used. (c) The viscosity of HPTC increases as the molecular weight of the CMC increases during the steady rate sweep rheological test. The viscosities of both the 90k and 250k did not change significantly from time 30 seconds to 600 seconds (p-value 0.799 = and 0.051 respectively), while the viscosity of the 700k dropped significantly from 30s to 600s with a p-value of 0.0011, suggesting a either mechanical disruption of the interpenetrating polymer network or decrease in entanglement from the continuous shearing for 600s. (d) The percentage loss in G' range from 69% to 83%, and they

are not significantly different (t values of all combinations larger than 0.05) among the three molecular weight CMC HPTC samples. In all the graphs above, the HPTC samples are at the optimal 12.6% TEGDMA, 87.5% water, and lower than optimal CMC concentration of 0.05g/ml due to the limitation of dissolving the 700k CMC in a higher concentration.

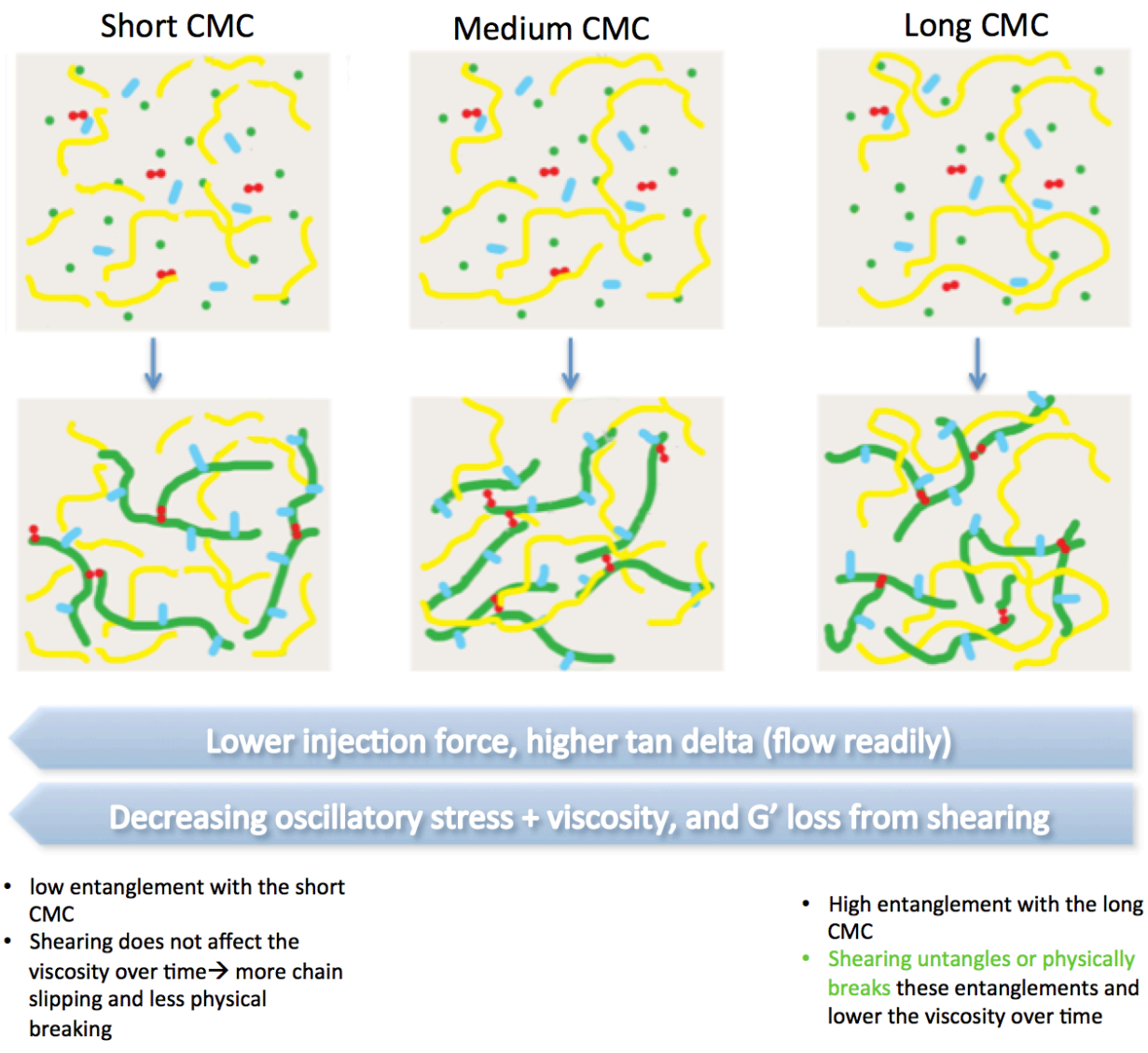

Figure 15. The effects of the molecular weight of CMC on HPTC's viscoelasticity and injectability are summarized in the schematic. With low concentration of CMC limited by the maximum CMC solubility in the long CMC sample, the degree of polymerization of the polymer chains are expected to be similar among the 3 different CMC MW.

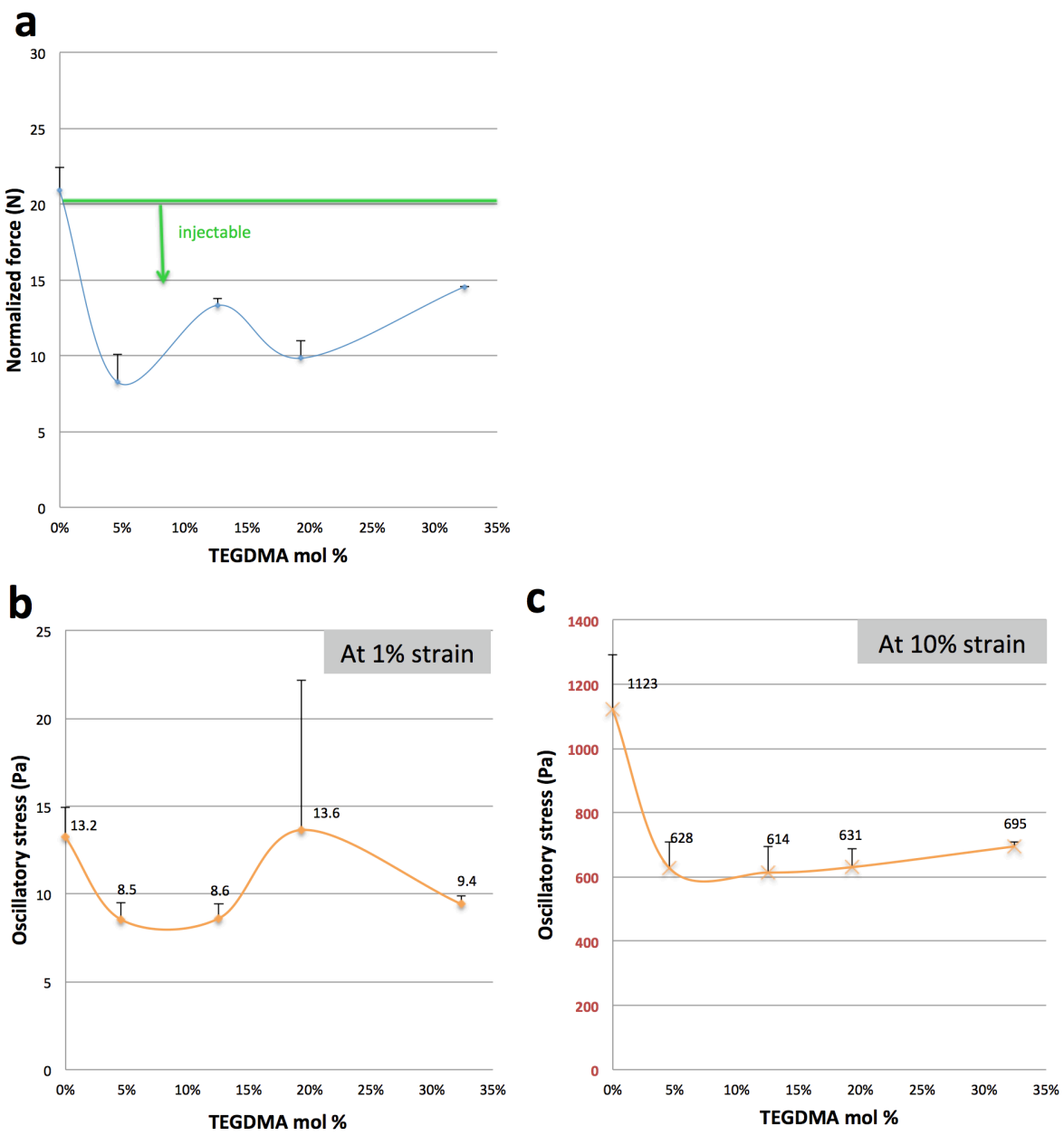

Figure 16. Having no TEGDMA significantly increases the force of injection, and it has a significantly higher oscillatory stress at 10% strain during strain sweep in rheological testing. (a) Instron mechanical testing of HPTC made with increasing TEGDMA mol %, 0%, 4.6%, 12.6%, 19.3% and 32.4% showed a significant drop in the force of injection between 0% and 4.6% TEGDMA (p=0.005), while increasing the TEGDMA percentage from 4.6% to 32.4% 4.6%. There is also a significant increase in injection force, at 13.2N at the next TEGDMA %, with p-value of 0.02. At 19.3% TEGDMA, the force drops again significantly (p = 0.045)(and it climbs back up again at 32.4% (p = 0.008). (a) Rheological testing shows that increasing the TEGDMA mol % from 0 to 4.6% significantly decreases the oscillatory stress during strain sweep at 10% strain, while this drop was not observed at 1% strain during the test. An increase of TEGDMA mol % from 4.6% to 32.4% did not significantly change the oscillatory stress in both 1% strain and 10% strain. In these graphs, HPTC samples are at 87.5% water, with 0.125g/ml 90k CMC.

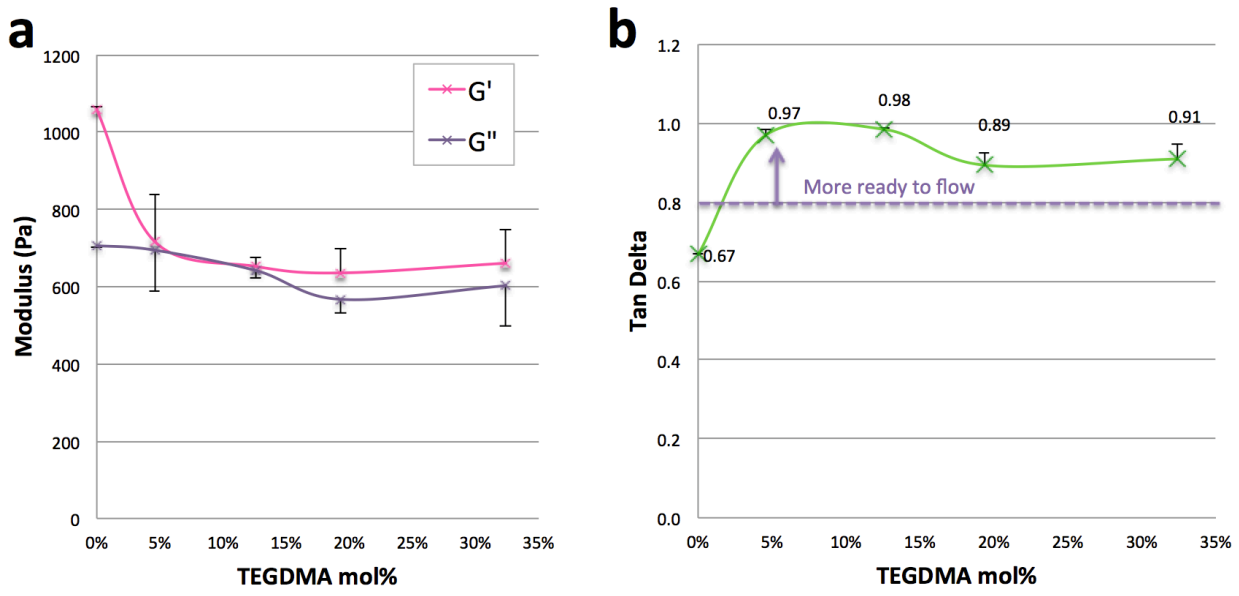

Figure 17. Increasing the TEGDMA mol % from 0 to 4.6% significantly decreases the elastic modulus G', and further increase in TEGDMA concentration does not change the G' and G" significantly. The Tan delta peaked at 4.6% and 12.6% TEGDMA. HPTC made with increasing TEGDMA mol %, 0%, 4.6%, 12.6%, 19.3% and 32.4% showed (a) decrease in G' from 0 to 4.65 TEGDMA, while the rest of the samples with higher TEGDMA % have similar G'. There is no significant difference in the G" of all samples during frequency sweep; (b) when TEGDMA is at 0%, HPTC has the lowest tan delta and does not flow well. Once the TEGDMA % increases to 4.6% and 12.6%, the Tan delta significantly increase to 0.97 and 0.98, and then at higher percentages, they drop down slightly to 0.89 and 0.91 for 19.3% and 32.4% respectively.

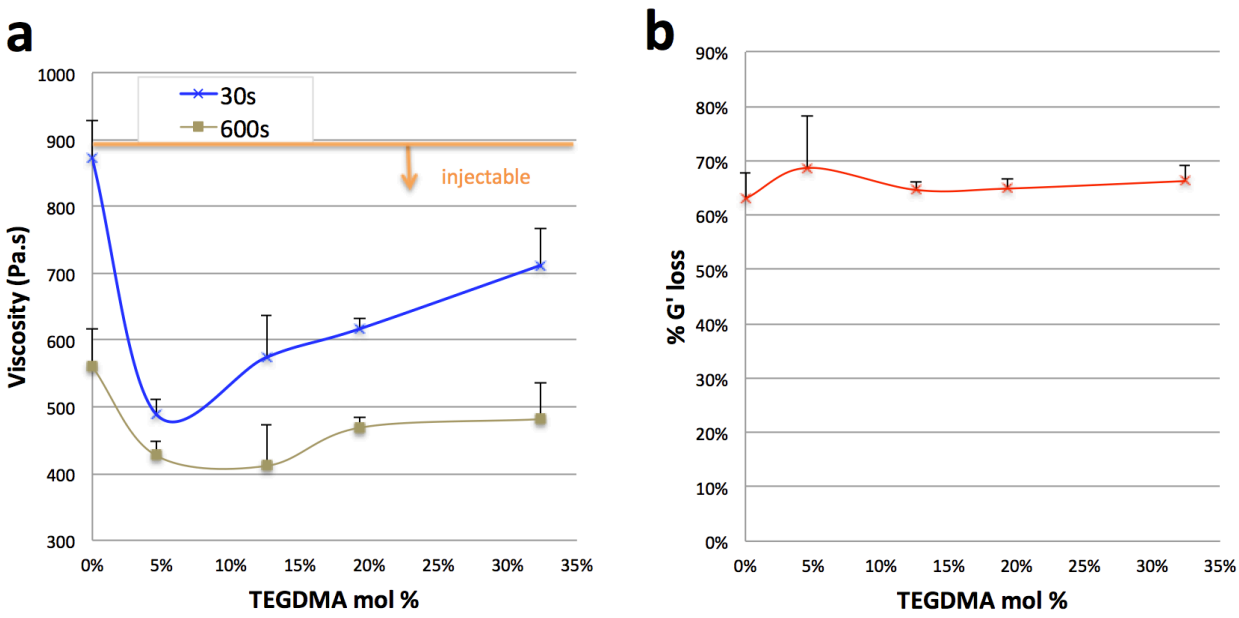

Figure 18. Increasing TEGDMA concentration from 0 to 4.6% dropped the viscosity significantly, and it increases gradually as the TEGDMA mol % increases (a). The G' loss after shearing is not significantly different between all TEGDMA % (b).

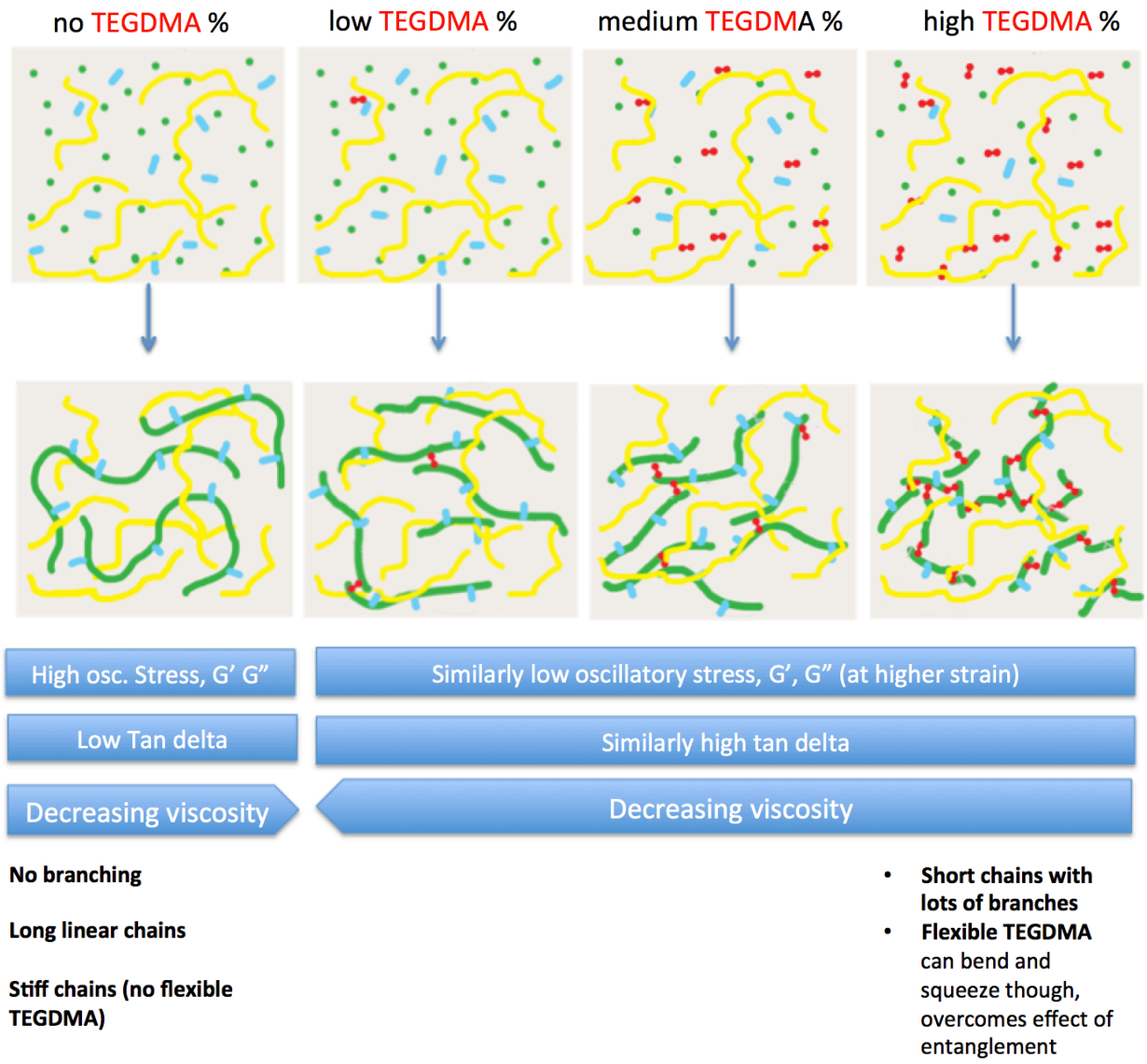

Figure 19. The effects of mole percentage of TEGDMA on HPTC's viscoelasticity and injectability are summarized in the schematic. With no TEGDMA, HPTC is at the borderline of being uninjectable, with significant increase in the force of injection, oscillatory stress, G' and G", and increased viscosity compared to the rest of the TEGDMA % tested, 4.6%, 12.6%, 19.3% and 32.4%. No TEGDMA HPTC also has lower tan delta. When the TEGDMA range is between 4.6 and 32.4%, there is no significant difference in the oscillatory stress, G', G" and Tan delta. However, the viscosity decreases from 32.6 TEGDMA to 4.6% TEGDMA. The hypothesis for this observation is that TEGDMA serves as a flexible crosslinker that helps HPTC squeeze through needles to be injected. Without it, the completely linear HEMA/PEGMA chains are stiff, making it more difficult to adjust its conformation and slip past the CMC entanglement to flow. With low percentage of TEGDMA, the improvement in injectability is seen, with more flexibility in the polymer network. Although at high TEGDMA % tested, HPTC is still injectable, the increased viscosity due to the increased crosslinking made it somewhat less desirable as an injectable for soft tissue.

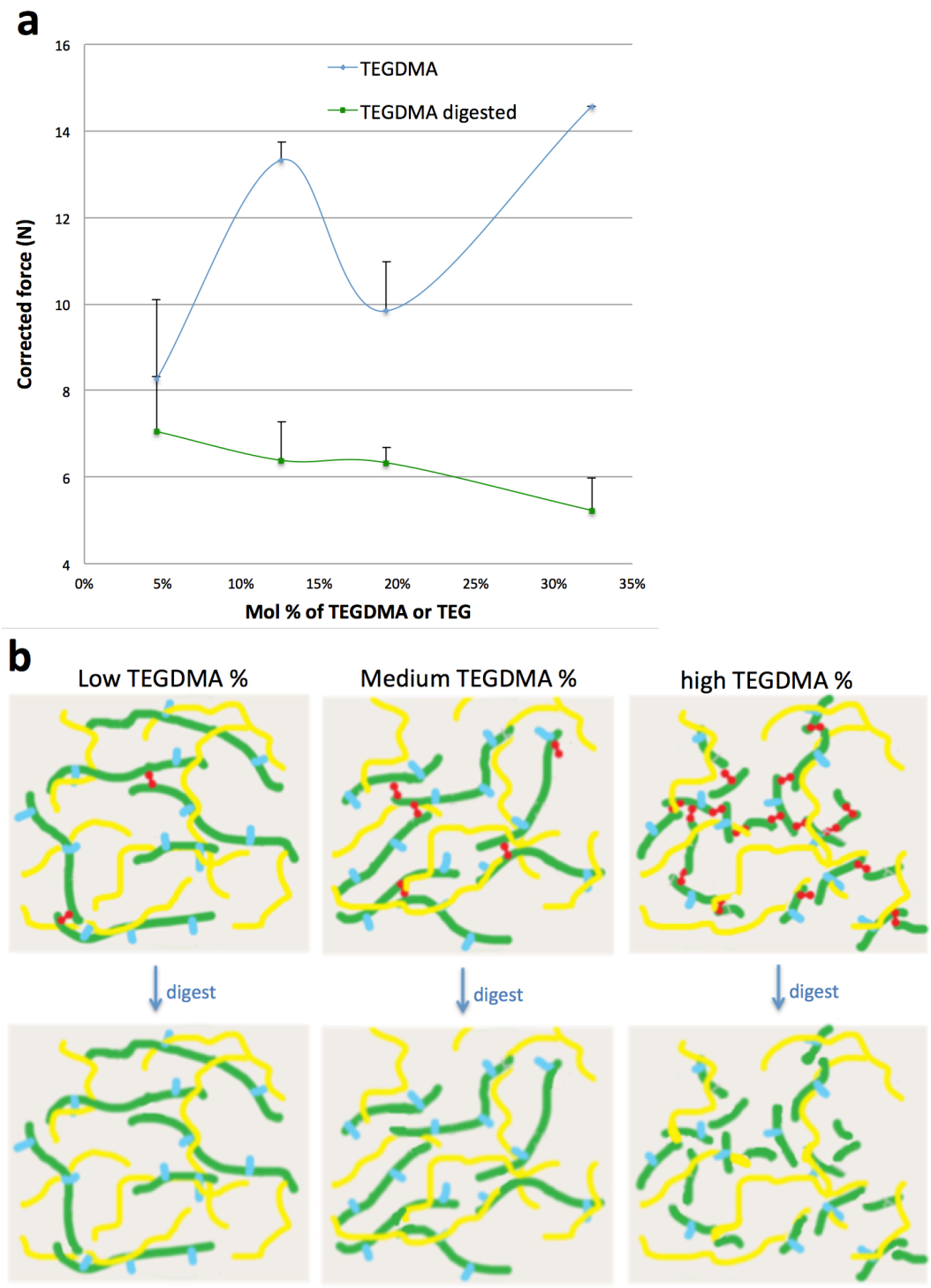

Figure 20. The force of injection of HPTC is the highest with 32.4% TEGDMA, but when the TEGDMA is digested with Fenton reaction, the force of injection dropped dramatically to the lowest, suggesting HPTC with 32.4% TEGDMA may have shorter HEMA/ PEGMA chains connected with more branching due to the increased percentage of TEGMDA. (a). The effect of TEGDMA digest is represented in the schematic in (b). All samples tested here contain 0.125g/ml 90k CMC, and 87.5% water.

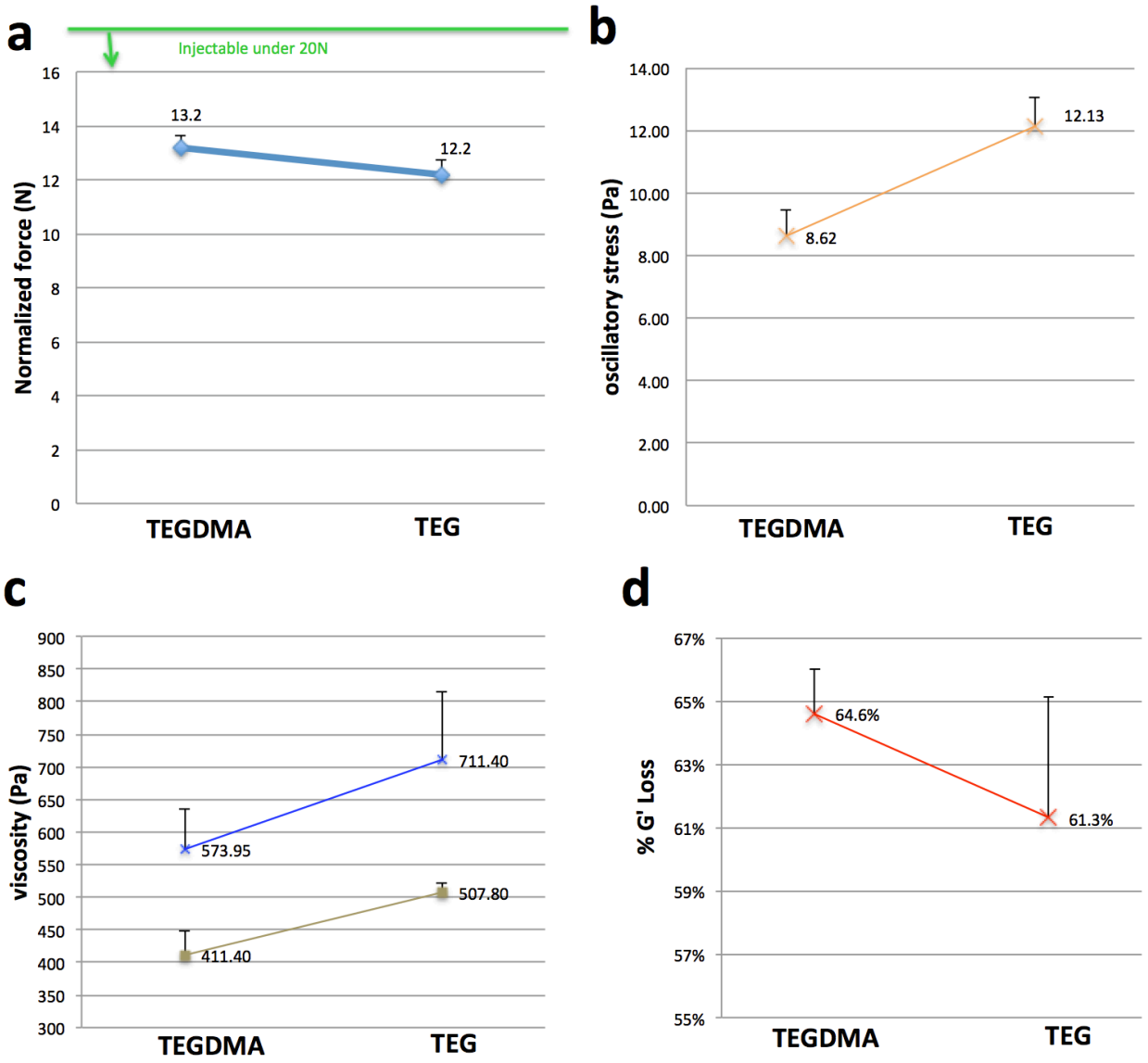

Figure 21. Substituting the polymerizing TEGDMA with non-polymerizing TEG does not significantly change the force of injection, oscillatory stress during strain sweep, viscosity, and percentage G' loss. HPTC polymerized with TEG in place of TEGDMA shows: (a) similar force required to inject through a 21G needle; (b) a small but statistically insignificant increase in the oscillatory stress during strain sweep, at 1% strain, with $p = 0.057$; (c) insignificant changes in both G' and G" during frequency sweep at 1Hz with p-values of 0.25 and 0.07 respectively ; and (d) insignificant change in percentage of G' loss ($p = 0.37$). In all of these graphs, HPTC samples are made with either 12.6% mol TEGDMA or TEG, 87.5% water, and 90k CMC concentration of 0.125 g/ml.

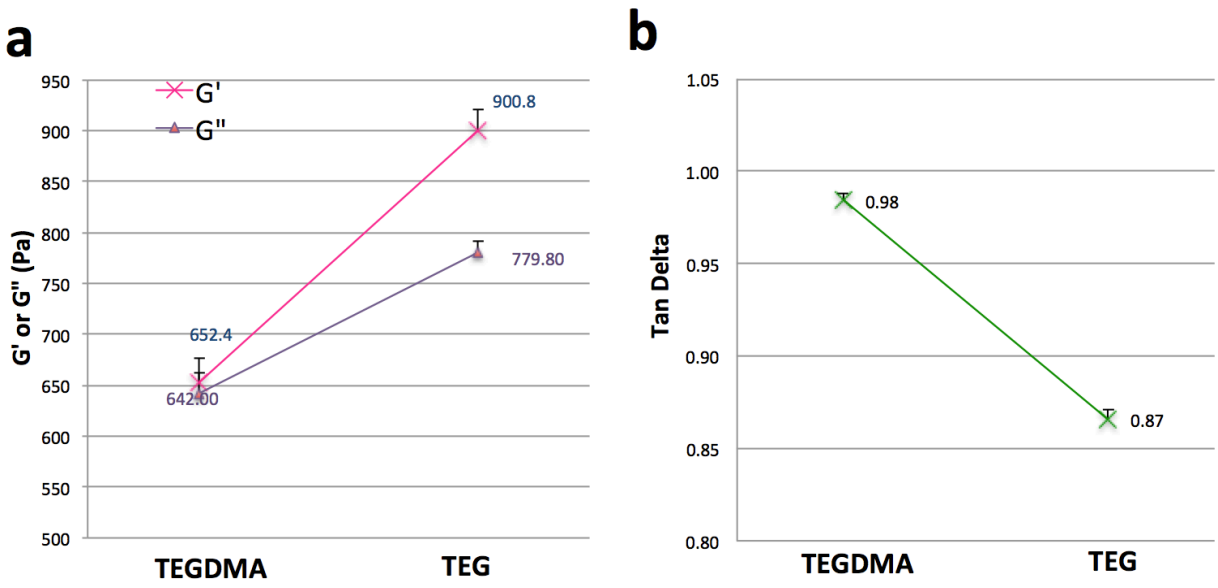

Figure 22. Substituting the polymerizing TEGDMA with non-polymerizing TEG significantly increases the elastic modulus G' and viscous modulus G", and significantly decreases the Tan delta during frequency sweep at 1Hz. HPTC made with TEG control instead of TEGDMA showed (a) an increase in G' ($p = 0.0002$*) and an increase in G" ($p = 0.045$*); (b) the Tan delta significantly decreases from 0.98 to 0.87 ($p = 0.003$*).

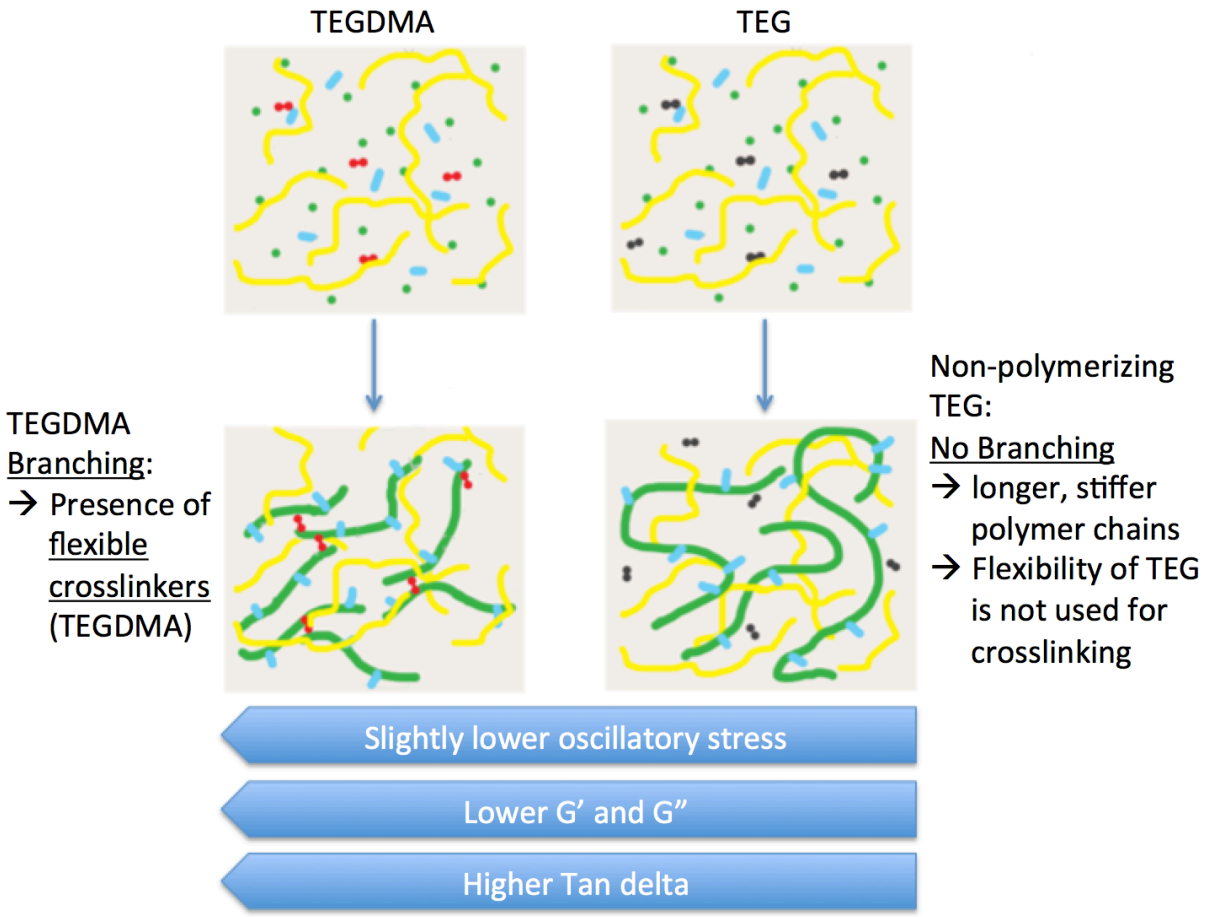

Figure 23. The effects of substituting 12.6% TEGDMA with 12.6% TEG on HPTC's viscoelasticity are summarized in this schematic. With low concentration of CMC limited by the maximum CMC solubility in the long CMC sample, the degree of polymerization of the polymer chains are expected to be similar among the 3 different CMC MW.

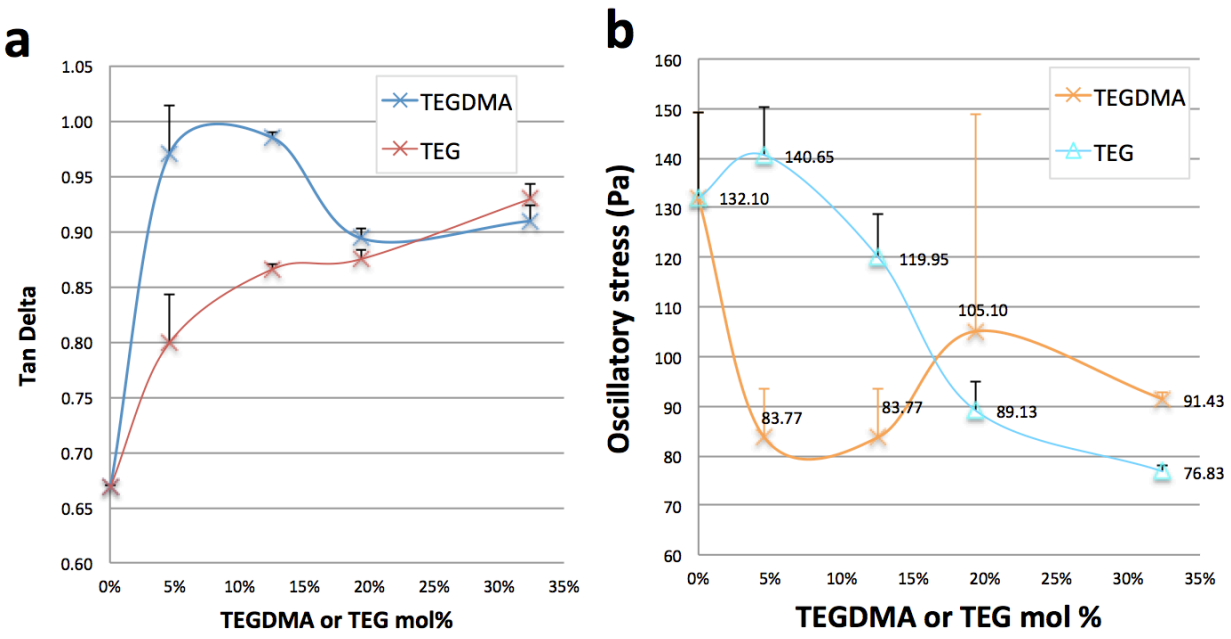

Figure 24. Effect of TEG substituting TEGDMA between mol % of 0 and 32.4% on Tan delta and oscillatory stress are shown. (a) As TEG % increases, the HEMA and PEGMA % decrease, resulting in shorter HEMA/PEGMA chains, which explains the increase in the flow property reflected in tan delta. On the other hand, TEGDMA at 4.6% and 12.6% have significantly higher tan delta than the slightly longer linear chains in TEG, suggesting that the presence of low density branch points that are flexible in TEGDMA improves the fluidity of HPTC, reflected in increased Tan delta at these low % TEGDMA. As the percentage of TEGDMA increases to 19.3 and 32.4%, the number of branch points would start to have an overpowering entanglement effect, not only with HEMA/PEGMA/ TEGDMA chains, but also with the surrounding CMC. Although the linkers are flexible, the added branch points increases the resistance of moment and lower the tan delta significantly. The resulting Tan delta between TEGDMA and TEG in this percentage range is similar between the two groups. (b) As the percentage of TEG increases the oscillatory stress of TEG decreases due to the shorter linear chains with lower entanglement and resistance to flow. TEG's oscillatory stress is higher than TEGDMA in the 4.6-12.5% range. It can be attributed to the flexibility of the low density flexible branch points that allow greater flow properties to lower the oscillatory stress.

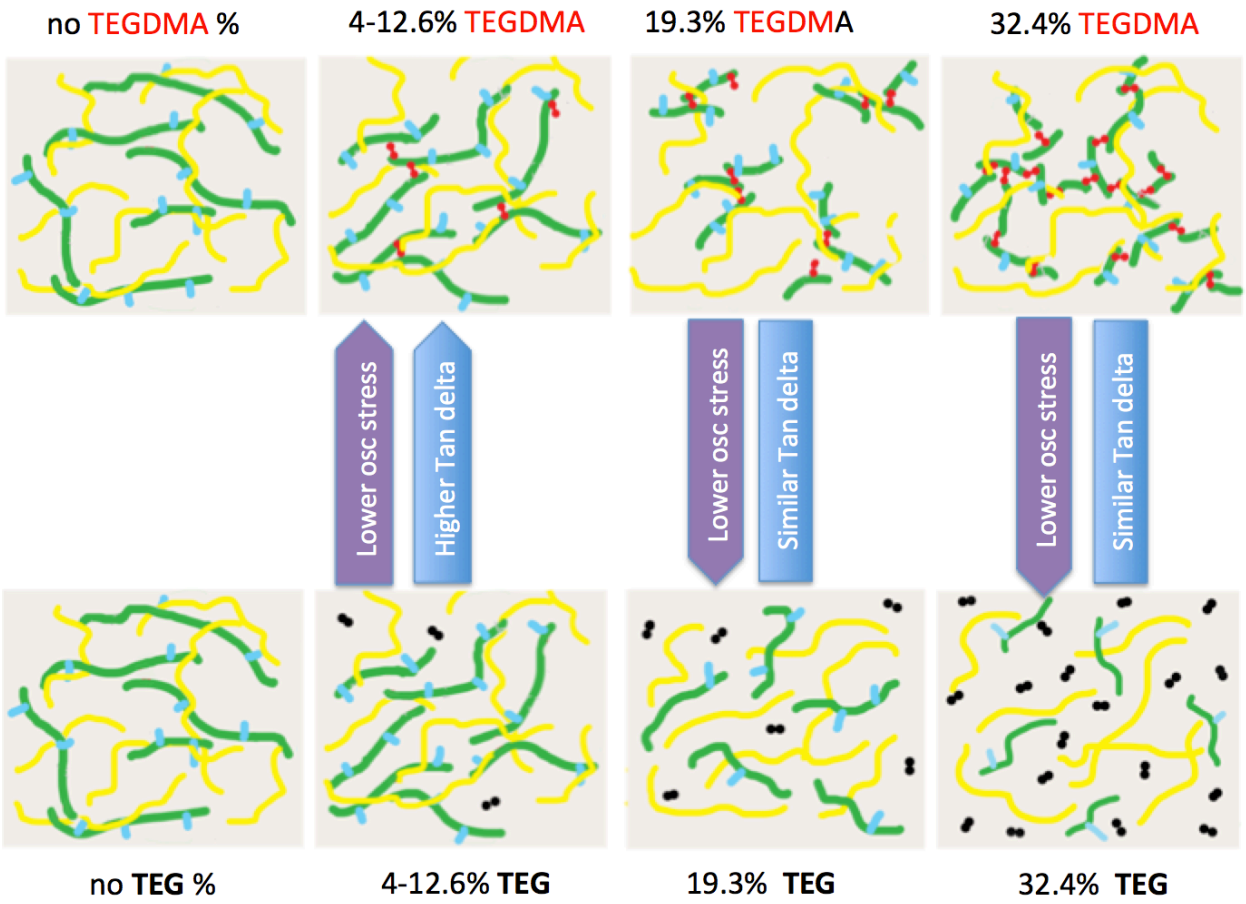

Figure 25. **The effects of mole percentage of TEGDMA vs. TEG on HPTC's viscoelasticity and injectability are summarized in this schematic.** With no TEGDMA, HPTC is at the borderline of being uninjectable, with significant increase in the force of injection, oscillatory stress, G' and G", and increased viscosity compared to the rest of the TEGDMA % tested, 4.6%, 12.6%, 19.3% and 32.4%. No TEGDMA HPTC also has lower tan delta. When the TEGDMA range is between 4.6 and 32.4%, there is no significant difference in the oscillatory stress, G', G" and Tan delta. However, the viscosity decreases from 32.6 TEGDMA to 4.6% TEGDMA. The hypothesis for this observation is that TEGDMA serves as a flexible crosslinker that helps HPTC squeeze through needles to be injected. Without it, the completely linear HEMA/PEGMA chains are stiff, making it more difficult to adjust its conformation and slip past the CMC entanglement to flow. With low percentage of TEGDMA, the improvement in injectability is seen, with more flexibility in the polymer network. Although at high TEGDMA % tested, HPTC is still injectable, the increased viscosity due to the increased crosslinking made it somewhat less desirable as an injectable for soft tissue.

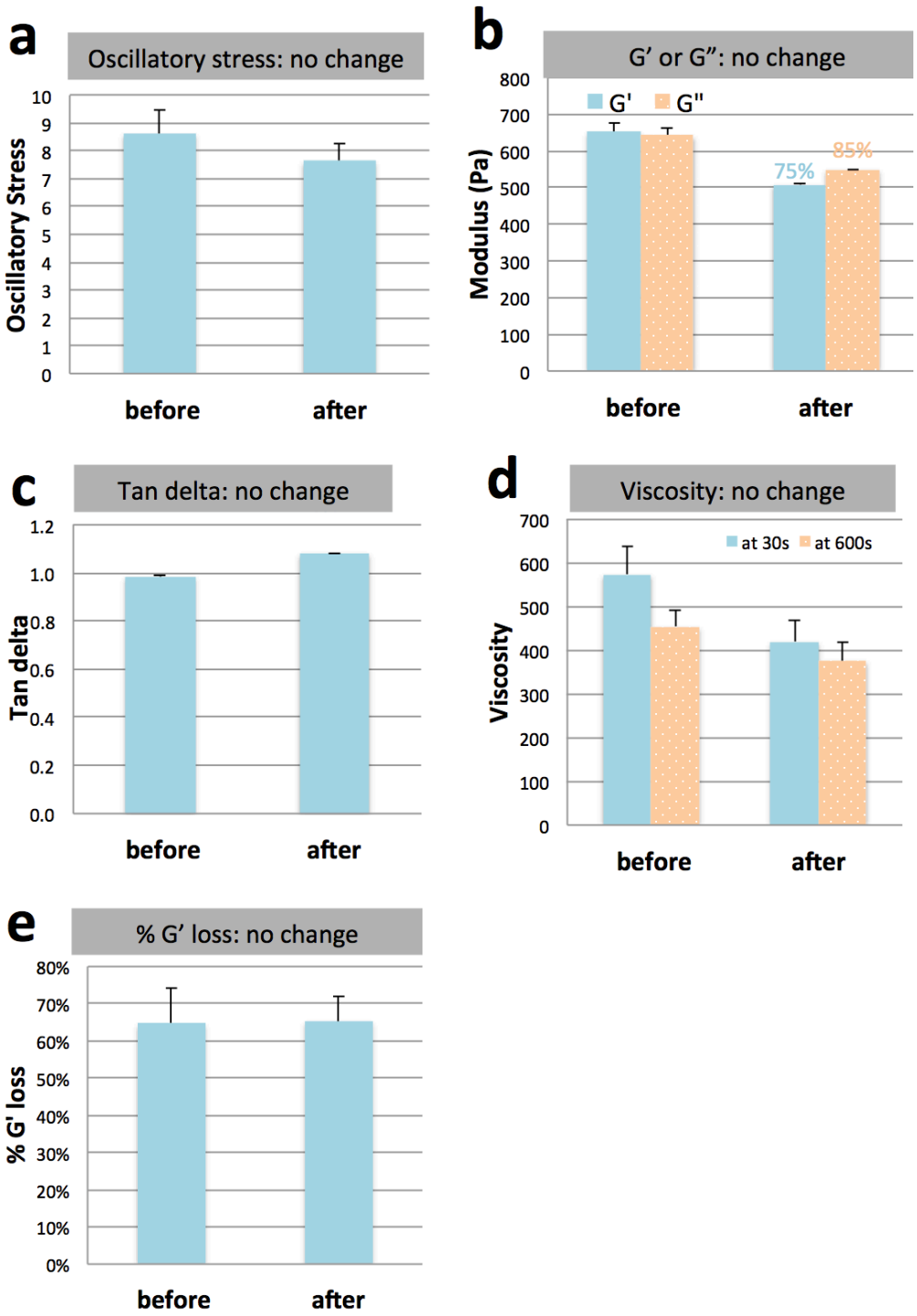

Figure 26. Passing HPTC through a 21G needle does not significantly affect its viscoelasticity. In the "before" samples, HPTC was simply scooped onto the bottom parallel plate of the rheometer for testing, while in the "after" samples, HPTC was injected through a 21G needle onto the same surface. T-test shows no significant difference in: (a) oscillatory stress ($p = 0.90$); (b) G' ($p = 0.21$) and G" ($p = 0.35$); (c) Tan delta ($p = 0.40$); (d) viscosity at 30s ($p = 0.17$) and 600s ($p = 0.30$); and (e) percentage G' loss ($p = 0.92$). N = 2 for all groups.

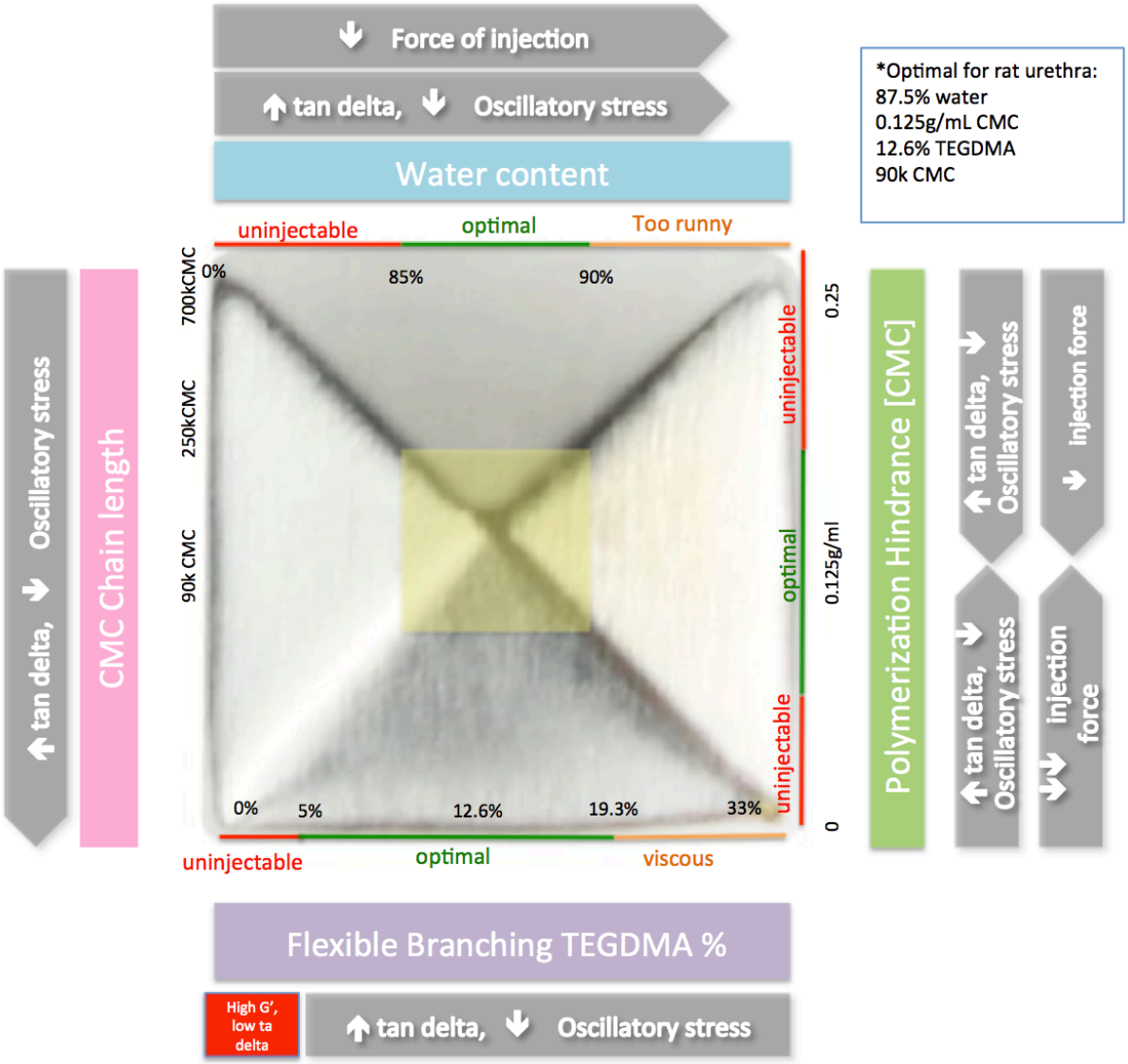

Figure 27. Shown here is a schematic that summarizes the four main parameters that define HPTC's injectability and viscoelastic properties. Clockwise from the top: Increasing water content decreases the force of injection, increases Tan delta and decreases oscillatory stress, which improves ease of injection. The optimal range is 85-90% water for best injectability. Increasing the polymerization hindrance or CMC concentration, from 0 to the optimal amount, 0.125g/ml in this case with MW 90k CMC, dramatically increases tan delta, decreases oscillatory stress, and dramatically reduces the injection force. Decreasing the CMC concentration from a high concentration of 0.25g/ml to the optimal concentration 0.125g/ml has similar effects as the above, except that the changes are not as dramatic. Increasing TEGDMA mole % from 0 to 32.4% shows an increase in Tan delta and decrease in oscillatory stress when there is as little as 4.6% TEGDMA present. The injectability of 0% TEGDMA HPTC is significantly lower than any TEGDMA concentrations tested. As CMC chain length decreases, the Tan delta increases and oscillatory stress decreases, making HPTC easier to inject.
The yellow shaded area represents a range that fulfills the criteria to be an injectable HPTC, within which it can have a wide range of characteristics for future customization use for different applications.

Reference

[1] J. Aleman, a. V. Chadwick, J. He, M. Hess, K. Horie, R. G. Jones, P. Kratochvil, I. Meisel, I. Mita, G. Moad, S. Penczek, and R. F. T. Stepto, "Definitions of terms relating to the structure and processing of sols, gels, networks, and inorganic-organic hybrid materials (IUPAC Recommendations 2007)," vol. 79, no. 10, pp. 1801–1829, 2007.

[2] A. Kretlow, J, Klouda, L, Mikos, "Injectable matrices and scaffolds for drug delivery in tissue engineering," *Adv. Drug Deliv. Rev.*, vol. 59, no. 4–5, pp. 263–273, 2007.

[3] X. Gao, Y. Zhou, G. Ma, S. Shi, D. Yang, F. Lu, and J. Nie, "A water-soluble photocrosslinkable chitosan derivative prepared by Michael-addition reaction as a precursor for injectable hydrogel," *Carbohydr. Polym.*, vol. 79, no. 3, pp. 507–512, 2010.

[4] T. Gan, Y. Zhang, and Y. Guan, "In situ gelation of P(NIPAM-HEMA) microgel dispersion and its applications as injectable 3D cell scaffold," *Biomacromolecules*, vol. 10, no. 6, pp. 1410–1415, 2009.

[5] J. Zhou, G. Wang, L. Zou, L. Tang, M. Marquez, and Z. Hu, "Viscoelastic behavior and in vivo release study of microgel dispersions with inverse thermoreversible gelation," *Biomacromolecules*, vol. 9, no. 1, pp. 142–148, 2008.

[6] T. Yoon, JJ, Chung, HJ, Park, "Photo-crosslinkable and biodegradable Pluronic/heparin hydrogels for local and sustained delivery of angiogenic growth factor," *J. Biomed. Mater. Res. A*, vol. 83A, no. 3, pp. 597–605, 2007.

[7] O. Wichterle and D. Lím, "Hydrophilic Gels for Biological Use," *Nature*, vol. 185, no. 4706, pp. 117–118, 1960.

[8] S. S. Lane, M. Morris, L. Nordan, M. Packer, N. Tarantino, and R. B. Wallace, "Multifocal intraocular lenses," *Ophthalmol. Clin. North Am.*, vol. 19, no. 1, pp. 89–105, 2006.

[9] T. Thomas, "Considerations affecting technique and results in keratoplasty.," *Trans. Ophthalmol Soc*, vol. 75, pp. 473–513, 1955.

[10] B. Y. R. Day, R. Day, I. C. La, U. R. E. Rge, and D. E. S. Ye, "ARTIFICIAL CORNEAL IMPLANTS BY Robert Day, M.D.," no. Figure i, 1877.

[11] A. DeVoe, "A Review of the techniques of keratoprostheses.," *Surv. Ophthalmol*, vol. 55, pp. 455–475, 1971.

[12] J. Aquavella, JV, Gullapalli, RN, Brown, AC, Harris, "Keratoprosthesis: Results, complications and management.," *Opthalmology*, vol. 89, pp. 655–660, 1982.

[13] S. D. Lee, G. H. Hsiue, C. Y. Kao, and P. C. T. Chang, “Artificial cornea: Surface modification of silicone rubber membrane by graft polymerization of pHEMA via glow discharge,” *Biomaterials*, vol. 17, no. 6, pp. 587–595, 1996.

[14] K. Kliment, M. Stol, K. Fahoun, and B. Stockar, “Use of spongy hydron in plastic surgery.,” *J. Biomed. Mater. Res.*, vol. 2, no. 2, pp. 237–243, 1968.

[15] S. H. Ronel, M. J. D’Andrea, H. Hashiguchi, G. F. Klomp, and W. H. Dobelle, “Macroporous hydrogel membranes for a hybrid artificial pancreas. I. Synthesis and chamber fabrication.,” *J. Biomed. Mater. Res.*, vol. 17, no. 5, pp. 855–864, 1983.

[16] G. F. Klomp, H. Hashiguchi, P. C. Ursell, Y. Takeda, T. Taguchi, and W. H. Dobelle, “Macroporous hydrogel membranes for a hybrid artificial pancreas. II. Biocompatibility.,” *J. Biomed. Mater. Res.*, vol. 17, no. 5, pp. 865–871, 1983.

[17] A. a. Obaidat and K. Park, “Characterization of protein release through glucose-sensitive hydrogel membranes,” *Biomaterials*, vol. 18, no. 11, pp. 801–806, 1997.

[18] I. S. Isayeva, B. T. Kasibhatla, K. S. Rosenthal, and J. P. Kennedy, “Characterization and performance of membranes designed for macroencapsulation/implantation of pancreatic islet cells,” *Biomaterials*, vol. 24, no. 20, pp. 3483–3491, 2003.

[19] C. M. Keow, F. A. Bakar, A. B. Salleh, L. Y. Heng, R. Wagiran, and S. Siddiquee, “Screen-printed histamine biosensors fabricated from the entrapment of diamine oxidase in a photocured poly(HEMA) film,” *Int. J. Electrochem. Sci.*, vol. 7, no. 5, pp. 4702–4715, 2012.

[20] C. P. Quinn, C. P. Pathak, and J. a Hubbell, “of Dimethacrylate for and Biocompatibility of of Improving Biosensors Biosensors,” vol. V, no. 5, pp. 389–396, 1995.

[21] C. N. Kotanen, C. Tlili, and A. Guiseppi-Elie, “Bioactive electroconductive hydrogels: The effects of electropolymerization charge density on the storage stability of an enzyme-based biosensor,” *Appl. Biochem. Biotechnol.*, vol. 166, no. 4, pp. 878–888, 2012.

[22] A. Hejcl, L. Urdzikova, J. Sedy, P. Lesny, M. Pradny, J. Michalek, M. Burian, M. Hajek, J. Zamecnik, P. Jendelova, and E. Sykova, “Acute and delayed implantation of positively charged 2-hydroxyethyl methacrylate scaffolds in spinal cord injury in the rat.,” *J. Neurosurg. Spine*, vol. 8, no. 1, pp. 67–73, 2008.

[23] M. Baylatry, MT, Bisdorf-Bresson, A, Labarre, D, Laurent, A, Moine, L, Saint Maurice, JP, Slimani, K, Wassef, “(12) United States Patent,” US 8,673,264 B2, 2014.

[24] S. Mura, J. Nicolas, and P. Couvreur, “Stimuli-responsive nanocarriers for drug delivery.,” *Nat. Mater.*, vol. 12, no. 11, pp. 991–1003, 2013.

[25] X. Z. Zhang, R. X. Zhuo, J. Z. Cui, and J. T. Zhang, “A novel thermo-responsive drug delivery system with positive controlled release,” *Int. J. Pharm.*, vol. 235, no. 1–2, pp. 43–50, 2002.

[26] Z. Kerem, W. Bao, and K. E. Hammel, “Rapid polyether cleavage via extracellular one-electron oxidation by a brown-rot basidiomycete.,” *Proc. Natl. Acad. Sci. U. S. A.*, vol. 95, no. 18, pp. 10373–10377, 1998.

[27] a. Jayakrishnan, B. C. Thanoo, K. Rathinam, and M. Mohanty, “Preparation and evaluation of radiopaque hydrogel microspheres based on PHEMA/iothalamic acid and PHEMA/iopanoic acid as particulate emboli,” *J. Biomed. Mater. Res.*, vol. 24, no. 8, pp. 993–1004, 1990.

CHAPTER 3

EVALUATION OF THE BIOCOMPATIBILITY OF HPTC AND ITS EFFICACY IN TREATING URINARY INCONTINENCE IN RATS

3.1 INTRODUCTION

Poly-(HEMA)-based hydrogels have been studied extensively as a biomaterial for intraocular lenses[1-2], artificial cornea [3-4], biosensor coating[5-7], contact lenses[8]. However, since it is to our knowledge that this is the first successful attempt at fabricating a classically solid pHEMA into a an injectable form that is nondegradable, it is essential to study its biocompatibility and assess its efficacy in augmenting soft tissue. In this study, we use the rat incontinence model to evaluate HPTC's efficacy in treating the soft tissue, urethra, by augmenting it to help it restore the voiding pressure to the pre-operation level.

3.2 MATERIALS AND METHODS

3.2.1 Materials

All animal experiments were approved by the Animal Research Committee and the Animal Research Committee of the Office for Protection of Research Subjects at University of California , Los Angeles. Lewis rats (strain code 004) were purchased from Charles River (Wilmington, MA). Anti-FGFR4 antibody [5B5] for the visualization of fibroblasts was purchased from abcam (catalog no.: ab44971, Abcam, Cambridge, MA) MTT reagent (catalog no.: M6494) was purchased from Thermo Fisher Scientific (Waltham, MA). Vybrant® DiI cell-labeling solution (Catalog no. V-22885) was purchased from Life Technologies (Waltham, MA).

J774A.1 mouse monocyte/ macrophage cell line(catalog no. J774A.1 ATCC TIB-67) was purchased from ATCC (Manassas, VA).

3.2.2 Cell harvest and culture

Human PLA cells were isolated as described [9-10]. Cells were plated in Dulbecco's Modified Eagle's Media (DMEM; Mediatech, Herndon, VA) supplemented with 10% FBS (FBS; HyClone, Logan, UT) and 1% from a 100× concentrated antibiotic–antimycotic solution (penicillin G/amphotericin B/streptomycin; Mediatech) at a density of 5×10^6 cells per 100-mm tissue culture dish. To expand the cells, adherent cells were allowed to grow to near confluency, washed with PBS, and harvested by using 0.25% trypsin/1 mM EDTA. The cells were replated 1:4 and allowed to grow.

774A cells from ATTC is grown in conditions to keep the cells differentiated as described elsewhere [11]. Namely, cells are never allowed to reach confluency on cell culture dish, and maintained in DMEM containing 4.5g/L D-glucose, pyruvate, 10% Fetal Bovine Serum, 100U/mL penicillin, 100ug/ml 2mM Glutamax™.

3.2.3 HPTC injection onto the urethra in the rat incontinence model

Survival surgery was performed on 2-6 month-old Lewis rats that have preoperative urodynamic testing performed. Surgical introduction of incontinence with urethrolysis was performed in all the animals as previously described [12-13]. The proximal urethra is detached from the surrounding tissues and the vagina, by isolating the urethra with combination tiny incisions in the connective tissues, and firm separation using sterile cotton swabs. The isolation of the urethra is continued down to the distal urethra, by detaching it from the pubic bone.

For groups that have HPTC injection, HPTC is injected in either r 60 µl or 30 µl total volume at 3-4 injection sites of the urethra in the proximal/ mid-urethra regions only. The success of injection can be visualized as white blobs on the urethral wall.

The number of animals used in each group is: 1. Urethrolysis only (10 animals, 1 deceased due to surgical complications on day 4); 2. Urethrolysis + 60 µl HPTC injection (10 animals, 1 deceased due to surgical complications on day 3); 3. Urethrolysis + 30 µl HPTC (9 animals). Animals were evaluated for urethral function.

3.2.4 HPTC co-injection with cells in the rat incontinence model

The potential of using HPTC as a vehicle for cell therapy is tested by co-injecting HPTC along with PLA cells.

First, we tested the biocompatibility of HPTC with co-injected DiI-labeled cells in the bladder environment. Cell-labeling steps were performed per manufacturer's guidelines. 100 µl of HPTC was injected onto the bladder wall, and 2 million cells suspended in 50 µl was injected as close to the injection site of the HPTC as possible. This was performed on 2 animals. In the negative control, only cells alone were injected onto the bladder wall (without HPTC). A size 6 PDS suture was placed directly on top of the injection site for easy identification of location for tissue harvest in 4 weeks. We harvested the bladders at 4 weeks and evaluated them for the appearance of the tissues and presence of cells.

Second, we assessed the potential for using HPTC along with cells for the treatment of incontinence. The same procedures as outlined in section 3.2.3 was performed, with the addition

of injection of 2 X 10^6 DiI labeled cells suspended in sterile 30 µl 1X HBSS into the urethra next to the HPTC injection sites.

3.2.5 Urethral function with urodynamic studies when animals are under light anesthesia

Urodynamic studies were performed to study the urethral function of the animals preoperatively and 2, 4, 9 and 24 weeks postoperatively. The number of animals tested in each group and each time point is presented in Table 1. All animals are anesthetized with 80mg/kg body weight ketamine and 15mg/kg body weight xylazine intraperitoneal injection. The urinary bladder was emptied before insertion of a 2F microtip transurethral catheter connected to a pressure transducer (Duet Logic, Medtronic, Denmark) connected to a syringe pump (Harvard Apparatus, Holliston, MA) that controls 100ul/min saline transfusion into the bladder during the urodynamic experiment. The details of the procedure can be found in Rodríguez et al.[12]. First, the bladder capacity and voiding pressure is first determined. Second, the ALPP is measured with a rectal transducer, to measure the abdominal pressure. The bladder is emptied and then filled up to half its capacity, and the exterior of the abdomen is gently and gradually pressed down with 4 fingers to increase the abdominal pressure. The ALPP is determined as the abdominal pressure (measured through the rectal transducer) at which the first flow of fluid exits the urethra.

3.2.6 Surgical placement of the Suprapubic tube for awake cystometry in ambulatory urodynamic study

The main goal of this experiment is to determine whether a group of animals shows any signs of bladder obstruction due to the presence of the injectable material. Regular urodynamic

studies can potentially mask problems with urinary obstruction, because of the placement of transurethral catheter that can temporary dislodge the obstruction, and the presence of anesthesia may somewhat affect the animal's voiding function, to void smaller volumes when they under the effect of anesthesia.

Suprapubic tube is placed to solve this problem because it will allow direct urodynamic testing while the rats are awake, and no transurethral catheter is necessary.

To gain access to the animals' bladder for urodynamic test without having to use a transurethral catheter, a sterile suprapubic tube (PE 50) is placed on the bladder's detrusor dome at the time immediately following urethrolysis. This flexible suprapubic tube is slightly melted and gently folded over to create a "notch" to prevent it form slipping off the bladder, and it connects the interior of the bladder to an outlet between the ears of the animal, but tunneling the tube to outside the abdominal muscle layer on the abdomen, and then tunneling it all the way around the body on the right side, and to finally have it emerge out of an incision behind the ears to prevent the animal from getting easy access to destroy it. The Suprapubic tube is secured with silk sutue at the bladder, abdominal muscle wall and near the outlet. The tube is sealed with a cautery iron to prevent infection. Before closing the incision on the abdominal wall, 60 μl of HPTC is injected onto the urethra (urethrolysis is already performed earlier), to prevent too accidental pushing and handling of the material before the animal is closed.

This outlet can later be assessed and connected to the urodynamic set up to perform awake cystometry. Four animals have been used for the study and they are separate from the groups in Table 1.

3.2.7 **Urethral function with ambulatory urodynamic studies to test for the presence of urinary obstruction**

Ambulatory urodynamic was used to exclusively study the separate group of animals described in 3.2.6 to determine whether an obstructive urethra is involved with HPTC injection. The outlet of the suprapubic tube is cut open with scissors to allow access for the bladder. The rat, which is awake, is placed in a metabolic cage with a scale at the bottom to catch the volume of urination. The tubing is connected to the syringe pump as well as the Duet Logic transducer. The tube is infused with water at 100ul/min, and the voiding pressure and volume is observed for a period of 30 minutes.

3.2.8 **Cytotoxicity—assessment of In vitro cell viability when HPTC is co-cultured with cells**

HFF cells were plated on 24 well plates in triplicates for each group at 50% confluency. In the first group, HFF cells are just incubated with culture medium alone. In the second group, 0.2ml HPTC was loaded directly on top of the cells as a think layer that cover the surface of the cells, before adding the same amount of medium. The last set of wells simply has medium and no cells in it. The culture is allowed to grow at 37°C for 3 days.

All media and HPTC are removed by aspiration and washed twice with sterile 1X PBS. MTT assay is carried out for 30 minutes as per the manufacturer's instructions. The increase in absorbance at 490nm should indicate the relatively amount of live cells in each well. The absorbance is read on an automated Bio-rad plate reader (xMark Microplate Absorbance Spectrophotometer).

3.2.9 Histological assessment of the injection sites

Animals are sacrificed and their bladder or urethral tissues are harvested and placed immediately in 10% neutral buffered formalin overnight. The tissues are then rinsed under running water for 2 minutes, and then placed in 30% sucrose solution to dehydrate for at least 24 hours. Transverse section of the urethra are made on the area of injection and embedded with OCT for cryosection. 5um sections were cut and put on glass slide. One section per animal was further stained with H&E stain.

3.2.10 Assessment of macrophage-mediated erosion on HPTC

We evaluated the biodegradation of HPTC in vivo as well as in vitro by culturing macrophage line J774.1A directly on top of HPTC for 2 weeks in quadruplicate. Our goal is to determine whether extracellular enzymes secreted by macrophage could digest the polymer, creating craters on the surface that has been reported[11] in for biodegradable polymers with digestable ester bonds in the backbone.

2 samples were trypsinized before 3 1XPBS washes. 2 samples were gently washed with PBS without trypsinization. The samples were then dried on top of parafilm in a vacuum desiccator for 3 days. Dried samples were processed by gold sputtering. Nova 600 DualBeam™ SEM/FIB was used to visualize the surface topology of HPTC cultured with J774A for 2 weeks.

3.2.11 Assessment of whether HPTC migrates to other organs

To test for the potential migration of HPTC, presence of trace amount were tested in spleen, lungs, liver, inguinal land iliac lymph nodes was investigated. Whole organ tissue digest was

performed on at least 3 animals per group per time point listed in Table 1. Samples were submerged in 1.0 M Potassium Hydroxide (KOH) incubation for 2 weeks, until organic matters were liquefied. Samples were centrifuged for 15 minutes at 15000g to pellet down the inorganics or non-degradable biomaterials at the bottom. These positive controls were used to check the validity of the test and its sensitivity. (A) Half a bladder injected with 30 µl of HPTC; (B) half a bladder injected with 5 µl of HPTC, (C) Half a bladder injected with 2 µl HPTC, and (D) just HPTC alone without digest. The entire pellet layer is transferred to the reader of the Fourier transform infrared spectroscopy (FTIR) machine, and the absorbance is read at the range of 400 to 4000nm. Peaks specific to HPTC absorbance are compared to the pellets of the KOH digested fractions.

3.3 RESULTS

3.3.1 HPTC augments the bladder wall and integrates well with the native tissue

HPTC was very easy to inject through 25G needle, which is the needle size appropriate for the animal injection (Figure 1a). Injection was smooth and the control of the volume is excellent compared to sub-optimal formulations of HPTC (which can be too runny and hard to have fine control of the volume, or too hard to inject). Injection of HPTC into the bladder wall was used as an assessment method for its biocompatibility, in terms host response, presence of fibrous capsule, integration of the hydrogel with the native tissue, inflammatory response. The injected HPTC shows a distinct outline on the bladder wall (Figure 1b), and it is elastic enough to stay put in the injection site without leaking out the puncture point where the needle was inserted.

Histology of the tissues shows that HPTC augments the bladder wall well with a bulking appearance (Figure 2) in all the bladders harvested at various time points (1 hour, 1 day, 2 weeks, 4 weeks, 6 weeks and 24 weeks post-injection). The general appearance of the injection site is similar at all time points, with a bulking effect that augments the tissue, and absence of any fibrous capsules detected by H&E and immunofluorescence staining with anti-fibroblast antibody (Figure 3) that showed positive staining in the spleen positive control. In contrast, Macroplastique at 3 weeks elicited extensive fibrous capsule around all the injected materials (Figure 3C), and showed poor signs of tissue integration.

3.3.2 Cells, predominantly histiocytes, infiltrate HPTC, but HPTC is resistant to macrophage mediated degradation

Examination of the HPTC injection site reveals that large amount of cell infiltration is found 1 day of injection, whereas 1 hour post-injection, no cell infiltration is seen. It suggests that cell infiltration occurs between 1 hour and 1 day. In figure 4a, high density of cells infiltrated HPTC 1 day post-injection in the urethra. In figure 4b, the histiocytes seem to be less dense at 24 weeks, but still present.

Due to the large amount of histiocyte infiltration, the concern was raised that these tissue macrophages may phagocytose HPTC. We conducted an experiment to test HPTC's resistance to macrophage-mediated digestion. 4 HPTC were incubated with J774A grown directly on top of it for 3 weeks. For the HPTC gels with cells were trypsinized off of the surface, the topography of HPTC on SEM looked smooth, with no signs of erosion. For the HPTC gels with cells still attached to them, SEM images showed that the surface of HPTC remained smooth, with no signs of material degradation underneath the cells. In contrast, biodegradable material

polytrimethylene carbonate (Figure 5c, adapted from Bat et al.[11]) that has undergone the same treatment shows severe surface erosion by J774A. Histological images also display an abundance of HPTC after 24 weeks, thus further weaken the concern over biodegradation over time due to the presence of histiocytes.

3.3.3 HPTC is likely to be non-cytotoxic, but does show a drop in cell number when co-cultured with HPTC on top

HFF cells grown direct contact with the injectable material on top of the monolayer of cells for three days shows a decreased number of cells as the MTT absorbance at 490nm decreased from HFF cells at 1.67±0.06 to HFF cells with HPTC on top , at1.32±0.04 (which is 79.2% of the HFF value) (Figure 6). There is a significant difference in the cell number with a p-value of 0.00073. A certain degree of decrease in the cell number is expected just due to the fact that nutrient and oxygen diffusion into the cells with a mass of HPTC sitting on top would be somewhat hindered compared with pure medium culture in the cell only group. A decrease of the value to 79.2% of the positive control indicates that it is unlikely to be a cytotoxic event because the percentage is still relatively high.

3.3.4 HPTC has good potential to be co-injected with cells for cell-based treatment

Co-injection of processed lipoaspirate cells with pHEMA material to test the potential of using the material as a vehicle for cell therapy—cells premixed or just injected directly next to the pHEMA injection sites on the bladder are found in abundance inside the HPTC injection site 4 weeks post-operative (found in 2 out of 2 rats). When cells are injected alone, they mostly dissipated with only few cells remaining, given the same conditions. Along with the finding that

there is an abundance of host cells that infiltrate into the pHEMA material within 1 day of injection, and the fact that a high percentage of DiI labeled cells are retained at the injection site, they suggest that the pHEMA can potentially be used in conjunction with cell therapy, or be used as a cell delivery vehicle for treatment of soft tissue defects.

3.3.5 HPTC successfully restores urethral function in the animal incontinence model for up to 24 weeks

The average ALPP for healthy Lewis rats is 16.1±5.5 cmH_2O, as shown in the preoperational ALPP in Figure 9a. Following the urethrolysis procedure, ALPP falls to 3.7±1.8, 5.1±2.3, and 3.1±1.3 cmH_2O 2, 9 and 24 weeks post-operation, when no treatment was given (Figure 10a).

However, urethral function in animals receiving 60 µl of HPTC injection was immediately improved at 2 weeks when the animals recover enough from the surgery to have urodynamic procedure performed, compared to its urethrolysis only counterpart. The post-operation ALPP for this group receiving 60 µl HPTC after urethrolysis had the ALPP restored to a level similar to the pre-operation average, at 17.5±5.6, 17.7±4.1, 10.2±1.0 cmH_2O at 2, 9 and 24 weeks respectively. Urethral function based on ALPP is significantly improved compared to the urethrolysis only group using the hierarchical linear model with random intercepts statistical analysis.

3.3.6 HPTC restoration of urethral function is dose-dependent treatment

We tested the dose-dependence of the amount of HPTC injected. For this group, we injected only half the amount, 30 µl HPTC instead of 60 µl after urethrolysis. The results show

that the improvement in ALPP was in between no injection and the 60 µl injection, at 8.8±3.6, 13.3±3.6, 9.6±3.6 cmH_2O at 2, 9 and 24 weeks respectively, indicating that the injection volume plays an important role in the success in restoring the pre-operational ALPP value of the bulking in the urethra. The ALPP improvement lasts 24 weeks for this group as well.

3.3.7 HPTC is a longer-lasting and more effective treatment option than injecting PLA cells alone for incontinence

Co-injection of DiI labeled ASC with 60 µl of pHEMA material resulted in a smaller improvement in ALPP compared to just the 60 µl material alone. Comparison of FDA-approved Macroplastique and Coaptite were attempted in the rat model with the injection performed with a performed with a 21G needle instead of a 25G needle because it would not flow through that needle size, and the results were only arbitrary because the injury on the urethra created by the oversized needle shaft could have contributed to the limited improvement in ALPP, when the animals survived the procedure (mortality rate of 3 out of 5 animals for Macroplastique and 2 out of 3 for Coaptite).

3.3.8 No urinary obstruction observed in rats receiving 60 µl of HPTC injection

Ambulatory urodynamic study showed that all three animals implanted with suprapubic tubes on the bladder dome (for urethral augmentation during urodynamics studies) for 2 weeks showed no sign of urinary retention or blockage of urethra. They were all capable of voiding large, normal voiding volumes when they were not under any anesthesia.

3.3.9 HPTC is durable in vivo and still remain in tissues at 24 weeks

As HPTC is formed as a covalent interpenetrating network with a robust backbone, it is not expected to be easily degradable over time, even in the presence of enzymes commonly found in tissues such as lysozymes, hyaluronidase and collagenase. Figure 2b shows that at 24 weeks, HPTC injected in the bladder wall is still highly intact and have a similar appearance to the bulking effect seen when the injection is initially performed. Presence of HPTC in the 24 week sample of the urethral section also suggests its non-degradability. This finding is consistent with the observation that HPTC is resistant to macrophage digestion in vitro.

3.3.10 The occurrence of urethral reattachment to the vagina 24 weeks post-operation is much more prominent in animals receiving 30 or 60ul of HPTC in the urethra following urethrolysis

In Figure 14, the pictures showing typical urethras for the urethrolysis only group, urethrolysis 30ul HPTC, and urethrolysis + 60ul HPTC are shown. The urethras of rats with urethrolysis alone usually have the entire urethra still detached from the vagina even at 24 weeks (2 out of 8 animals), and all of the animals examined with the 30ul HPTC injection (3 out of 3 animals, Figure 14 b) and 60 ul injection (6 out of 6 animals) (Figure 14d) showed vaginal reattachment. The percentage of the vaginal reattachment is shown in figure 14a, where .the urethrolysis only group has 25% vaginal reattachment at 24 weeks, while urethrolysis + 30 ul HPTC or 60ul HPTC has 100% vaginal reattachment.

3.3.11 No sign of HPTC migration is detected

We inspected 14 HPTC-injected animals' spleen, lungs, liver, inguinal lymph nodes, pelvic lymph nodes for signs of material migration by FTIR. 4 animals are sacrificed at 2 weeks post-injection, 4 animals at 4 weeks, 4 animals at 9 weeks, and 2 animals at 24 weeks. No trace of HPTC had been detected by this method in any of these organs, while the positive control with whole organ digest containing 2 μl of HPTC showed 4 peaks that are specific to the presence of HPTC.

3.4 DISCUSSION

This study describes a novel synthetic interpenetrating polymer network, HPTC, that is formed with HEMA, PEGMA and TEGDMA precursors polymerized around a suspended mass of CMC chains in water, during free radical polymerization. The resulting hydrogel, HPTC, has a range of mechanical properties when polymerized under different conditions. The optimal mechanical property was chosen for the purpose of using HPTC as an injectable, nondegradable HEMA-based hydrogel that has a elastic modulus close to that of soft tissues. HPTC with 87.5% water, precursor composition of 87.2 mol % HEMA, 0.19 mol % PEGMA, and 12.6 mol % TEGDMA, 0.125 g/ml 90k CMC was used, because of its optimal injectability, combined with its ability to stay in the injection site, while having the ability to stay intact at the injection site short term (within minutes) and long term (months).

HPTC in the above composition is easy to inject through a 25G needle, in order to be used for ultimately injecting into the very small urethra in the rat model. The injected HPTC into the bladder wall shows a distinct outline, and feels supple to the touch. It is also excellent at staying at the injection site and has no problem leaking out the puncture point, where it was a

problem for some other formulations of HPTC where they are not as viscous or have high enough modulus.

In vivo assessment of HPTC shows excellent tissue integration in the bladder and urethra, with cell infiltration into the entire area of the injection site, even deep inside the HPTC material. Bulking appearance can be easily observed in the tissues, and no fibrous capsule can be found in any injection site in over 30 animals at different time points, 2, 4, 6 and 24 weeks.

Histiocytes are observed in the HPTC injection site as soon as 1 day after injection, and although the intensity of histiocytes co-localization subsided over time, they are still present at 24 weeks. To evaluate whether HPTC is resistant to the degradation of macrophages as histiocytes are tissue macrophages, we cultured differentiated macrophage J771A directly on the surface of HPTC for 3 weeks, and then analyzed the topography of the surface with and without the cells trypsinized off of the surface. There was no sign of surface erosion on the HPTC surface, and the topography looked smooth under SEM, suggesting that HPTC is resistant to macrophage erosion. Even though histiocytes are still found within the HPTC implant up to 24 weeks after injection, we do not have evidence that shows that HPTC can be broken down by them, and HPTC is still abundant in both the bladder and urethral tissues at that time point. However, since we did not further investigate the consequences of having the histiocytes present within the HPTC implant at 24 weeks, we are uncertain about the microenvironment within the HPTC site. We are not certain if those histiocytes become frustrated phagocytes and release cytotoxic mediators and proteolytic enzymes[14] to the surrounding environment. We are also not certain if there is any vicious cycle involved between the inflammatory cells and the histiocytes. Such concern was raised when Vijayasekaran et. al. found the association of frustrated phagocytes on the calcium deposit in their poly(HEMA) sponges implanted into rabbit

eyes, where the phagocytes were unable to digest the mineral particles, and as a consequence, inflammatory cells were re-recruited to attempt to clear the debris, which then trigger the degenerating phagocytic cells to become nuclei for further calcification [15]. Although we have not observed any signs of classically activated phenotype in the form of giant cells at any of the HPTC sites, the fate of these histiocytes remain unknown and need to be studied in the future to ensure the implant's safety in the host, and that the surrounding tissues remain normal and healthy. At this point, we cannot rule out the possibility of frustrated phagocytic attempt of the non-degradable HPTC that can consequently release cytotoxic mediators, or cross talk with the inflammatory cells.

HPTC has an interesting tendency to attract cell infiltration in vivo. In as little as one day after injection, cell infiltration is obvious throughout the implant. The mechanism by which the cells are attracted to HPTC is not fully understood, but one or more of the following might shed light to the observation:

(1) HPTC is highly porous and hydrophilic in nature, containing 80-90% of water. Therefore, movement of cells into the implant is non-tortuous due to the lack of physical hindrance.

(2) The majority of the polymeric network is very hydrophilic, consisting of mostly pHEMA and CMC. Cells tend to present favorable morphology and adhesion towards these hydrophilic surfaces. Most synthetic biodegradable polymers require hydrophilic surface modification for desired cellular responses if they are not hydrophilic in nature[16], and increased hydrophilicity of many biomaterials such as nanofibers that have inherently lower hydrophilicity, air or Argon plasma treatment has been widely adapted as a method to improve cell adhesion and proliferation[17-20].

(3) Infiltration of initial cells may facilitate further infiltration of cells through secretion of extracellular matrix or other cytokines. One example of cell-mediated of cell migration into a synthetic scaffold was found in xyloglucan-graft-poly-D-lysine (LCL) hydrogels implanted into caudate putamen of adult rats[21], where initial migration of astrocytes attracted other types of neuronal cells into the implant.

(4) Foreign body response is triggered and inflammatory cells are attracted to the implant due to tissue injury and the nature of the biomaterial. The degree and extent of such foreign body response are affected by the composition, contact duration, degradation rate, morphology, porosity, roughness, shape, size, sterility and surface chemistry of the implant [22]. Chronic inflammation is characterized by the presence of macrophages, monocytes and lymphocytes, along with the increase in blood vessels and connective tissues to the restructured area [23-26]. The end stage of foreign body reaction is usually the formation of a 50-200μm thick fibrous capsule that walls the implant off from the interacting surrounding tissue, but this end stage has not been found in any of the tissue harvested from the animals at up to 24 weeks.

HPTC has been shown in this study to effectively treat incontinence in the rat animal model or urethrolysis by injection of 60μl of HPTC into the urethra, to restore the normal ALPP. Continence has been restored to the normal level of continence prior to the injury model of incontinence. We have ruled out the possibility of urethral obstruction for the restoration of continence with HPTC, by showing that the animals could void normally in large volumes under ambulatory conditions. We have further shown that the treatment with HPTC in the urethra is dose-dependent, as half the volume of he effective dose, 30 μl of HPTC only partially restores the ALPP, to the level between the urethrolysis only control and the 60μl HPTC treatment.

We further evaluated the efficiency of treating incontinence with 60ul of HPTC with 30ul of cells. The ALPP restoration was not as great as the HPTC only group, and we postulated that the total volume loaded could have been too high for the small urethra to handle, and trauma was introduced during the process of the injection of the 90µl volume. We have further evidence of urethrolysis + 60ul HPTC + 30 µl saline that it has a similar ALPP as the urethrolysis + 60µl HPTC + 30µl group, pointing to the likelihood that the reduced efficacy of treatment might be due to volume overload.

We do find that HPTC is a longer-lasting and more effective treatment option than just injecting PLA cells alone for incontinence. The problem with injecting cells alone is that the cells disperse to the surroundings in a short time, in this case, almost completely within 9 weeks post-injection, confirmed by immunofluorescence of the tissue sample and the ALPP (5.1 cmH_2O which is the same as the urethrolysis only level), making cell-only injection a poor choice of long-term treatment for incontinence in the rat model. However, when HPTC is co-injected with the same number of cells, the ALPP maintained at a higher level at 9 weeks (12.2 cmH_2O) and even at 24 weeks (11.5 cmH_2O).

No trace of HPTC was found in the tissue digest of other organs such as spleen, lungs, liver, inguinal and pelvic lymph nodes by FTIP. It is consistent with the abundance of HPTC found in the injection site based on histology and the high ALPP in urodynamic studies even at late time points such as 9 weeks and beyond.

An unexpected observation of the rat urethra from rats with or without the HPTC injection was that rats receiving HPTC injecting have shown a very high rate (100%) of vaginal reattachment to the urethra after the urethrolysis procedure at 2 weeks, while the rats with no treatment only had 25% occurrence of vaginal reattachment. The exact mechanism to which

HPTC might promote vaginal reattachment to the urethra is not known. A possible explanation is that the inflammatory response of the HPTC injection contributed to the production of collagen and other extracellular matrix at the injury site, and that in turn promoted the reattachment of the vagina back to the urethra due to improved adhesion. Another possible explanation is that the cells infiltrated into the HPTC implants excrete cytokines or other cellular signals that promote local repair, and attracted cells that are responsible for improved tissue adhesion.

3.5 CONCLUSION

HPTC has been shown to be biocompatible with no sign of fibrotic capsule formation in vivo, good integration with the soft tissue being augmented, with cell infiltration. Although HPTC attracts histiocytes in vivo, there was no sign of macrophage degradation observed based on in vitro co-culture with the macrophage cell line. MTT assay shows that when HFF cells are grown in direct contact with HPTC immediate on top of the cell monolayer, the MTT absorbance only drops to 79% of its value when there is no material sitting on top of the gel. We evaluated the potential to co-inject cells with HPTC at adjacent injection sites, and showed that the cells seem to be attracted by the HPTC material and strongly co-localized with HPTC 4-weeks post-injection, while the cell-only cells have mostly migrated away, leaving only a few cells behind at the injection site.

HPTC has also been evaluated for its effectiveness as a soft tissue injectable to treat urinary incontinence in the rat model, by injecting HPTC onto the urethral wall immediately following the surgical injury model for urinary incontinence, urethrolysis. First, when 60ul of

HPTC is injected to the urethra of the incontinence model, the ALPP restored to the normal level as soon as we could measure it with urodynamic test at 2 weeks, and the ALPP restoration lasts up to 24 weeks, which is 1/3 of the lifetime of the rat. Second, we found that HPTC treatment is dose-dependent, as half the volume improved the ALPP hallway between the 60ul volume and the urethrolysis only group. Third, we attempted to evaluate the efficiency of treating incontinence with co-injection for HPTC with cells, but due to circumstances related to the injection volume chosen for the experiment being traumatic for the urethral tissue, it was inconclusive whether cells with HPTC can have better potential in improving the urethral function. We found no signs of urinary obstruction in rats receiving 60ul of HPTC as a treatment method, with normal voiding volume and normal voiding pressure. And lastly, reattachment of the urethra to the vagina is dramatically increased with the treatment of HPTC. We postulate that the potential reason for this reattachment is due to cytokine secreted by cells inside of HPTC, that may signal host cells for healing and production of more collagen production, but further studies are necessary to have a better understanding of the observed phenomenon.

3.6 Table

	week				
	0	2	4	9	24
pre-operation	26				
urethrolysis only		8	6	6	9
urethrolysis + 60 µl HPTC		8	5	6	9
urethrolysis + 30 µl HPTC		6	6	3	6
urethrolysis + 60 µl HPTC + 30 µl cells		2	2	2	2
urethrolysis + 60 µl HPTC + 30 µl saline			2		
urethrolysis + 30 µl cells		2	2		
urethrolysis + 60 µl Macroplastique (21G)					2

Table 1. Number of animals used for each group at each time point for urodynamic studies.

3.7 Figures

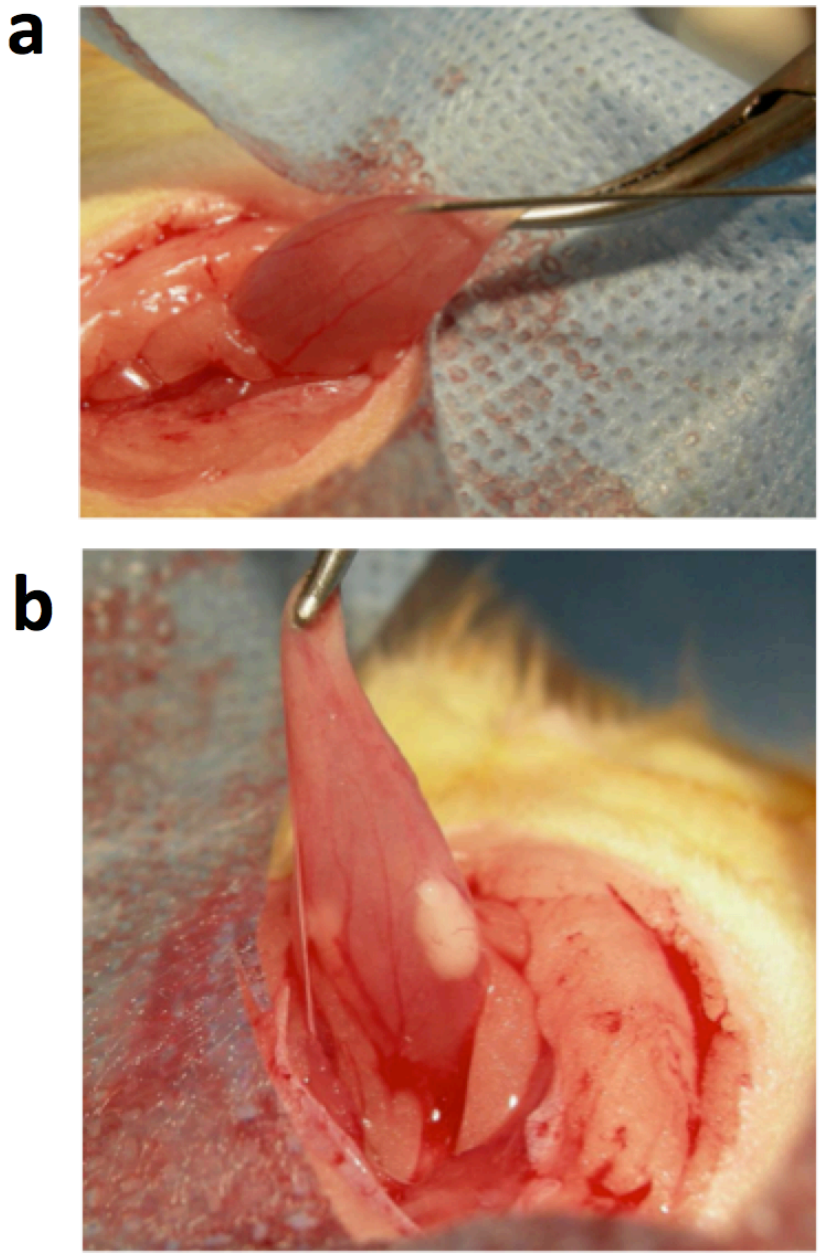

Figure 1. HPTC is injected in to the submucosa of the rat bladder to assess its biocompatibility and ability to augment soft tissue. Optimal HPTC determined in Chapter 2 can be injected through 25 G needles easily with very good volume control with the desirable balance between elastic and fluid property. (a). The injected HPTC with the desirable characteristics identified in Chapter 2 shows a well-defined outline at the injection site, with no leakage of HPTC through the puncture site of the injection.

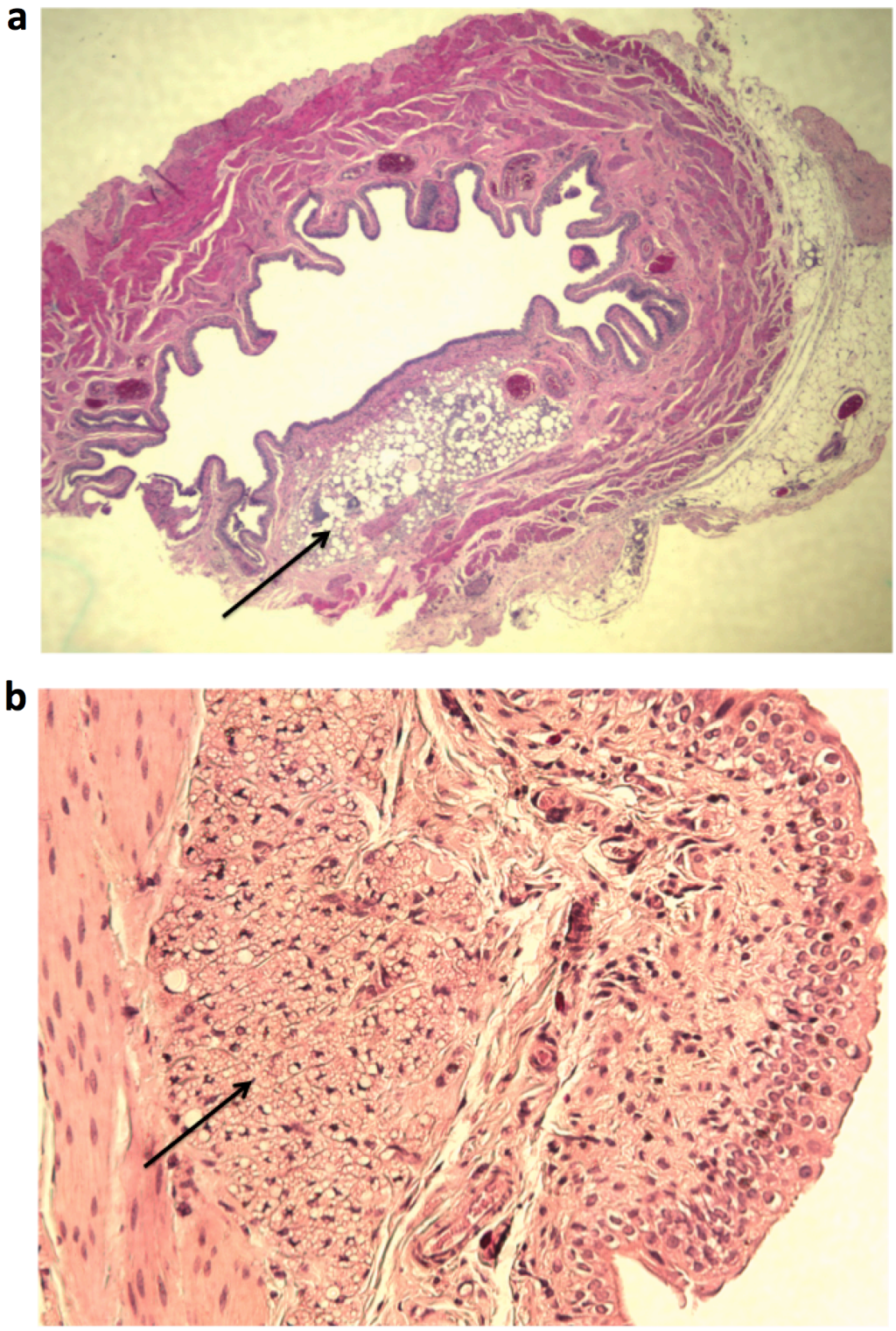

Figure 2. HPTC augments the bladder wall and integrates well with the native tissue. HPTC injected into the submucosal of the bladder shows a bulking effect at (a) 4 weeks post-operation), similar to other soft tissues fillers, with good integration with the native tissues, and (b) 24 weeks post-operation still shows the presence of HPTC, indicating its durability.

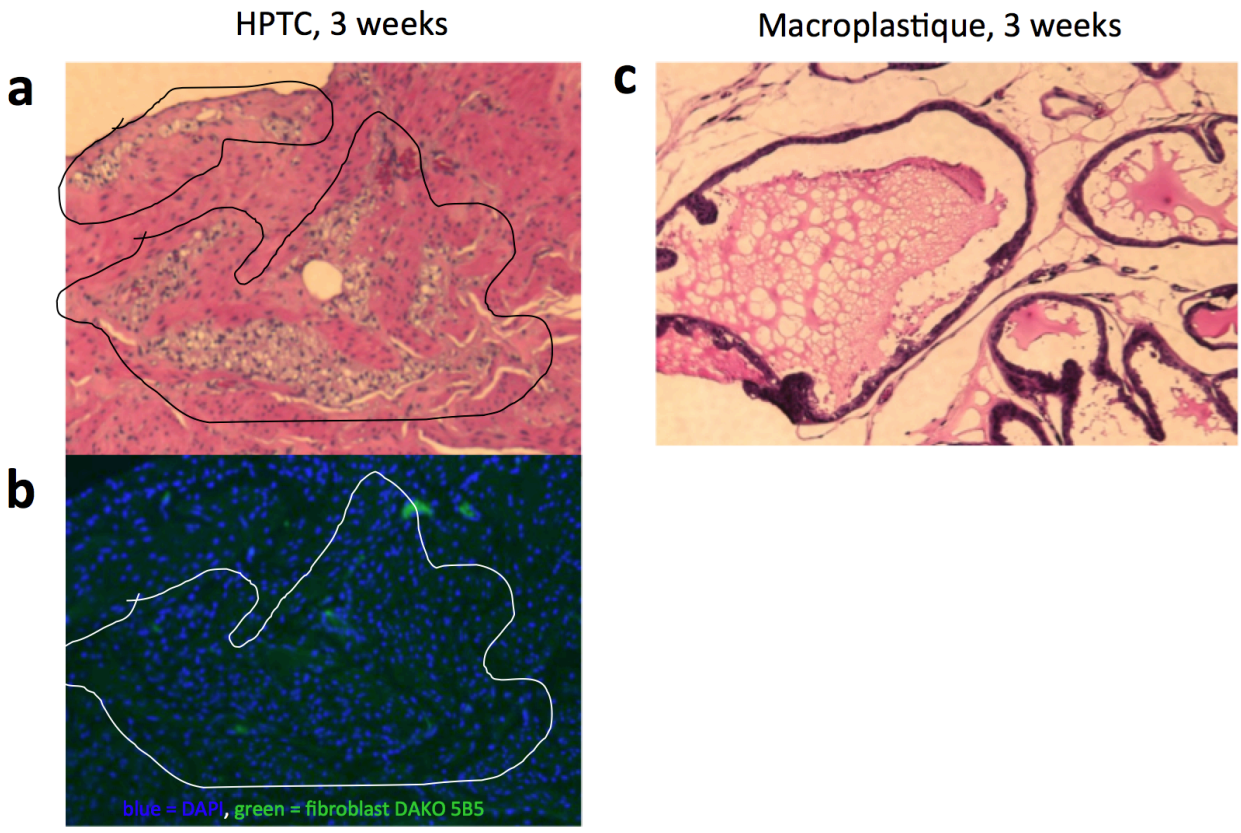

Figure 3. Fibrotic tissues are not found around HPTC injection sites. Shown here in (a) is a 3 weeks post-injection of HPTC onto the bladder wall, showing no signs of fibrosis on H&E staining and immunofluorescence staining with anti-fibroblast antibody DAKO 585 on an adjacent section of the same bladder, (b) whereas for Macroplastique injection, thick fibrotic tissue is evident around the injected elastomeric particles. The positive control for the DAKO 5B5 on spleen tissue confirmed positive fibroblast staining (not shown). No fibrotic capsules have been found in any of the animal tissues with HPTC injection at 2, 4, 9, 16 and 24 weeks.

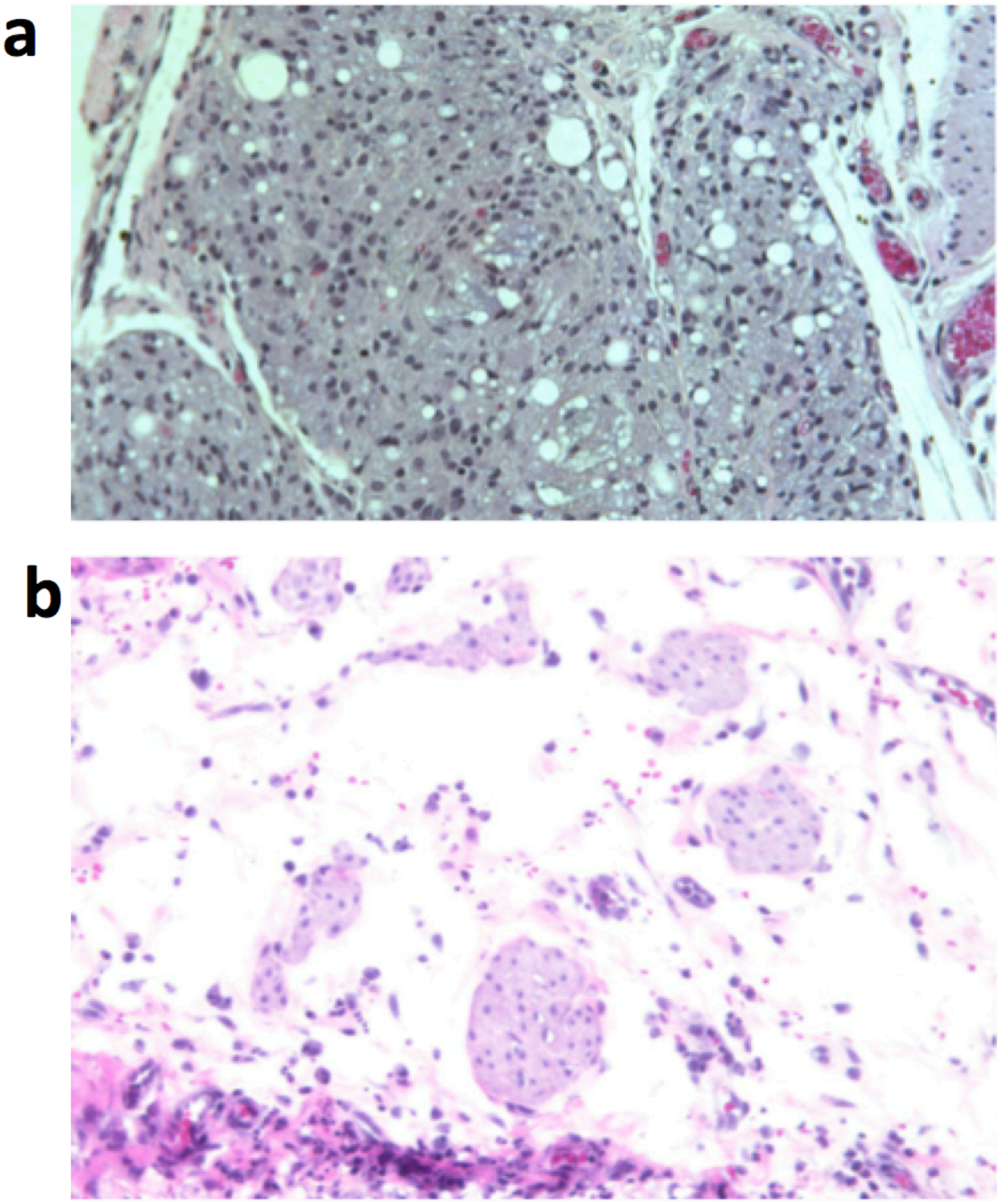

Figure 4. Large number of cells, predominantly histiocytes, infiltrate into HPTC after bladder or urethral injection.(a) 1 day H&E stain of HPTC-injected urethra shows cell infiltration as early as that time point. When the same experiment was repeated at 30 minute time point post-injection, the gel was blank without cells, indicating cell infiltration happens between 30 minutes and 1 day (not shown). (b) Histiocyte density seems to decrease in general at later time points such as 9 weeks or later. Shown here is a urethral section with HPTC injection at 24 weeks.

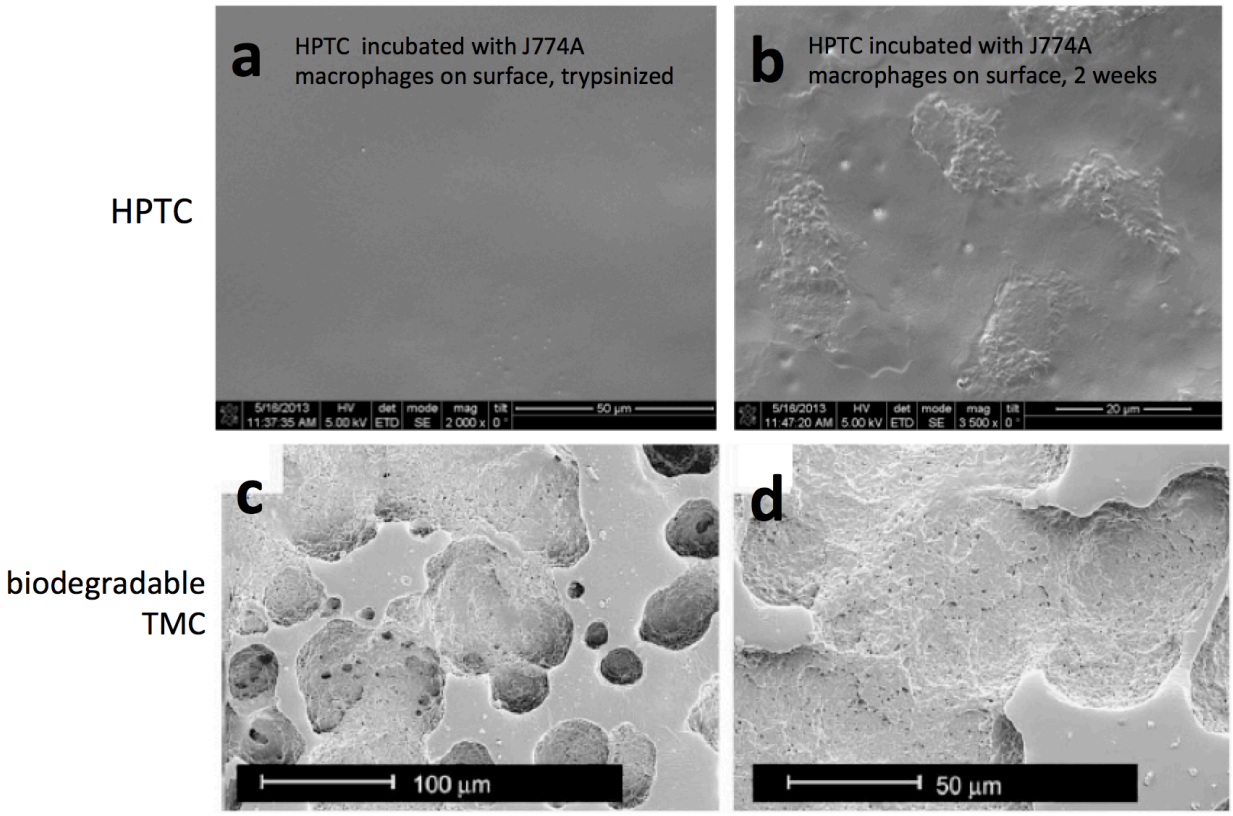

Figure 5. HPTC resists digestion by macrophages.(a) differentiated macrophage cell line J744A is grown directly on top of HPTC surface for 2 weeks, and before the processing of the SEM sample, the cells are trypsinized off the HPTC surface. No signs of surface erosion is observed. (b) HPTC with differentiated J774A cells still attached (not trypsinized here) is subjected to SEM, and no HPTC erosion can be found in areas under the cells. In contrast, SEM images adapted from Bat et. al. [11] (c-d) with J774A cells grown on top of trimethylene carbonate, which has ester backbones prone to degradation, shows 100-100um diameter signs of erosion.

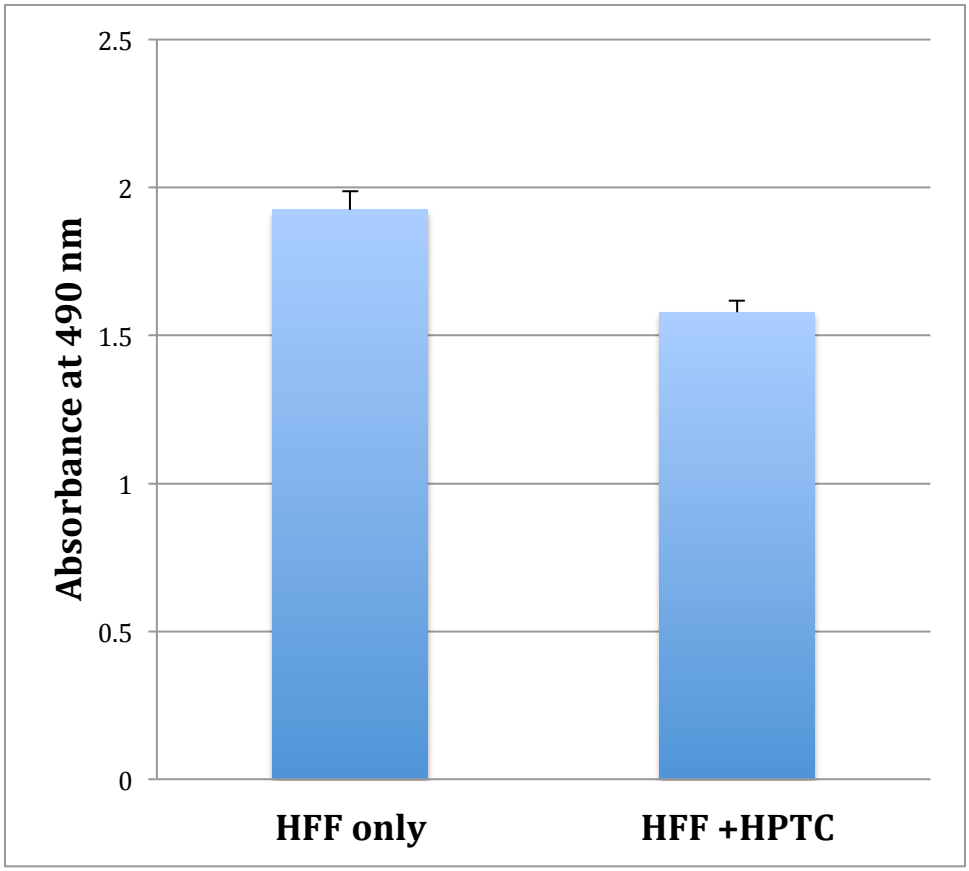

Figure 6. HFF cells co-cultured with HPTC have an 82% survival rat compared to cells cultured alone. MTT assay shows that HFF cells grown together with HPTC showed an 18% reduction in cell number compared to just HFF cells only, over a period of 3 days ($p = 0.0007$*).

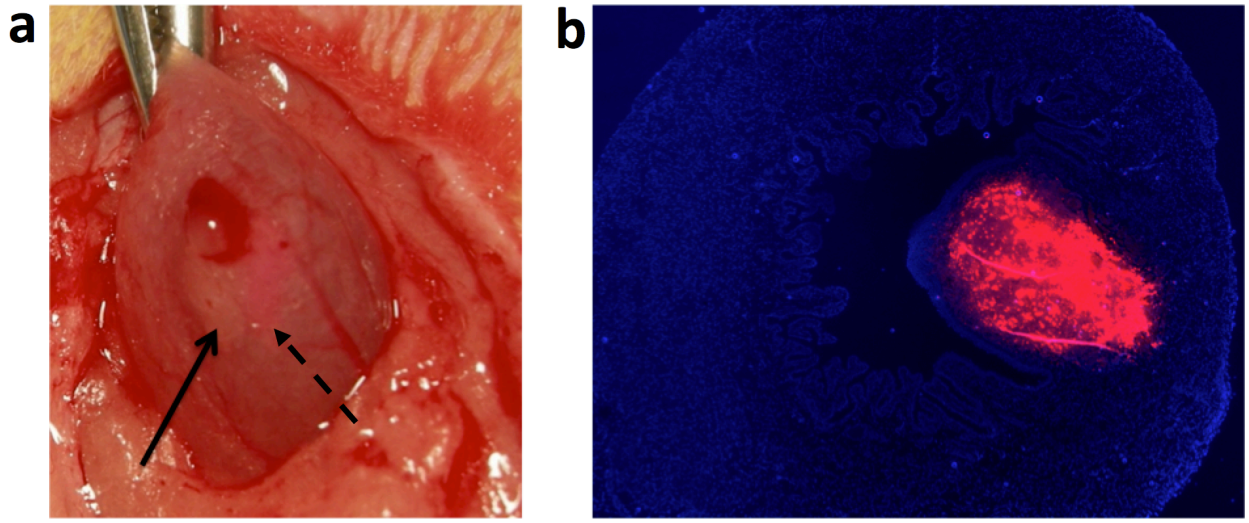

Figure 7. Co-injection of PLA cells directly adjacent to HPTC shows that cells migrate into the HPTC and remain highly localized there even 4 weeks post-injection, at which point cells would normally migrated away if only cells are injected alone.
(a) pHEMA gel was first delivered into the bladder wall (solid arrow) and $2X10^6$ DiI-labeled PLA cells were injected to the immediate right (dashed arrow) (b) immunofluorescence with just DAPI stain demonstrates that the cells are distinctly localized to the pHEMA injection site after 4 weeks, which would otherwise have been dispersed with cell injection only(data not shown).

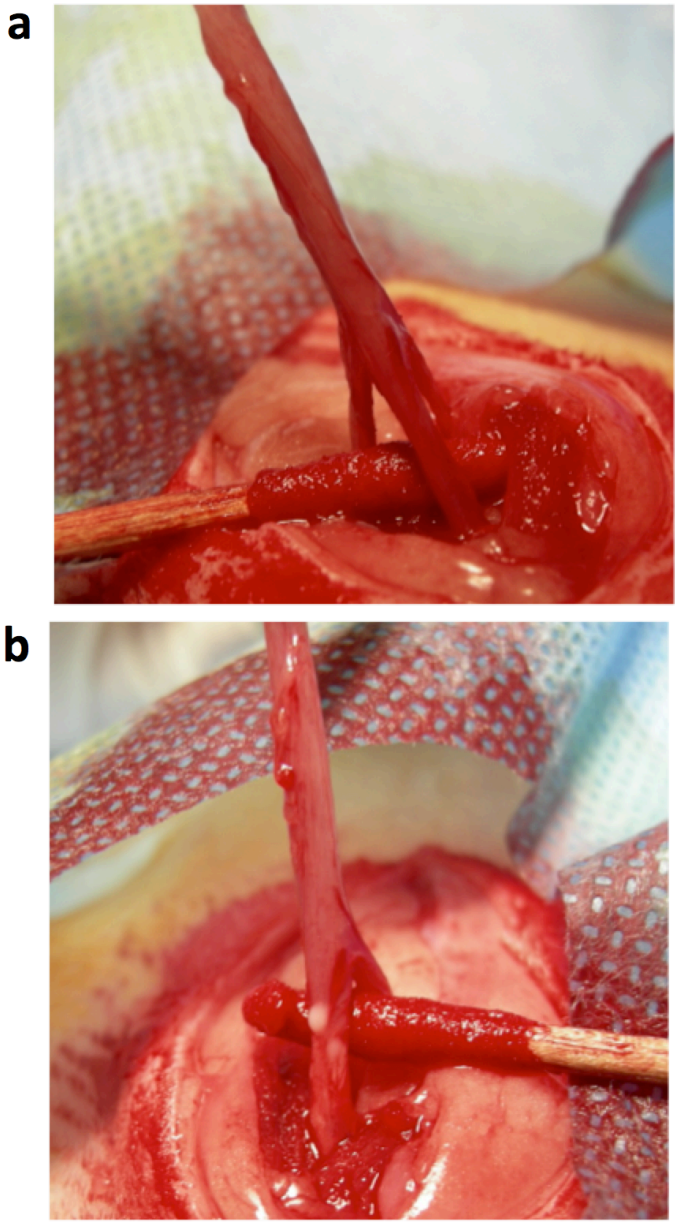

Figure 8. Surgical model of urinary incontinence, urethrolysis, followed by injection of HPTC onto the urethra as an augmentation method. (a) Urethrolysis is performed on healthy, young (2-6 months old) Lewis rats to create an incontinence model by disconnecting the urethra from all connective tissues and adjacent organs. (b) HPTC is injected onto the urethral wall at 3-4 spots around the urethra after urethrolysis, and they can be seen as white globules with well-defined borders post-injection.

a

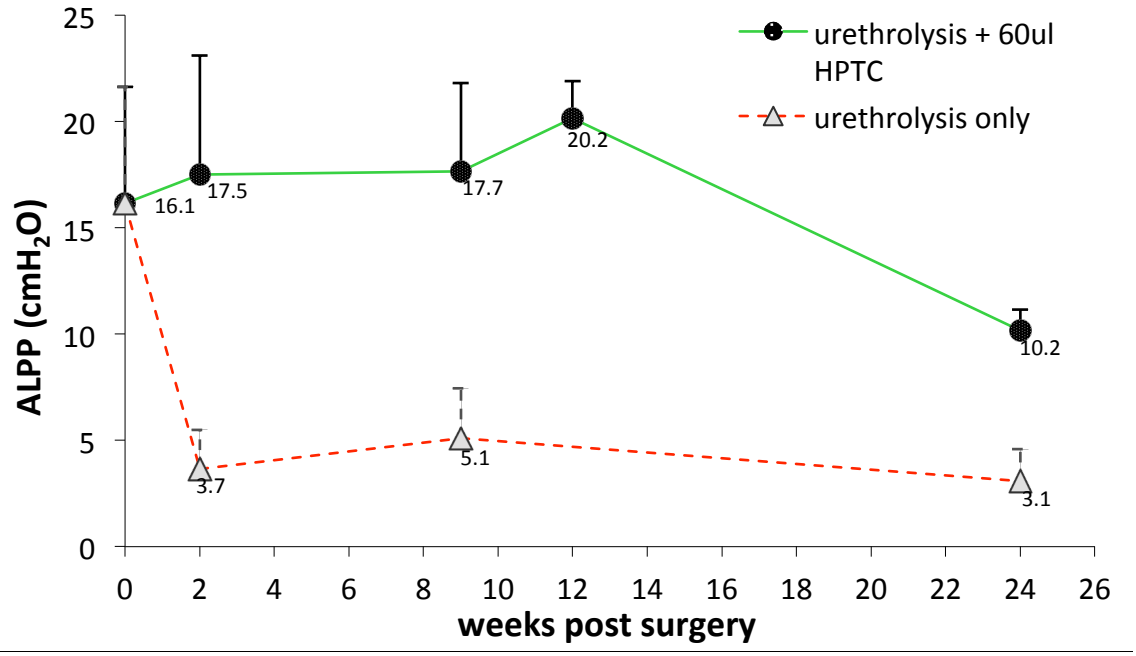

b

ALPP	week	chi2	P>chi2
urethrolysis + 60 µl pHEMA vs. urethrolysis only	0	0.01	0.9169
urethrolysis + 60 µl pHEMA vs. urethrolysis only	2	16.1	0.0001*
urethrolysis + 60 µl pHEMA vs. urethrolysis only	9	22.5	0.0000*
urethrolysis + 60 µl pHEMA vs. urethrolysis only	24	5.37	0.0205*

Figure 9. Abdominal Leak-Point Pressure (ALPP) of rats receiving no injection after urethrolysis dropped dramatically, while rats receiving injections of 60 µl pHEMA have significant restoration to the pre-op level ALPP. The group of rats that received no injection has reduced ALPP following the urethrolysis procedure, the surgical model of incontinence by disconnecting the urethra from the neighboring tissues and severing the majority of the blood supply for the urethra. The impairment in urethral function after the urethrolysis procedure has been shown to sustain for up to 24 weeks, with the ALPP reduced from the average of 16.1 cmH_2O pre-operation, to between 3 and 6 cmH_2O up to 24 weeks post-operation. Similar observations have also been reported by other studies [Zhang et al, 2005]. However, the group of rats that received injections of 60 µl of pHEMA material on the urethral wall immediately after the urethrolysis procedure had the ALPP restored to the pre-operation level, with the effect lasting up to 24 weeks. Figure 9b. The ALPP of the rats in the two groups are statistically different at 2, 9 and 24 weeks *.

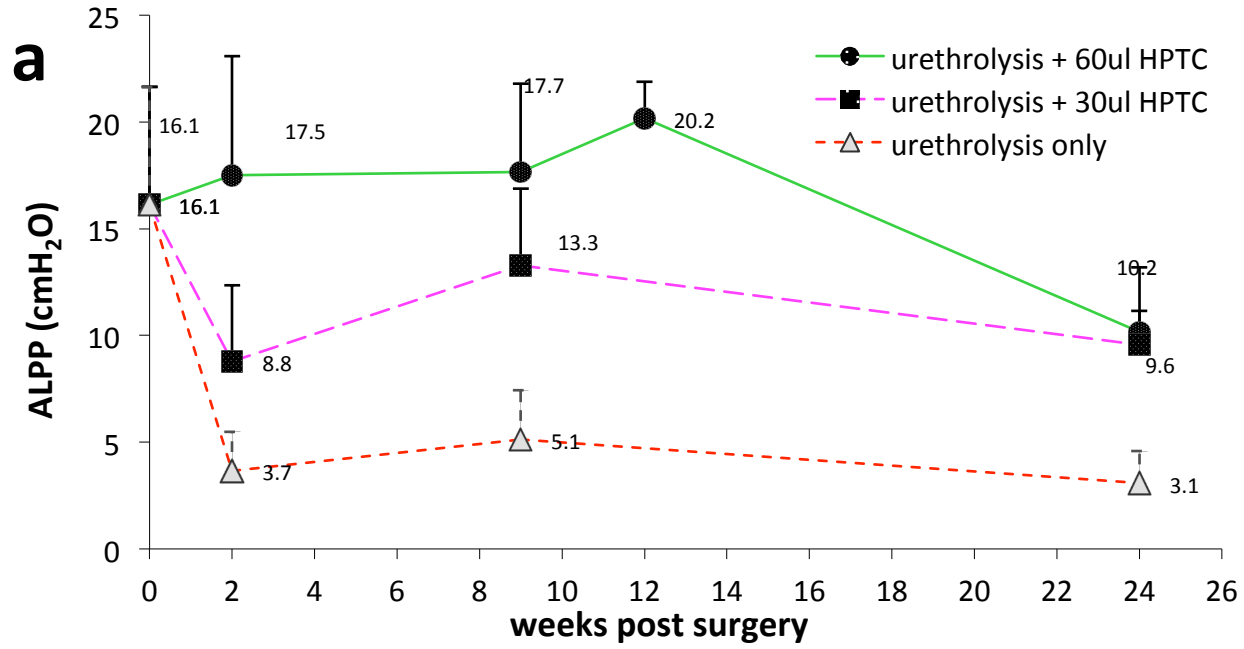

b

ALPP	week	chi2	P>chi2
urethrolysis + 60 µl pHEMA vs. urethrolysis + 30 µl pHEMA	0	1.69	0.1931
urethrolysis + 60 µl pHEMA vs. urethrolysis + 30 µl pHEMA	2	0.1	0.7525
urethrolysis + 60 µl pHEMA vs. urethrolysis + 30 µl pHEMA	9	0.14	0.7104
urethrolysis + 60 µl pHEMA vs. urethrolysis + 30 µl pHEMA	24	0.87	0.3502

Figure 10. Restoration of ALPP with the pHEMA injection is dependent on the volume of material injection. When 30 µl of pHEMA is injected instead of 60 µl, the ALPP is somewhere in between the urethrolysis only group and the one receiving 60 µl material. The 30 µl group is significantly different from the urethrolysis group, while not significantly different from the 60 µl pHEMA injection group at 2, 9 and 24 weeks.

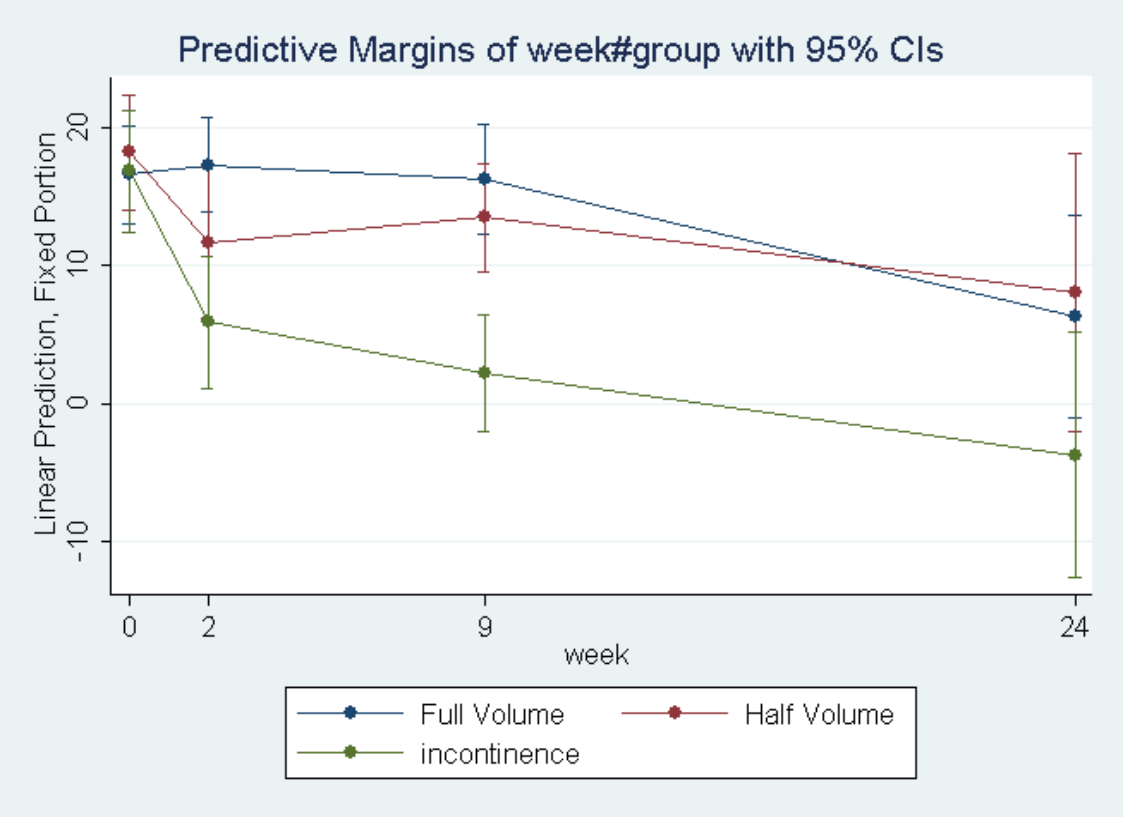

Figure 11. Hierarchical linear model with random intercepts by rat to control for repeated measures by rat reveals that all groups are statistically significantly different from each other at 2, 9 and 24 weeks.

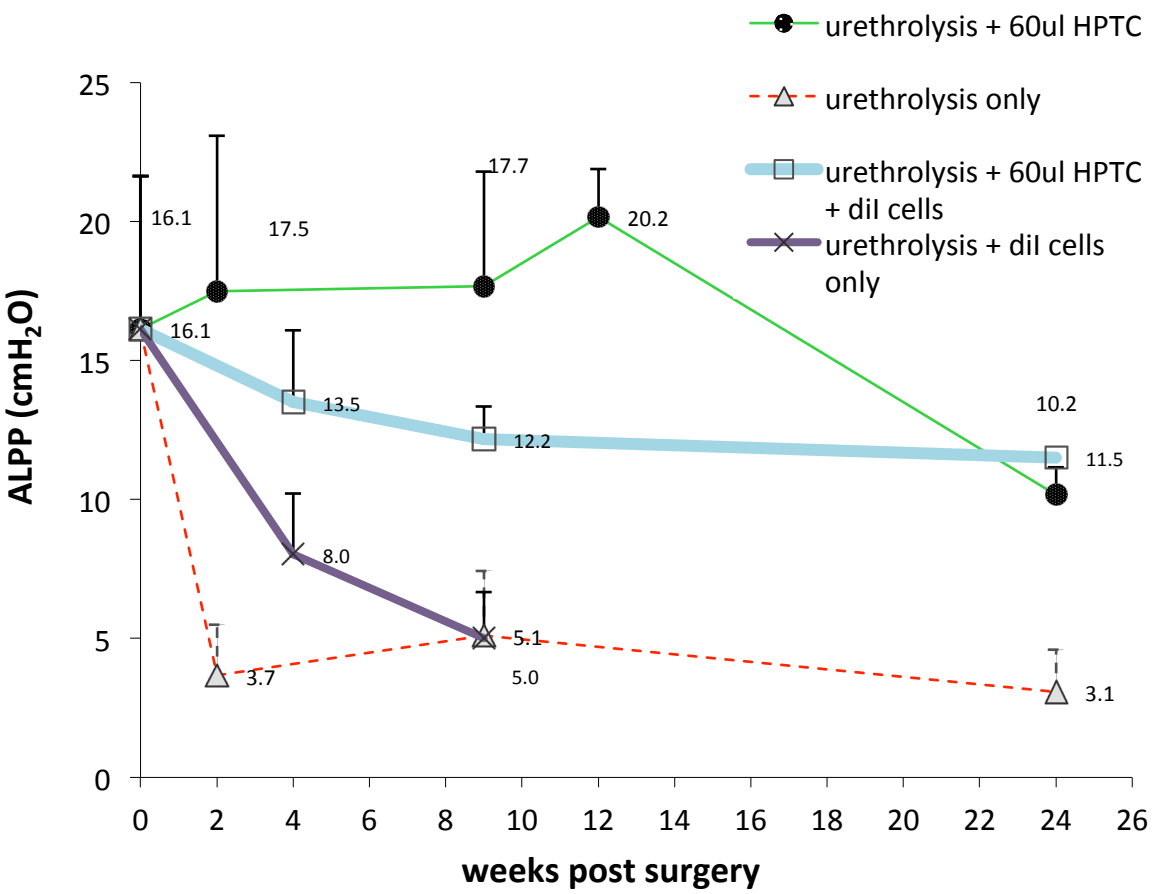

Figure 12. Co-injection of HPTC with PLA cells shows improvement in ALPP compared to treatment with 30 µl PLA cells alone, but compared to treatment with just HPTC alone, it did not improve ALPP quite as well. Injection of cells only (thick solid purple line with cross markers) shows some improvement in ALPP at 4 weeks, and the cells' bulking effect dissipated completely by 9 weeks. Cells co-injected with 60 µl HPTC (solid light blue line with open square makers) has higher ALPP compared to cells alone at 4 and 9 weeks, and the effect is sustained up to 24 weeks. The hypothesis for this line to be not at the same or higher level than the HPTC alone (solid think green line) is that the total volume injected, 90ul, (60 µl of HPTC with 30 µl of cells), might be too large a volume for the urethra to handle and it causes trauma to the urethra.

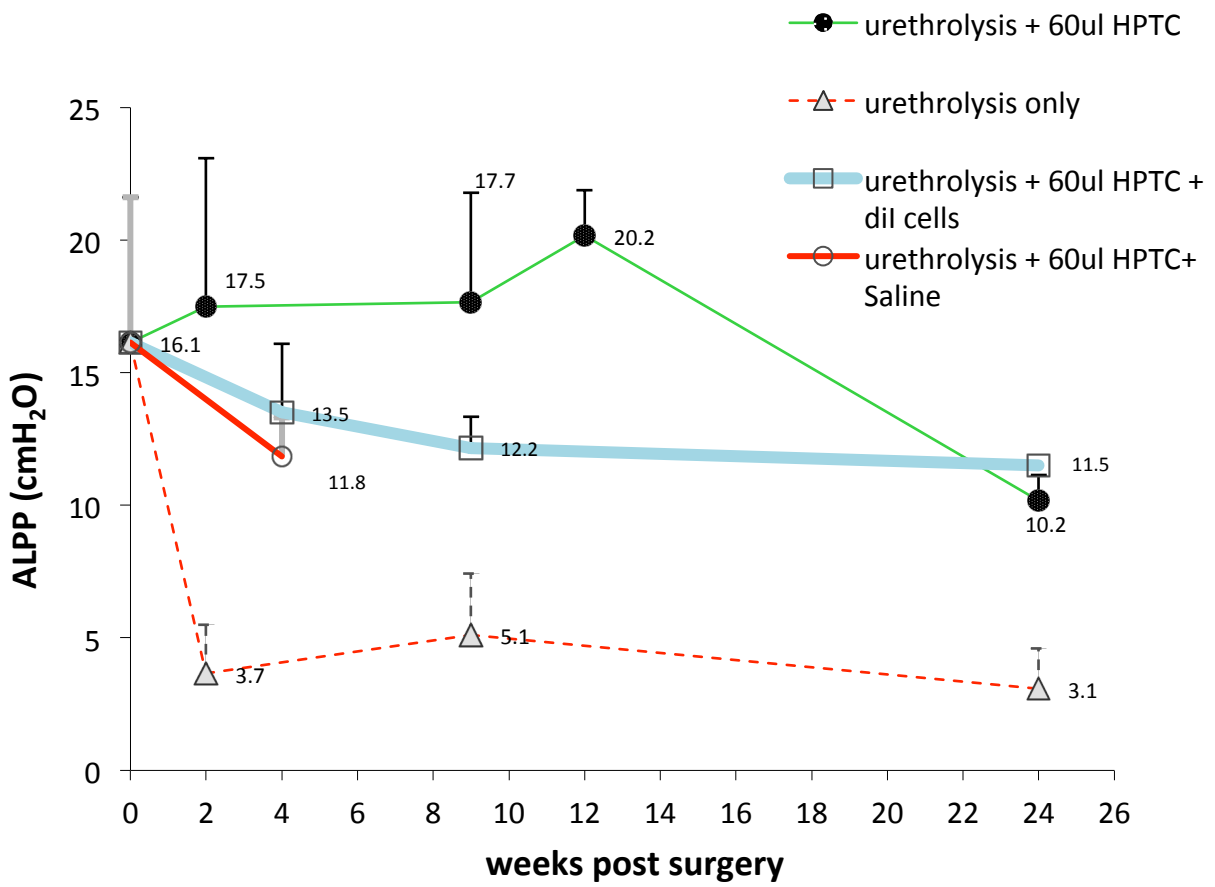

Figure 13. Injecting an oversized volume could reduce the restoration potential with HPTC-cell co-injection. To test the hypothesis that injecting 90 µl total volume might be the reason why the restoration of ALPP for 60 µl HPTC + 30 µl cells is not as big an improvement as injection of 60 µl HPTC only (green line with circles markers), we inject the same total volume using 60µl HPTC and 30 µl saline in one more group of animals (solid red line with open circle markers) to test if it has a lower ALPP compared to just 60 µl HPTC alone. The red solid line shows that the ALPP indeed is lower than that with 60 µl HPTC alone, suggesting the 90 µl is an overloading volume that could be detrimental to the urethra itself, and ALPP restoration by HPTC is not as prominent due to the possible trauma.

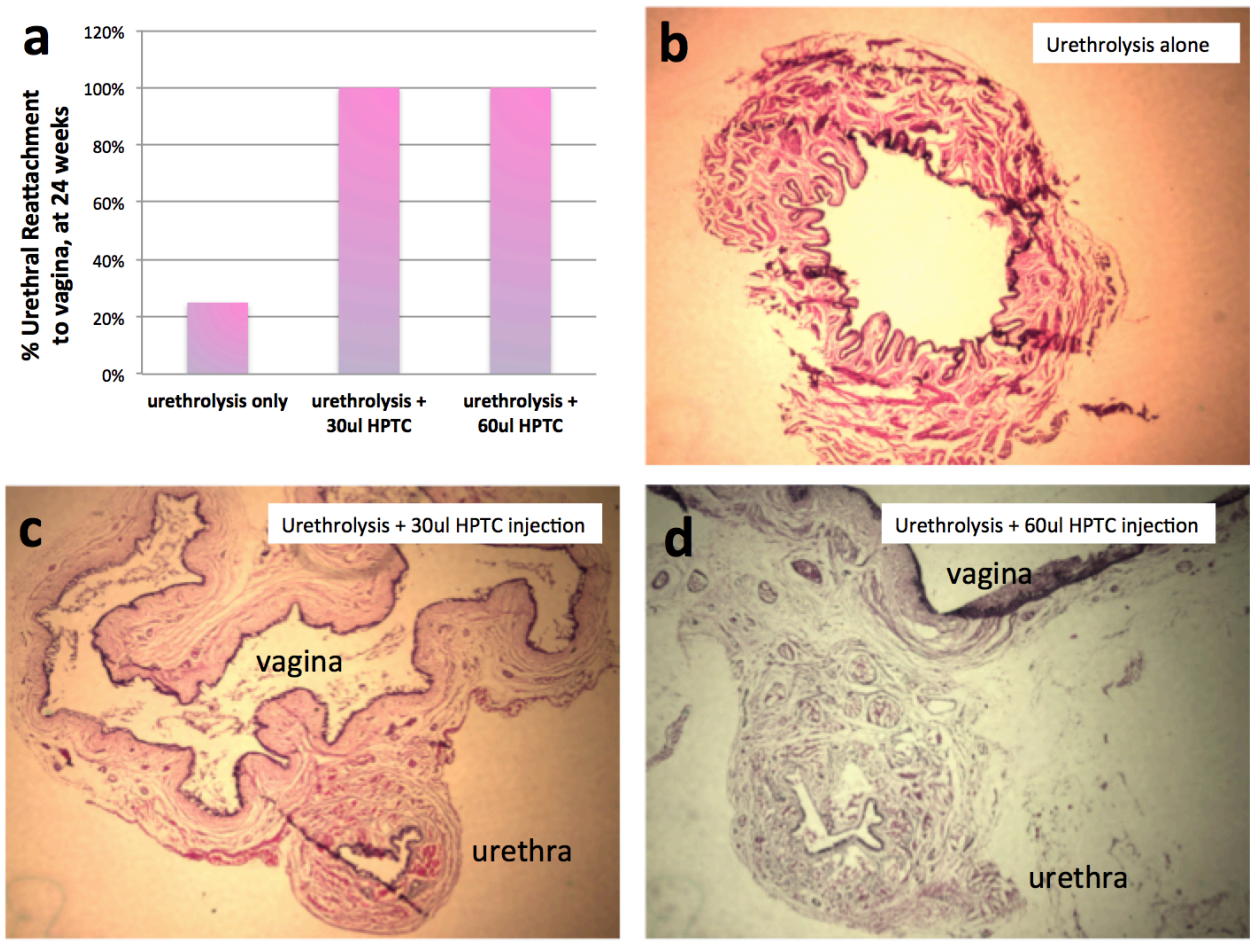

Figure 14. Urethral reattachment to the vagina after urethrolysis at 24 weeks is dramatically improved HPTC injection. (a) Urethra after urethrolysis typically remains detached from the vagina at 24 weeks without treatment. Shown on the graph for urethrolysis only, the percentage of urethral reattachment to the vagina is only about 25% (2 out of 9 animals). However, the percentage of urethral reattachment to the vagina dramatically increases as HPTC is injected into the urethral wall, at 100% reattachment rate for both 30 µl and 60 µl HPTC (3 out of 3 animals and 6 out of 6 animals). The p-value for these

References

[1] S. S. Lane, M. Morris, L. Nordan, M. Packer, N. Tarantino, and R. B. Wallace, "Multifocal intraocular lenses," *Ophthalmol. Clin. North Am.*, vol. 19, no. 1, pp. 89–105, 2006.

[2] G. Barrett, "Multicenter Trial of an intraocular hydrogel lens implant," *J. Cataract Refract. Surg.*, vol. 13, no. 6, pp. 621–626, 1987.

[3] Q. Zhang, Z. Fang, Y. Cao, H. Du, H. Wu, R. Beuerman, M. B. Chan-Park, H. Duan, and R. Xu, "High refractive index inorganic-organic interpenetrating polymer network (IPN) hydrogel nanocomposite toward artificial cornea implants," *ACS Macro Lett.*, vol. 1, no. 7, pp. 876–881, 2012.

[4] S. D. Lee, G. H. Hsiue, C. Y. Kao, and P. C. T. Chang, "Artificial cornea: Surface modification of silicone rubber membrane by graft polymerization of pHEMA via glow discharge," *Biomaterials*, vol. 17, no. 6, pp. 587–595, 1996.

[5] C. M. Keow, F. A. Bakar, A. B. Salleh, L. Y. Heng, R. Wagiran, and S. Siddiquee, "Screen-printed histamine biosensors fabricated from the entrapment of diamine oxidase in a photocured poly(HEMA) film," *Int. J. Electrochem. Sci.*, vol. 7, no. 5, pp. 4702–4715, 2012.

[6] C. N. Kotanen, C. Tlili, and A. Guiseppi-Elie, "Bioactive electroconductive hydrogels: The effects of electropolymerization charge density on the storage stability of an enzyme-based biosensor," *Appl. Biochem. Biotechnol.*, vol. 166, no. 4, pp. 878–888, 2012.

[7] C. P. Quinn, C. P. Pathak, and J. a Hubbell, "of Dimethacrylate for and Biocompatibility of of Improving Biosensors Biosensors," vol. V, no. 5, pp. 389–396, 1995.

[8] P. C. Nicolson and J. Vogt, "Soft contact lens polymers: An evolution," *Biomaterials*, vol. 22, no. 24, pp. 3273–3283, 2001.

[9] L. V Rodríguez, Z. Alfonso, R. Zhang, J. Leung, B. Wu, and L. J. Ignarro, "Clonogenic multipotent stem cells in human adipose tissue differentiate into functional smooth muscle cells.," *Proc. Natl. Acad. Sci. U. S. A.*, vol. 103, no. 32, pp. 12167–12172, 2006.

[10] P. a Zuk, M. Zhu, H. Mizuno, J. Huang, J. W. Futrell, a J. Katz, P. Benhaim, H. P. Lorenz, and M. H. Hedrick, "Multilineage cells from human adipose tissue: implications for cell-based therapies.," *Tissue Eng.*, vol. 7, no. 2, pp. 211–228, 2001.

[11] E. Bat, T. G. van Kooten, J. Feijen, and D. W. Grijpma, "Macrophage-mediated erosion of gamma irradiated poly(trimethylene carbonate) films," *Biomaterials*, vol. 30, no. 22, pp. 3652–3661, 2009.

[12] L. V Rodríguez, S. Chen, G. S. Jack, F. De Almeida, L. V Rodrı, K. W. Lee, R. Zhang, V. Larissa, and D. Almeida, "New objective measures to quantify stress urinary incontinence in a novel durable animal model of intrinsic sphincter deficiency New objective measures to quantify stress urinary incontinence in a novel durable animal model of intrinsic sphincter deficien," vol. 90024, pp. 1332–1338, 2006.

[13] A. Hijaz, F. Daneshgari, K.-D. Sievert, and M. S. Damaser, "Animal models of female stress urinary incontinence.," *J. Urol.*, vol. 179, no. 6, pp. 2103–2110, 2008.

[14] E. E. Gardiner, S. S. Mok, a Sriratana, H. C. Robinson, B. J. Veitch, D. a Lowther, and C. J. Handley, "Polymorphonuclear neutrophils release 35S-labelled proteoglycans into cartilage during frustrated phagocytosis.," *Eur. J. Biochem.*, vol. 221, no. 2, pp. 871–879, 1994.

[15] S. Vijayasekaran, T. V Chirila, T. a Robertson, X. Lou, J. H. Fitton, C. R. Hicks, and I. J. Constable, "Calcification of poly(2-hydroxyethyl methacrylate) hydrogel sponges implanted in the rabbit cornea: a 3-month study.," *J. Biomater. Sci. Polym. Ed.*, vol. 11, no. 6, pp. 599–615, 2000.

[16] H. S. Yoo, T. G. Kim, and T. G. Park, "Surface-functionalized electrospun nanofibers for tissue engineering and drug delivery," *Adv. Drug Deliv. Rev.*, vol. 61, no. 12, pp. 1033–1042, 2009.

[17] X. Zhu, S. C. Kerm, M. B. E. Chan-Park, and T. L. Seng, "Effect of argon-plasma treatment on proliferation of human-skin-derived fibroblast on chitosan membrane in vitro," *J. Biomed. Mater. Res. - Part A*, vol. 73, no. 3, pp. 264–274, 2005.

[18] J. Venugopal, S. Low, A. T. Choon, a. Bharath Kumar, and S. Ramakrishna, "Electrospun-modified nanofibrous scaffolds for the mineralization of osteoblast cells," *J. Biomed. Mater. Res. - Part A*, vol. 85, no. 2, pp. 408–417, 2008.

[19] J. Jia, Y. Y. Duan, J. Yu, and J. W. Lu, "Preparation and immobilization of soluble eggshell membrane protein on the electrospun nanofibers to enhance cell adhesion and growth," *J. Biomed. Mater. Res. - Part A*, vol. 86, no. 2, pp. 364–373, 2008.

[20] M. P. Prabhakaran, J. Venugopal, C. K. Chan, and S. Ramakrishna, "Surface modified electrospun nanofibrous scaffolds for nerve tissue engineering.," *Nanotechnology*, vol. 19, no. 45, p. 455102, 2008.

[21] D. R. Nisbet, A. E. Rodda, M. K. Horne, J. S. Forsythe, and D. I. Finkelstein, "Implantation of functionalized thermally gelling xyloglucan hydrogel within the brain: associated neurite infiltration and inflammatory response.," *Tissue Eng. Part A*, vol. 16, no. 9, pp. 2833–2842, 2010.

[22] J. M. Morais, F. Papadimitrakopoulos, and D. J. Burgess, “Biomaterials/tissue interactions: possible solutions to overcome foreign body response.,” *AAPS J.*, vol. 12, no. 2, pp. 188–196, 2010.

[23] E. J. Kovacs, “Fibrogenic cytokines: the role of immune mediators in the development of scar tissue.,” *Immunol. Today*, vol. 12, no. 1, pp. 17–23, 1991.

[24] S. M. Wahl, H. Wong, and N. McCartney-Francis, “Role of growth factors in inflammation and repair.,” *J. Cell. Biochem.*, vol. 40, no. 2, pp. 193–199, 1989.

[25] W. J. Williams, “Review article Granulomatous inflammation - a review,” pp. 723–733, 1983.

[26] J. Pober and R. Cotran, “The role of endothelial cells in inflammation,” *Transplantation*, vol. 50, no. 4. pp. 537–544, 1990.

CHAPTER 4

POTENTIAL TO USE HPTC TO DELIVER ADIPOSE DERIVED STEM CELLS IN THE INJECTION SITE—ADVANTAGE OF A LOW MODULUS AND DURABLE FILLER FOR SOFT TISSUE

4.1 INTRODUCTION

Adipose stem cells (ASCs) have first been reported by Zuk et al[1] in 2001 as a pluripotent adult cell source, and has since been studied for the potential to be used in regenerative medicine[2-4], with 20 approved ongoing or completed clinical trials to-date (Table 1) (www.clinicaltrials.gov/) for treatment of a variety of conditions, from wound healing, pain treatment for amputation stumps, various nervous system diseases, erectile dysfunction, osteoarthritis, dry macular degeneration, degenerative disc disease, tendon injury, fistulas, cardiac function anomaly, Crohn's disease, incontinence, cancer and various use for cosmetic procedures. The major advantage of adipose stem cells is that they can potentially be harvested from the patient autologously at any age through minimally invasive procedure, with the pluripotent cell yield in the order of 400,000 per mL of lipoaspirate[5], which is much higher than the typical yield from mesenchymal stem cell extraction from other parts of the mesoderm including bone marrow[6-7], umbilical cord[6], placenta[8-9], muscle, corneal stroma or dental pulp [10].

Despite the promising potential of autologous ASCs in tissue regeneration and repair, having an efficient vehicle that can deliver ASCs to the target site in the body, maintaining a high cell number at the target site over an extended period of time in order

to have any therapeutic effect, and promoting ASC's differentiation once delivered in the target site remain challenging aspects of using ASC for tissue regeneration in practice.

There is an increasing body of evidence that points to the overwhelming importance of mechanical environment in the modulation of cell fate by mechanicotransduction via stretch-sensitive ion channels, cytoskeleton modification, stress fiber orientation, integrins, gravity, and signaling molecules [11-15]. Cells have the ability to respond drastically differently to mechanical cues of the substrate or matrix on which they are exposed to, often with as much importance as the chemical environment[16]. As the scientific community started to gain more understanding on the importance of mechanical stimuli and surface topography in the remodeling of the cytoskeleton, and in turn, signal transduction and cell fate, more attention has been garnered for providing conducive mechanical environment for maximum potential of differentiating stem cell into the target lineage for tissue regeneration [11, 17]. There are numerous reports that point to the importance of having relatively low elastic modulus (<40kPa) growth surface in order to best induce soft tissue morphology and phenotype under controlled environments [11] [18-22]. The exact elastic modulus conducive for different cells and final desired cell fate varies, and it is dependent on the origin of the cell type, chemical cues available, surface chemistry and topography specific for the system tested, and the type of final soft tissue fate desired.

Despite the current understanding of the importance of having mechanically conducive environment for cell delivery in tissue engineering applications, extremely limited long-lasting vehicles are available which fulfills the requirement of providing conducive mechanical environment, which is relatively low in elastic modulus, for soft

tissues. There are currently three main types of materials as vehicles for delivery: natural, synthetic, and hybrid of the two. Most cell delivery vehicles being explored currently are derived from natural resources, but they are not long-lasting in the body, namely protein-based polymers such as collagen, gelatin, silk fibroin, fibrin, and polysaccharidic polymers such as chitosan, alginate and hyaluronic acid (HA) [23], with a degree of degradation to 50% of the original mass in 2 months or less. Synthetic polymers have properties that are easily controlled, and the most widely used ones include poly(ethyl glycol) (PEG) [24], poly (vinyl alcohol) (PVA) but they have been shown to have poor adhesion and interaction with cells and led to anoikis due to the lack of matrix interactions[23], and therefore not ideal for long-term success as cell delivery vehicles. Hybrids of polymers found in the nature and synthetic polymers were investigated, such as an injectable hydrogel made of a blend of HA, collagen and ether tetrasuccinimidyl glutarate for cell delivery in the nucleus pulposus [25], and a blend of HA with methylcellulose[26] for the treatment of retinal degenerative diseases [26]. Most of these new hybrids investigated fall short in terms of providing durability and therefore limits its potential for extended use.

There is a lack of cell delivery vehicle that is long-lasting and yet matches the modulus of the soft tissue. Currently, durable delivery vehicles and low elastic modulus materials seem mostly mutually exclusive. The invention of biomaterials that that fulfill both criteria at once will be an important contribution to the research of using stem cells as a long-term treatment method, where the prolonged presence of the cells at the delivery site has often been called to question.

In this study, we demonstrate the degree of myogenic differentiation of two types of stem cells, Adipose derived stem cells (ASC), and bone marrow stromal cells (BMSC), to the varying elastic modulus of the hydrogel system, to attempt to show proof of concept that that mechanical property is indeed a crucial aspect of maintaining cell phenotype similar to the cells at the site of injection. Myogenic differentiation is of interest in this study as we are most interested in the regeneration of the smooth muscle in urethra and musculature for cosmetic purposes, both of which important for soft tissue regeneration. If the cells do express higher myogenic potential at certain elastic modulus, we can use that information to customize the HPTC's modulus that can be conducive for stem cells' differentiation and injectability.

4.2 MATERIALS AND METHODS

Hydrogels with controlled elastic moduli were fabricated with 88.2 mol % HEMA, 6.1 mol % PEGMA and 5.7 mol % TEGDMA as the sole precursors, which are then mixed with 20 to 80% water to alter its moduli without changing other chemical compositions of the hydrogel, including the branching frequencies. CMC is left out of this composition to help achieve a smoother surface for the ease of hydrogel fabrication in the form of 1mm thick, 15mm diameter cylinders. This composition is termed HPT gel, which stands for HEMA, PEGMA and TEGDMA. The gels are polymerized between 2 glass plates with a 1mm spacer by heat-activated free radical polymerization at 80°C under dry heat for half an hour with 1.0 wt % Azobisisobutyronitrile (AIBN). The glass plates are then separated and the gel sheet

sandwiched in between is then cut with a circular cutter at 15mm diameter. HPT gels with 6 different elastic moduli, 2.5, 5, 15, 50, 125 and 200 kPa were made.

One side of each circular gel is then coated with a layer of RGDS functional group for improved cell spreading through integrin interactions. Namely, RGDS peptide (Sigma, A9041) is allowed to react with PEG-200-monomethylether-monomethacrylate (Polysciences 16664-100) to form RGDS-PEG-aryloyl. RGDS-PEG-acryloyl is then mixed with the appropriate % of precursors (88.2 mol % HEMA, 6.1 mol % PEGMA and 5.7 mol % TEGDMA) and water to form a RGDS layer with the same elastic modulus on each disc, at a final coating volume of 60µl, by heat polymerization at 80°C in a water bath for 10 minutes. The RGDS coating is covalently bound to the resulting polymer mix. Discs of RGDS-functionalized hydrogels are then briefly disinfected by soaking in 70% ethanol for 5 minutes, and then subsequently washed in sufficient 1X PBS three times, with the last wash lasting more than 2 hours to remove all traces of ethanol. UV light exposure for 15 minutes was used as an additional disinfection method.

Two types of cells were seeded and cultured on the RGDS-coated HPT discs with 6 different elastic moduli. Adipose derived stem cells (ASC) harvested from young adult Lewis rats as described in Rodriguez et. al.[27], and Bone marrow stromal cells (BSMC) derived from young adult Lewis rats as well, as previously described[28, 29]. Cells were initially seeded onto the RGDS coated HPT discs with DMEM with 10% fetal bovine serum, let acclimate for 3 days, before switching to their respective myogenic media. ASC were maintained in smooth muscle maintenance media SMIM [27] and BMSC were maintained in myogenic growth factors (5ng/ml platelet-derived growth factor (PDGF-BB) and 2.5ng/ml transforming growth factor (TGF-

b1)[28]. Cells were allowed to grow on the surfaces for 3 weeks, with refreshment of the medium every 2-3 days, before RNA is harvested from the cells with the Qiagen RNeasy kit.

Myogenic marker expression was assessed by real time PCR. Two markers, ACTA2 and MYH11 expression were evaluated, compared to the baseline of day 0 of culture on the gel discs. Real time PCR using Roche FastStart SYBR green master mix on the Mx3000 system (Agilent Technologies, Inc) referencing the level of housekeeping 18S ribosomal mRNA. ACTA2 to 18S mRNA ratio and MYH11 to 18S mRNA level were recorded at the log phase of each PCR copy number growth curve. The baseline expression level for ACTA2 and MYH11 day 0 were set at 1.

4.3 RESULTS

HPT hydrogels with a range of elastic moduli from 2.5 to 200 kPa, but with the same branching ratio and chemistry, were successfully made. The only variable present, which determines the elastic moduli, is the water content. The elastic moduli chosen are 1, 15, 50, 100, 200 and >2000 kPa, at 20%, 37%, 48%, 56%, 60% and 71% precursor percentage (figure 1), where the remaining percentage is pure water.

For BMSC, the ACTA2 expression decreased after growing on the RGDS-functionalized HPT gel discs at all the elastic moduli tested, with expression level between 0.01 and 0.4 compared to day 0 of culture (figure 2a). MYH11 expression for BMSC increased for the lower elastic moduli 1kPa and 15kPa, at 11.0 and 17.8 fold increase compared to day 0 respectively (figure 2b). For the higher elastic moduli, between 50 and >2000 kPa, the MYH11 expression

decreased, suggesting that they are not conducive mechanical environment for BMSC myogenic differentiation.

For ASCs, the ACTA 2 expression increased for all the elastic moduli tested, with 1kPa substrate being the highest, at 10.2 fold increase, followed by 15kPa at 4.9 fold increase, and100kPa at 4.6 fold increase (figure 2a). MYH 11 expression for ASC increased the most at 1kPa elastic modulus as well, with a 20.3 fold increase compared to the expression on day 0. The second highest increase is at 100kPa, at 14.3 fold increase, followed by 15kPa at 6.0 fold increase. ASCs have the strongest myogenic expression according to both ACTA2 and MYH11 expression at 1kPa elastic modulus provided by RGDS functionalized HPT hydrogel.

4.4 DISCUSSIONS

We have successfully created an in vitro hydrogel system for cell culture with a smooth and even surface, functionalized with RDGS peptides that are covalently integrated with the hydrogel for improved cell adhesion and spreading, with a range of elastic modulus ranging from 1 to over 2000kPa just by changing the water content alone. The gels with different moduli have exactly the same branching ratio and chemistry.

Under the smooth-muscle-inducing culture conditions (SMIM media), ASCs cultured on the RGDS-functionalized HPT surfaces with elastic moduli ranging from 1 to >2000kPa seem to express higher levels of smooth muscle specific markers, ACTA2 and MYH11, in general, compared to day 0, when ASCs are solely cultured on high modulus tissue culture dish, and not under chemical induction of SMIM media. Among these moduli, ASCs showed by far the highest myogenic expression of both ACTA2 (10.2 times higher expression) and MYH11 (20.3

times higher expression) when cultured on 1kPa HTP surface. At 15kPa, ASCs shows promising myogenic potential, with ACTA2 expressed 4.9 times more than the time 0 baseline, and MYH11 expressed 6 times more. ASCs respond differently to varied matrix stiffness. Based on Engler et al.'s study[11], a different source of stem cells, MSCs showed the most prominent myogenic expression at 11kPa, with 6 times more myogenic message being expressed. Having the ASC respond the best in myogenic differentiation at a relatively low elastic modulus is consistent with Engler's finding.

For BMSC, expression of ACTA2 was lower than the day 0 level across the board of all the different moduli. However, the highest MYH11 expression does peak at 15kPa at 17.8 times the baseline expression. The peak at which the highest myogenic expression is found is similar to the one reported by Engler at al. fir BMSC, 10kPa. BMSC is also shown to respond differently to the same chemical environment but different mechanical support.

We have shown that the two types of stem cells tested, ASC and BMSC both respond to mechanical cues in the environment while the chemical environments are kept identical, with highest myogenic potential towards the lower elastic modulus range of 1-15kPa. Since HPTC injectable gel has a modulus close to this modulus range, cells that might be co-injectaed are believed to in a conducive mechanical environment to differentiate into the myogenic lineage, if the other factors, such as chemical cues are also beneficially aligned.

4.5 CONCLUSIONS

An in vitro hydrogel cell culture system with a wide range of adjustable elastic moduli (1- >2000 kPa) but identical chemical environment was described in this study. Real time PCR

study of marker expression of ASCs and BMSCs grown on these surfaces reveal that these cells indeed respond to different matrix stiffness. Highest myogenic expression was seen at 1kPa for ASC, while 15kPa was observed for BMSC.

4.6 Table

Condition	Status	ID	Institution
Anal Fistula	completed	NCT00475410	Cellerix
The Sequelae Caused by Severe Brain Injury	completed	NCT01649700	Oscar Kuang-Sheng Lee
Peripheral Vascular Diseases; Cardiovascular Diseases	completed	NCT01211028	University Hospital, Toulouse
Buerger's Disease	completed	NCT01302015	K-Stemcell Co Ltd
Knee Osteoarthritis	Active	NCT02142842	University of Science Ho Chi Minh City
Type 1 Diabetes Mellitus	Active	NCT00703599	Adistem Ltd
Osteoarthritis	Active	NCT01885832	Translational Biosciences
Amputation Stumps; Pain	Active	NCT01645722	University of Pittsburgh
Critical Limb Ischemia	Active	NCT01745744	Iniciativa Andaluza en Terapias Avanzadas
Critical Limb Ischemia (CLI); Diabetes	Active	NCT01257776	Iniciativa Andaluza en Terapias Avanzadas
Autoimmune Diseases; Immune System Diseases; Demyelinating Diseases; Nervous System Diseases	Active	NCT01056471	Iniciativa Andaluza en Terapias Avanzadas
Dry Macular Degeneration	recruiting	NCT02024269	Bioheart
Degenerative Disc Disease	recruiting	NCT02097862	Bioheart, Inc.
Rotator Cuff Tear	recruiting	NCT02298023	Seoul National University Hospital
Osteoarthritis	recruiting	NCT02241408	StemGenex
Rheumatoid Arthritis	recruiting	NCT02348086	StemGenex
Multiple Sclerosis	recruiting	NCT02157064	StemGenex
Chronic Obstructive Pulmonary Disease	recruiting	NCT02161744	Arkansas Heart Hospital
Graft Versus Host Disease; Chronic and Expanded Graft Versus Host Disease; Immune System Diseases	recruiting	NCT01222039	Iniciativa Andaluza en Terapias Avanzadas
Chronic Obstructive Pulmonary Disease	recruiting	NCT02216630	Kimera Society Inc
Erectile Dysfunction; Peyronie' Disease	recruiting	NCT02414308	Khaled Abdulmoneim Gadalla
Micromastia	recruiting	NCT02116933	Joel A. Aronowitz
Low Back Pain	recruiting	NCT02338271	Inbo Han
Erectile Dysfunction	recruiting	NCT02087397	Ageless Regenerative Institute
Lateral Epicondylitis	recruiting	NCT01856140	Sun Gun Chung
Clinical Patient Safety of Allogeneic Stem Cell Therapy	recruiting	NCT02387723	JKastrup, Rigshospitalet, Denmark
Ulcerative Colitis	recruiting	NCT01914887	Instituto de Investigación Hospital Universitario La Paz
ARDS	recruiting	NCT01902082	Shaoxing Second Hospital
Faecal Incontinence	recruiting	NCT02292628	Iniciativa Andaluza en Terapias Avanzadas
Critical Limb Ischemia	recruiting	NCT02099500	Ageless Regenerative Institute
Wounds	not yet recruiting	NCT02314416	Georgia Regents University
Erectile Dysfunction; Cardiac Disease	not yet recruiting	NCT02107118	Mohit Khera
Chronic Obstructive Pulmonary Disease	not yet recruiting	NCT02348060	StemGenex
Cancer	not yet recruiting	NCT02439047	Centre Oscar Lambret
Lipodystrophies; Aesthetics Procedure	not yet recruiting	NCT02034786	Cryopraxis Criobiologia Ltda
Parkinson's Disease	unknown	NCT02184546	StemGenex
Complex Perianal Fistula	unknown	NCT01314092	Anterogen Co., Ltd.
Crohn	unknown	NCT01440699	Anterogen Co., Ltd.
Lipodystrophy	unknown	NCT00715546	Irmandade Santa Casa de Misericórdia de Porto Alegre
Crohn Disease	unknown	NCT01157650	Clinica Universidad de Navarra, Universidad de Navarra

Table 1. Approved completed, ongoing and future clinical trials to-date registered with the U.S. National Institute of Health (www.clinicaltrials.gov).

4.7 Figures

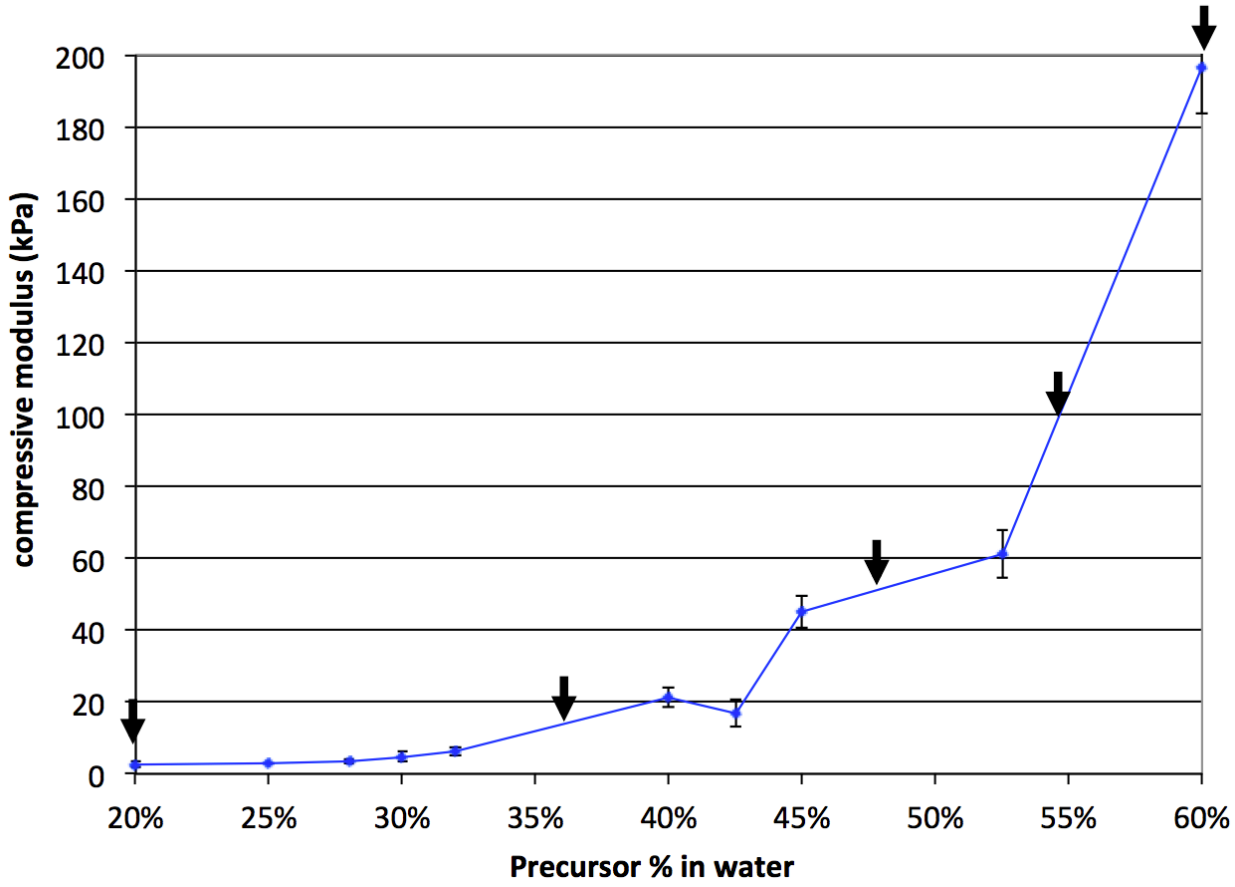

Figure 1. HPT hydrogel with increasing compressive moduli while maintaining the same chemical composition was achieved by increasing the precursor percentage (88.2 mol % HEMA, 6.1 mol % PEGMA and 5.7 mol % TEGDMA), which is essentially decreasing water percentage. The compressive modulus was tested with Instron compressive testing in quadruplicates. The moduli used for the subsequent experiments with defined moduli are indicated with the arrows (except for 2000kPa which is off the scale), at 1, 15, 50, 100, 200 and >2000 kPa.

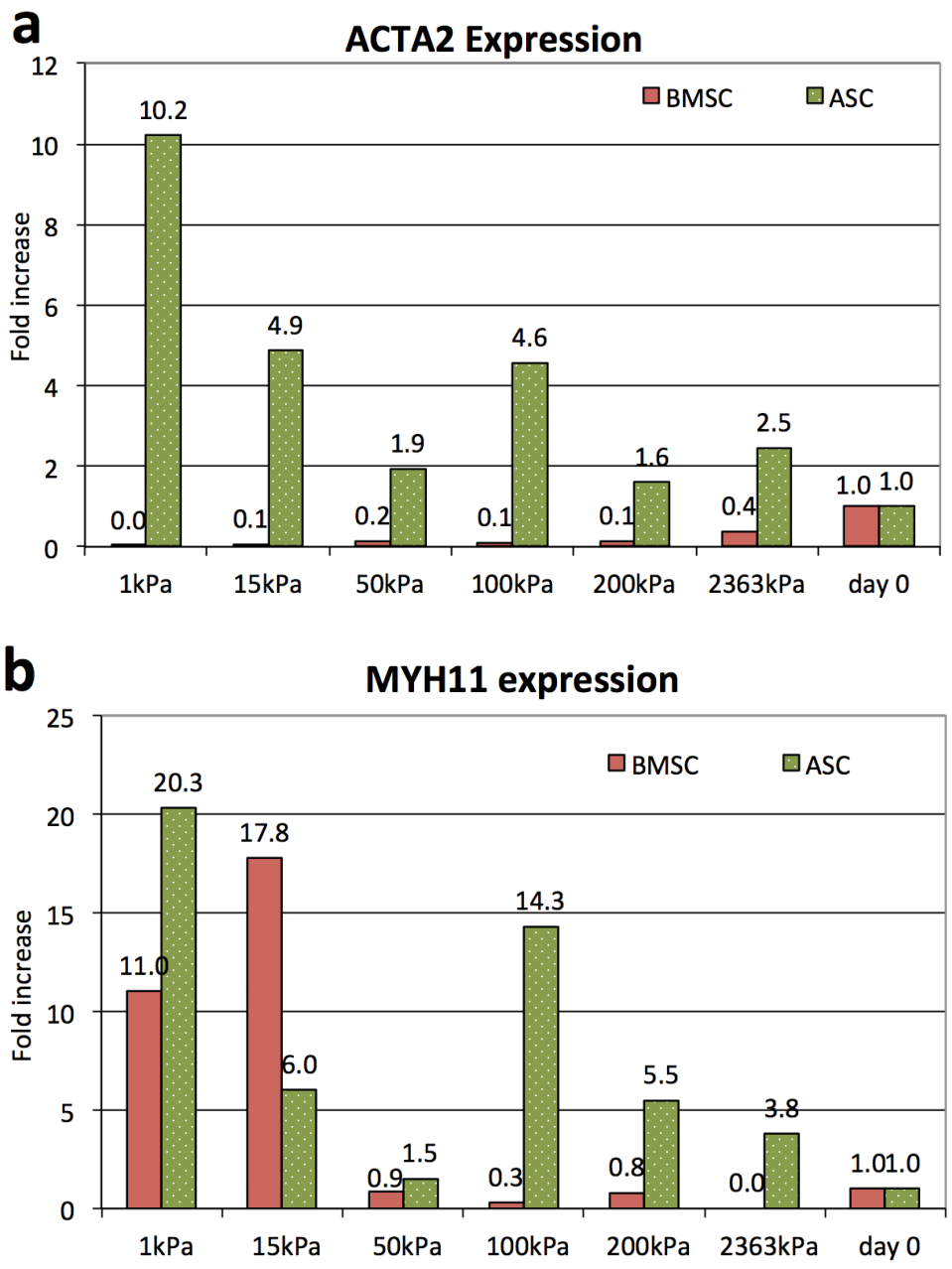

Figure 2. Real time PCR reveals that the highest increase in ACTA2 (smooth muscle Actin) expression is observed for rat ASCs grown on the 1kPa HPT surface, at 10.2 fold compared to day 0, and the highest hold increase in MYH11 (smooth muscle myosin heavy chain) expression is also for the 1kPa HPT surface, at 202.7 fold compared to day 0. The reference gene used was 18S. All the ASCs on HPT surface was grown for a total of 3 weeks, with DMEM for 1 week and then switched to SMIM medium for 2 weeks, before RNA harvesting. BMSC have decreased ACTA2 expression when cultured on HPT surface compared to day 0 (a), however, they have increased MYH11 expression at low modulus (1kPa and 15 kPa) HPTC surfaces (b).

Reference

[1] P. a Zuk, M. Zhu, H. Mizuno, J. Huang, J. W. Futrell, a J. Katz, P. Benhaim, H. P. Lorenz, and M. H. Hedrick, "Multilineage cells from human adipose tissue: implications for cell-based therapies.," *Tissue Eng.*, vol. 7, no. 2, pp. 211–228, 2001.

[2] A. Mizuno, H, Tobita, M, Uysal, "Concise review: genetically engineered stem cell therapy targeting angiogenesis and tumor stroma in gastrointestinal malignancy," *Stem Cells*, pp. 227–235, 2013.

[3] J. M. Gimble, A. J. Katz, and B. a. Bunnell, "Adipose-derived stem cells for regenerative medicine," *Circ. Res.*, vol. 100, no. 9, pp. 1249–1260, 2007.

[4] S. Lendeckel, A. Jödicke, P. Christophis, K. Heidinger, J. Wolff, J. K. Fraser, M. H. Hedrick, L. Berthold, and H. P. Howaldt, "Autologous stem cells (adipose) and fibrin glue used to treat widespread traumatic calvarial defects: Case report," *J. Cranio-Maxillofacial Surg.*, vol. 32, no. 6, pp. 370–373, 2004.

[5] L. Aust, B. Devlin, S. J. Foster, Y. D. C. Halvorsen, K. Hicok, T. du Laney, a Sen, G. D. Willingmyre, and J. M. Gimble, "Yield of human adipose-derived adult stem cells from liposuction aspirates.," *Cytotherapy*, vol. 6, no. 1, pp. 7–14, 2004.

[6] S. Kern, H. Eichler, J. Stoeve, H. Klüter, and K. Bieback, "Comparative analysis of mesenchymal stem cells from bone marrow, umbilical cord blood, or adipose tissue.," *Stem Cells*, vol. 24, no. 5, pp. 1294–1301, 2006.

[7] C. Bourzac, L. C. Smith, P. Vincent, G. Beauchamp, J. P. Lavoie, and S. Laverty, "Isolation of equine bone marrow-derived mesenchymal stem cells: a comparison between three protocols," *Equine Vet. J.*, vol. 42, no. 6, pp. 519–527, 2010.

[8] Z. Miao, J. Jin, L. Chen, J. Zhu, W. Huang, J. Zhao, H. Qian, and X. Zhang, "Isolation of mesenchymal stem cells from human placenta: Comparison with human bone marrow mesenchymal stem cells," *Cell Biol. Int.*, vol. 30, no. 9, pp. 681–687, 2006.

[9] O. Parolini, F. Alviano, G. P. Bagnara, G. Bilic, H.-J. Bühring, M. Evangelista, S. Hennerbichler, B. Liu, M. Magatti, N. Mao, T. Miki, F. Marongiu, H. Nakajima, T. Nikaido, C. B. Portmann-Lanz, V. Sankar, M. Soncini, G. Stadler, D. Surbek, T. a Takahashi, H. Redl, N. Sakuragawa, S. Wolbank, S. Zeisberger, A. Zisch, and S. C. Strom, "Concise review: isolation and characterization of cells from human term placenta: outcome of the first international Workshop on Placenta Derived Stem Cells.," *Stem Cells*, vol. 26, no. 2, pp. 300–311, 2008.

[10] G. T.-J. Huang, S. Gronthos, and S. Shi, "Mesenchymal stem cells derived from dental tissues vs. those from other sources: their biology and role in regenerative medicine.," *J. Dent. Res.*, vol. 88, no. 9, pp. 792–806, 2009.

[11] A. J. Engler, S. Sen, H. L. Sweeney, and D. E. Discher, “Matrix Elasticity Directs Stem Cell Lineage Specification,” *Cell*, vol. 126, no. 4, pp. 677–689, 2006.

[12] D. E. Ingber, “Tensegrity: the architectural basis of cellular mechanotransduction.,” *Annu. Rev. Physiol.*, vol. 59, pp. 575–599, 1997.

[13] D. E. Ingber, “Tensegrity II. How structural networks influence cellular information processing networks.,” *J. Cell Sci.*, vol. 116, no. Pt 8, pp. 1397–1408, 2003.

[14] P. a. Janmey and D. a. Weitz, “Dealing with mechanics: Mechanisms of force transduction in cells,” *Trends Biochem. Sci.*, vol. 29, no. 7, pp. 364–370, 2004.

[15] F. H. Silver and L. M. Siperko, “Mechanosensing and mechanochemical transduction: how is mechanical energy sensed and converted into chemical energy in an extracellular matrix?,” *Crit. Rev. Biomed. Eng.*, vol. 31, no. 4, pp. 255–331, 2003.

[16] R. M. Tenney and D. E. Discher, “Stem cells, microenvironment mechanics, and growth factor activation,” *Curr. Opin. Cell Biol.*, vol. 21, no. 5, pp. 630–635, 2009.

[17] F. Guilak, D. M. Cohen, B. T. Estes, J. M. Gimble, W. Liedtke, and C. S. Chen, “Control of Stem Cell Fate by Physical Interactions with the Extracellular Matrix,” *Cell Stem Cell*, vol. 5, no. 1, pp. 17–26, 2009.

[18] G. C. Reilly and A. J. Engler, “Intrinsic extracellular matrix properties regulate stem cell differentiation,” *J. Biomech.*, vol. 43, no. 1, pp. 55–62, 2010.

[19] A. J. Engler, M. a. Griffin, S. Sen, C. G. Bönnemann, H. L. Sweeney, and D. E. Discher, “Myotubes differentiate optimally on substrates with tissue-like stiffness: Pathological implications for soft or stiff microenvironments,” *J. Cell Biol.*, vol. 166, no. 6, pp. 877–887, 2004.

[20] A. S. Rowlands, P. a George, and J. J. Cooper-White, “Directing osteogenic and myogenic differentiation of MSCs: interplay of stiffness and adhesive ligand presentation.,” *Am. J. Physiol. Cell Physiol.*, vol. 295, no. 4, pp. C1037–C1044, 2008.

[21] D. E. Discher, P. Janmey, and Y.-L. Wang, “Tissue cells feel and respond to the stiffness of their substrate.,” *Science*, vol. 310, no. 5751, pp. 1139–1143, 2005.

[22] J. S. Park, J. S. Chu, A. D. Tsou, R. Diop, Z. Tang, A. Wang, and S. Li, “The effect of matrix stiffness on the differentiation of mesenchymal stem cells in response to TGF-β,” *Biomaterials*, vol. 32, no. 16, pp. 3921–3930, 2011.

[23] P. B. Malafaya, G. a. Silva, and R. L. Reis, “Natural-origin polymers as carriers and scaffolds for biomolecules and cell delivery in tissue engineering applications,” *Adv. Drug Deliv. Rev.*, vol. 59, no. 4–5, pp. 207–233, 2007.

[24] S. J. Bryant, K. L. Durand, and K. S. Anseth, “Manipulations in hydrogel chemistry control photoencapsulated chondrocyte behavior and their extracellular matrix production.,” *J. Biomed. Mater. Res. A*, vol. 67, no. 4, pp. 1430–1436, 2003.

[25] E. C. Collin, S. Grad, D. I. Zeugolis, C. S. Vinatier, J. R. Clouet, J. J. Guicheux, P. Weiss, M. Alini, and A. S. Pandit, “An injectable vehicle for nucleus pulposus cell-based therapy,” *Biomaterials*, vol. 32, no. 11, pp. 2862–2870, 2011.

[26] B. G. Ballios, M. J. Cooke, D. van der Kooy, and M. S. Shoichet, “A hydrogel-based stem cell delivery system to treat retinal degenerative diseases,” *Biomaterials*, vol. 31, no. 9, pp. 2555–2564, 2010.

[27] L. V Rodríguez, Z. Alfonso, R. Zhang, J. Leung, B. Wu, and L. J. Ignarro, “Clonogenic multipotent stem cells in human adipose tissue differentiate into functional smooth muscle cells.,” *Proc. Natl. Acad. Sci. U. S. A.*, vol. 103, no. 32, pp. 12167–12172, 2006.

[28] Y. S. Yoon, A. Wecker, L. Heyd, J. S. Park, T. Tkebuchava, K. Kusano, A. Hanley, H. Scadova, G. Qin, D. H. Cha, K. L. Johnson, R. Aikawa, T. Asahara, and D. W. Losordo, “Clonally expanded novel multipotent stem cells from human bone marrow regenerate myocardium after myocardial infarction,” *J. Clin. Invest.*, vol. 115, no. 2, pp. 326–338, 2005.

[29] M. a Eglitis and E. Mezey, “Hematopoietic cells differentiate into both microglia and macroglia in the brains of adult mice.,” *Proc. Natl. Acad. Sci. U. S. A.*, vol. 94, no. 8, pp. 4080–4085, 1997.

Chapter 5

5.1 CONCLUSIONS

This dissertation presents a novel approach in fabricating a long lasting, non-biodegradable hydrogel that is easily injectable, in the attempt to solve the major problems with the currently existing semi-permanent to permanent injectable implant for the soft tissue augmentation. The size of the soft tissue fillers market is a multibillion dollar market worldwide. Other than the extremely high demand to have improvements of materials in the cosmetic procedure industry, various medical conditions frequently use soft tissue fillers as a minimally invasive treatment, including urinary incontinence, vesicoureteral reflux, fecal incontinence, and vocal cord repair procedures. Our main interest for this study is to fabricate a material for the treatment of urinary incontinence. Our main goal is to address these major issues with the existing available FDA-approved products:

(1) to produce a durable injectable material that can be **easily injectable** without clogging the needle or require a piston-powered syringe to inject;

(2) to have the ability to **customize the viscoelastic property** of the material to fit specific requirements for different applications;

(3) to provide an injectable that has the potential to be co-injected with cells.

We produced an interpenetrating network of hydrogel that has a list of components that have good safety records for medical devices, with HEMA, PEGMA, TEGDMA and CMC, and we named this hydrogel HPTC. We have optimized and attempted to understand the parameters required to produce a range of HPTC that are injectable, but with different, customizable viscoelastic properties. The optimal concentration and size of each component is mixed together with water and a photoinitiator, and the polymerization of HEMA/PEGMA and

TEGDMA take place around the pre-existing CMC strands by photoinitiated free radical polymerization. The resulting HPTC has adjustable elastic modulus, viscous modulus, tan delta, oscillatory stress under strain, and viscosity by changing one or more of these conditions during processing: the water content, CMC concentration, molecular weight of the CMC, and the percentage of TEGDMA. We have optimized a specific formulation of HPTC that fit the desired characteristics for urethral augmentation for the treatment of urinary incontinence in the rat model.

We have tested the biocompatibility of HPTC in the rat and found that it integrates well within the native tissue, with lots of cell infiltration, no fibrous capsule, and the material remains in vivo for up to 24 weeks in the rat urethra. We have found that m0st of the cells infiltrated into HPTC are histiocytes, and a less dense amount of them still exist in the HPTC 24 weeks after injection. However, direct culturing of macrophage cells on top of HPTC shows that HPTC is resistant to macrophage-mediated erosion,. Evaluation of its effectiveness as a treatment method for restoring urethral function shows that restores continence in the animal when the appropriate volume is injected, with improvement of the abdominal leak-point pressure back to its pre-incontinence level for up to 24 weeks. We observed a potential to co-inject cells with HPTC as a treatment method that is not available in any other injectable fillers in the current market, as co-injected cells seem to highly co-localize within the HPTC material, which is not seen in the cell only group where the cells mostly migrate away at 4 weeks.

5.2 FUTURE DIRECTIONS AND SUGGESTED EXPERIMENTS

This report demonstrated the potential of HPTC as an injectable filler with improved injectability compared to the major FDA-approved products in the same category with

customizable properties. However, this is only the beginning of a new area of research in the realm of soft tissue fillers, and more work is ahead to investigate HPTC's short-term and long-term safety, inflammatory response, and efficacy in treatment. It will eventually be crucial to understand how human soft tissue responds to the material as well.

Histiocyte infiltration and its residence in HPTC at 24 weeks requires further research to investigate the state of these cells, the type of cytokines they send out at different stages, and whether or not they have a frustrated attempt to phagocytose the surface and releasing free radicals in the environment that could cause havoc to the system, or cause degradation of HPTC.

Though the observation that PLA cells highly co-localize in HPTC opens an interesting discussion whether using HPTC could be a good candidate to co-inject with cells for cell therapy application, a better understanding why the cells are attracted to HPTC in the first place would be an important question to address. It would be interesting to find out if HPTC attract adipose derived stem cells preferentially, or a combination of different types of host cells. If the cell attraction is not specific, it would be crucial to understand the type of cells attracted, and their fate, cytokine responses, and physical interaction with HPTC in the short and extended time scale.